NTNU – Trondheim
Norwegian University of
Science and Technology

Direct Charging of a Solar Thermal Battery

Direkte soloppvarming av et termisk batteri

Victoria Sivertsen

Master of Science in Mechanical Engineering
Submission date: December 2013
Supervisor: Ole Jørgen Nydal, EPT
Co-supervisor: Asfafaw Haileselassie, EPT

Norwegian University of Science and Technology
Department of Energy and Process Engineering

NTNU
Norwegian University
of Science and Technology

Department of Energy
and Process Engineering

EPT-M-2013-xx

MASTER THESIS

For

Victoria Sivertsen

Fall 2013

Direct Charging of a Solar Thermal Battery

Direkte soloppvarming av et termisk batteri

Background and objective

One method of collecting and storing high temperature solar energy is to illuminate the heat storage directly. The storage can be positioned in the focus point of a concentrating reflector. If the storage consists of a solar salt (Nitrate solution) which melts upon heating, the storage should not be illuminated from the bottom.

Top illumination can be achieved with a double reflector system, where a secondary reflector redirects the rays onto a heat storage positioned below an opening in the primary reflector. A system has been constructed and is ready for analysis, optimization and testing.

The objective of the work is to determine the efficiency of the heat charging of a storage in a double reflector system.

The following tasks are to be considered:

1 Assemble and instrument the complete system for testing

2 Perform tests in the sun with measurements of the charging process using thermo elements and a thermal camera.

3 Perform a thermal analysis of the system

4 Provide recommendations for the further development or for field tests

Within 14 days of receiving the written text on the master thesis, the candidate shall submit a research plan for his project to the department.

When the thesis is evaluated, emphasis is put on processing of the results, and that they are presented in tabular and/or graphic form in a clear manner, and that they are analyzed carefully. The thesis should be formulated as a research report with summary both in English and Norwegian, conclusion, literature references, table of contents etc. During the preparation of the text, the candidate should make an effort to produce a well-structured and easily readable report. In order to ease the evaluation of the thesis, it is important that the cross-references are correct. In the making of the report, strong emphasis should be placed on both a thorough discussion of the results and an orderly presentation.

The candidate is requested to initiate and keep close contact with his/her academic supervisor(s) throughout the working period. The candidate must follow the rules and regulations of NTNU as well as passive directions given by the Department of Energy and Process Engineering.

Risk assessment of the candidate's work shall be carried out according to the department's procedures. The risk assessment must be documented and included as part of the final report. Events related to the candidate's work adversely affecting the health, safety or security, must be documented and included as part of the final report.

Pursuant to "Regulations concerning the supplementary provisions to the technology study program/Master of Science" at NTNU §20, the Department reserves the permission to utilize all the results and data for teaching and research purposes as well as in future publications.

The final report is to be submitted digitally in DAIM. An executive summary of the thesis including title, student's name, supervisor's name, year, department name, and NTNU's logo and name, shall be submitted to the department as a separate pdf file. Based on an agreement with the supervisor, the final report and other material and documents may be given to the supervisor in digital format.

YES Work to be done in lab (outdoors solar tests)
NO Field work

Department of Energy and Process Engineering, 16 January 2013

Olav Bolland
Department Head

Ole Jørgen Nydal
Academic Supervisor

Co-supervisor: Asfafaw Hailesellassie (PhD)

Preface

This thesis was carried out as a continuation of the NUFU Network Project “Small scale concentrating solar energy system with heat storage”. The work was done in cooperation with the laboratory of the Department of Energy and Process Engineering (EPT) at the Norwegian University of Science and Technology (NTNU).

This thesis would not have been possible to complete without the help of the technical staff at the laboratory. I would like to thank Paul Svendsen for his support and input throughout the work. Also I want to thank Marius Østnor Døllner for the outstanding work with the tracking system, and completion of the double reflector. For assistance in designing components of the system, I am thankful for the help from Martin Bustadmo and Reidar Tellebon. For the execution of replacing the reflective film, I am grateful for the help and inspiration of Halvor Haukvik and Martin Trana.

And finally I would like to thank my supervisor Ole Jørgen Nydal and co-supervisor Asfafaw Haileselassie for valuable advice and discussion throughout the project period.

Abstract

Direct illumination of a thermal storage from a concentrating solar collector can be used to charge a phase change material (PCM) for the purpose of storing heat for cooking. Top illumination can be achieved by a double reflecting system to avoid any dangers of expansion from heating the storage from the bottom.

An experimental investigation of the double reflecting system has been conducted at the lab of the Department of Energy and Process. The main purpose of the experiments was to be able to conduct an efficiency measurement of the system's ability to charge the heat storage. A double reflective solar concentrator with a heat storage has been instrumented and made ready for testing. Two tests of the full system with direct illumination of the heat storage by the sun have been conducted. Temperature measurements were done by thermocouples in the heat storage and on the secondary reflector, and a thermal camera was used to monitor the temperature of the top plate of the heat storage. The tests were not satisfactory in that they did not succeed to melt the phase change material (PCM) in the storage, and an efficiency measurement could not be concluded. The reflective film was as a result of these tests changed to reflective aluminium tiles for a better performance.

Additional tests with a thin absorber plate of carbon steel were then conducted, since the sun was now too low on the sky to allow a complete test. The focal point on the thin absorber plate reached temperatures above 300°C, and the focusing power of the system was promising. A test procedure for tracing a laser ray from a self-adjusting laser diode to the absorber by utilizing a Computer Numerical Control machine (CNC-machine) and a digital camera for automation has been developed and tested. Post processing of images acquired has been programmed in the Matlab programming software to crate intensity plots of the focal point of the double reflector. By means of a grid paper on the absorber plate, the focal point of the primary reflector was found for the reflective film and for the reflective aluminium tiles to be 665 mm and 662 mm respectively. The secondary reflectors optimal position to be able to focus the rays on to an absorber plate placed at the base of the primary reflector has been investigated by the new test procedure, and found to be 683 mm, with a separation distance between the two foci of 21 mm. A simple analysis of the double reflector in a Ray Tracing program gave a separation distance of around 20 mm.

Sammendrag

En dobbeltreflekternede solfanger kan brukes til å varme opp et varmelager bestående av et faseendrende materiale ved direkte belysning av lageret. Oppvarming av lageret må skje fra toppen og ned for å unngå farene ved utviding. Varmen fra lageret kan senere brukes til matlaging etter solen har gått ned.

Den dobbeltreflekterende solfangeren har blitt testet eksperimentelt ved Varmeteknisk laboratorium ved instituttet for energi og prosess-teknikk på Norges tekniske og naturvitenskapelige universitet (NTNU). Hovedformålet med eksperimentene var å finne effektiviteten til systemet for oppvarming av et varmelager. En dobbeltreflektor har blitt instrumentert og gjort klar til testing. To forsøk med oppvarming av varmelageret ved direkte belysning fra dobbeltreflektoren har blitt utført. Temperaturene i lageret og på sekundærreflektoren ble målt av termoelementer, og et termisk kamera ble brukt til å følge temperaturutviklingen på overflaten av varmelageret. Det lyktes ikke å smelte det faseendrende materialet i varmelageret, og effektivitetsmålinger kunne ikke utføres. En belsutning om å skifte ut reflektivfilmen på primærbarabolen med reflekterende aluminiumsfliser ble derfor tatt.

Dobbeltreflektoren ble så testet i sola med en tynn absorbatorplate av svart stål da solen var for lav for å utføre tester med varmelageret. Fokuspunktet på absorbatorplaten ble målt til over 300°C. En forsøksprosedyre som går ut på å traversere en laserdiode over primærparabolen ved hjelp av en CNC-maskin for å se på refleksjonen på en absorbatorplate ble utviklet. Et kamera ble montert for å automatisk ta bilder av laserrefleksjonene, og etterbehandling av bildene ble programmert i Matlab for å finne optimal monteringshøyde av sekundærparabolen, og for å finne fordelingen av intennsitet i fokuspunktet til systemet. Ved hjelp av millimeterpapir ble fokuslengden til primærbarabolen undersøkt for reflektivfilmen og for aluminiumsflisene til å være henholdsvis 665 mm og 662 mm. Optimal høyde for sekundærparabolen ble bestemt til å være 683 mm fra primærparabolens bunnpunkt og opp til kanten av sekundærparabolen, med en avstand mellom fokuspunktene til de to parabolene på 21 mm. En enkel analyse av dobbeltreflektoren er gjort i et strålefølgende program, og separasjonsavstanden mellom fokuspunktene var her funnet til å være rundt 20 mm.

Table of contents

Table of figures

1 Introduction

One method of collecting and storing high temperature solar energy for cooking is to illuminate the heat storage directly. The storage can be positioned in the focus point of a concentrating reflector. If the storage consists of a solar salt (Nitrate solution) which melts upon heating, the storage should not be illuminated from the bottom. Top illumination can be achieved with a double reflector system, where a secondary reflector redirects the rays onto a heat storage positioned below an opening in the primary reflector.

Solar ovens have been around for decades, but traditional fuels of biomass are still the main source of energy for cooking in remote areas of the world, where electricity is not available. Many studies has focused on the dangers of cooking over an open fire, where women and children are the most vulnerable to the health risks associated with burning accidents and indoor smoke from fire places. Other studies have focused on the problems of deforestation caused by excessive burning of firewood by a growing population. Because of the increased scarcity of firewood, the price is in many areas pushed to a high level, leading to the fact that many cannot afford it and the collection of firewood become tedious task for women. The solar oven as we know it today comes in numerous sizes, qualities and functionalities. Yet, solar ovens has not been widely accepted and utilized in today's society.

Two factors that limit the use of traditional solar ovens are that usage is only possible in the hours of sunshine, and that they are often only capable of cooking at medium temperatures (in the range of 150 °C). Frying and baking usually require higher temperatures. Solar collectors focusing on heat storages has been investigated by, amongst others, the The Norwegian Programme for Development, Research and Education (NUFU) Network project, "Small scale concentrating solar energy system with heat storage". The scope is that such a system should be able to store high temperature heat in the range of 220 °C, suitable for frying and baking, and keep the heat stored so that cooking can be done at night. A system has been constructed and is ready for complete instrumentation, analysis, optimization and testing.

1.1 Backgroud

This thesis is a continuation of the research done in the NUFU Network Project, from the period of 2007−2011 (SIU), in a collaboration between the Norwegian University of Science and Technology (NTNU) and 5 African universities (Mozambique, Uganda and Ethiopia).

> *"The Norwegian Programme for Development, Research and Education (NUFU) supports partnership-based academic cooperation between researchers and institutions in developing countries and their partners in Norway focusing on research, education, capacity building and institutional development."*

The focus of the network project was on a traditional solar cooker with a heat storage that allows continuous energy use not limited to the hours of sunshine. The goal was that the implementation of a heat storage to the system can increase the acceptance of solar energy.

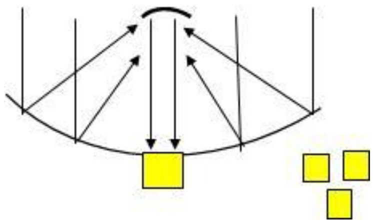

Figure 1.1 Illustration of a double reflector charging a heat battery.

This was to be done by studying prototypes of small scale concentrating collectors with integrated heat storage units with low cost solutions.

1.1.1 Stationary heat storage

The first concept is the idea of a stationary heat storage that can be heated via a heat carrier that circulates between the absorber and the heat storage. Air, oil and steam are examples of different heat carriers. The heat carrier transfers heat to the storage medium, e.g. a rock bed, accumulated or stationary oil, or a phase change material (PCM).

1.1.2 Heat batteries and direct illumination

In the second concept, the storage is to be illuminated directly using a secondary reflector. The storage is in this case smaller than the stationary type and portable. A larger storage unit could contain several smaller heat batteries. By illuminating the heat storage directly, there is no need for an additional circulation of HTF.

1.2 Problem statement

The problem faced by solar cookers, is the possibility to be a good replacement for other fuels in a way that is simple and safe to use, without adding too much complexity. Only then will it be accepted as an equal option to biofuels. The challenge of the double reflector solar collector is the need for accurate adjustment of the secondary reflector and an accurate tracking system. A final efficiency measurement is needed for the double reflecting solar cooker. A procedure for testing the systems optical efficiency is also needed to assess the focusing power of the system, and to be able to test solar collecting systems in the winter months of the year in the laboratory of Energy and Process Engineering.

1.3 Objective

The goal of this thesis is to instrument, and evaluate the potential of, a double reflective system, and to provide recommendations for the further development and for field tests. The evaluation is based on the following methods:

- Optical characterization from laser experiments in lab
- Thermal measurements and visualization from experiments in the sun
- Ray tracer analysis to support experimental results

1.4 Methodology

The methodology for the different test procedures and analysis will be described together with the experimental setup in Chapter 4 Tests and experimentation;

- Thermal test with heat storage
- Thermal test with thin absorber plate
- Experimental focal length of primary reflector
- Optimal placement of secondary reflector
- Image processing in Matlab

1.5 Scope and limitations

The main limitation for the project is the access to the sun and a clear sky, which is largely dependent of the amount of sunny days in Trondheim in the weeks available for testing after the summer. The scope of the thesis is to investigate the double reflectors ability to focus rays on to a storage.

1.6 Motivation

The motivation for this type of system is the possibility to store and use high temperature energy for cooking, and especially frying of the east African bread Injera.

The design of the system allows eliminating an additional heat transfer fluid for charging a movable storage unit containing PCM. Two parabolic reflectors will then guide the sunrays to reflect not once, but twice to come back down to the base of the primary reflector. This sets high demands for both tracking accuracy and the optical properties of the reflectors.

The main advantage of the double reflector system is the possibility to use the PCM solar salt (sodiun-potassium nitarate mixture). PCM storages has proved to store 5−14 times more heat per unit volume than sensible heat storage materials such as rock, shastry or water (Sharma).

A drawback is that cooking cannot be done while the heat storage is charging. The system also loses some energy due to the extra reflection required, but the motivation is that the benefits of not needing a HTF loop are greater than the drawbacks.

2 Litterature

In this chapter, the main concepts and definition for concentrating solar collectors is described.

2.1 Definitions

Spectral intensity
The spectral intensity of incident radiation is defined as the rate at which radiant energy for a certain wavelength λ, is incident from the directional angles θ and φ (in spherical coordinates), per unit area of the intercepting surface normal to this direction, per unit solid angle about this direction, and per unit wavelength interval around λ.

Reflectivity
Reflectivity is a property that determines how much of the incident radiation that is reflected by a surface. The property is essentially bidirectional, and depends not only on the direction of the incident radiation, but also on the direction of the reflected radiation.

Emissivity
The rate at which energy is released from a surface per unit area is known as the emissive power of the object. Emissivity is relative to the upper limit of radiant energy released defined by the Stefan−Boltzmannl law (if the object in question would have been an ideal radiator/blackbody) (Incopera 2007).

Irradiation
The rate at which radiant energy is incident on a unit area of a surface.

Solar noon:
The time of the day that the sun sits highest of the sky, in solar time defined to be at noon (12:00 AM)

Equinox, autumnal and vernal:
Defined by the FreeOnlineDictionary as:

> *"Either of the two times during a year when the sun crosses the celestial equator and when the length of day and night are approximately equal; the vernal equinox or the autumnal equinox".*

Solstice, summer and winter:
Defined by the FreeOnlineDictionary as:

> *"Either of two times of the year when the sun is at its greatest distance from the celestial equator. The summer solstice in the Northern Hemisphere occurs about June 21st, when the sun is in the zenith at the tropic of Cancer; the winter solstice occurs about December 21st, when the sun is over the tropic of Capricorn. The summer solstice is the longest day of the year and the winter solstice is the shortest."*

2.2 Solar declination

The earth's rotational axis is tilted 23.45 degrees with respect to the normal of the plane of the earth's elliptical orbit around the sun. Since the axis of rotation is kept at a constant direction while the earth orbits the sun, the sun has a seasonal variation across the year, measured in the declination angle δ.

The declination angle is equal to the local altitude angle, α_{loc}, at the sub solar point of our planet (the point at which the sun is directly overhead, i.e. in zenith position). This makes the sun decline $\delta = \pm 23.45°$ from the equinox position ($\delta = 0°$) during one year. The tilt of the earth's axis is towards the sun at summer time, and away from the sun at winter for the northern hemisphere. The dates for different declination angles are shown in Figure 2.1 (UCSB).

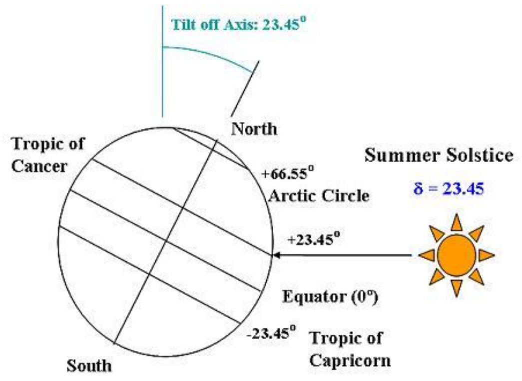

Declination (°)	Approximate dates
+23.45	June 22
+20	May 21, July 24
+15	May 1, Aug 12
+10	Apr 16, Aug 28
+5	Apr 3, Sept 10
0	Mar 21, Sept 23
−5	Mar 8, Oct 6
−10	Feb 23, Oct 20
−15	Feb 9, Nov 3
−20	Jan 21, Nov 22
−23.45	Dec 22

Figure 2.1. Declination angles with associated dates.

2.3 Concentrating solar collectors

A concentrating solar collector uses an optical device between the sun and the absorbing collector surface to concentrate the energy from the sun. The collector area is smaller on a concentrating collector than on a plate collector. Concentrators can be reflectors (e.g. parabolic trough, parabolic dish, compound parabolic trough) or refractors (e.g. lens, Fresnel lens), and receivers can have many different designs. The concentration ratio is defined as the aperture area to the absorber area ratio, and it varies for different concentrators. The greater the concentration ratio is, the more accurate the tracking system needs to be.

Tracking of the suns movement can be done in two principal methods, the altazimuth method and a one-axis method. The altazimuth method tracks the sun in both azimuth and altitude direction. This is the method used by the double reflector system, and most paraboloidal concentrators. One-axis tracking is the other principal method, and it tracks the sun in only one direction; east-west, or north-south. One-axis tracking is generally used on parabolic trough collectors. (Kalogirou 2004).

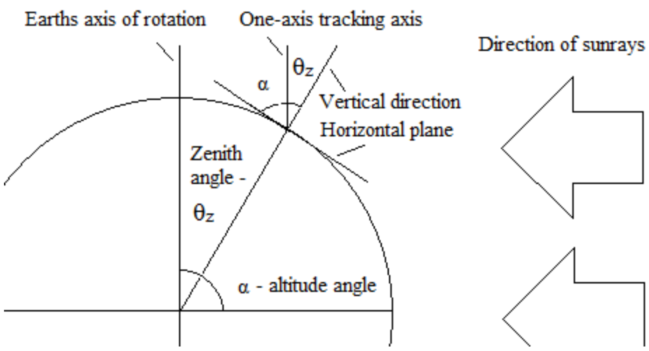

Figure 2.2. Accurate tracking using only one axis. Example at δ=0° (equinox).

There is also a method that can track the sun accurately using only one axis that is tilted, called the polar mount. This is done by inclining the axis in an angle parallel to the earth's axis, i.e. corresponding to the altitude angle of the local area, α_{loc} and facing south. This mode of tracking is also referred to as polar tracking east-west.

2.4 Concentration ratio

The concentration ratio is defined as the average energy on the receiver to that on the aperture.

$$C = \frac{A_c}{A_a} \tag{2.1}$$

Where A_c is collector aperture area, and A_a is the area of the absorber. (John A. Duffie 2006)

2.5 Parabolic dish reflector

A parabolic dish reflector (PDR) is one method for collecting energy from the sun. It has a point-focus, and must therefore track the sun fully with a two-axis tracking mechanism (or a polar mount tracking). A receiver is placed in the focal point. A parabolic dish reflector is only able to collect the direct solar radiation.

A parabolic curve with a vertical axis (principal axis) going through the focal point can be described by the equation (Blackwell and Thornton):

$$x^2 = 4fy \tag{2.2}$$

Where x is the distance from the vertical axis, y the height of a point on the parabola, and f is the focal length from the base of the parabola to the focal point. The point at which the parabola intersects with the principal axis is termed vertex.

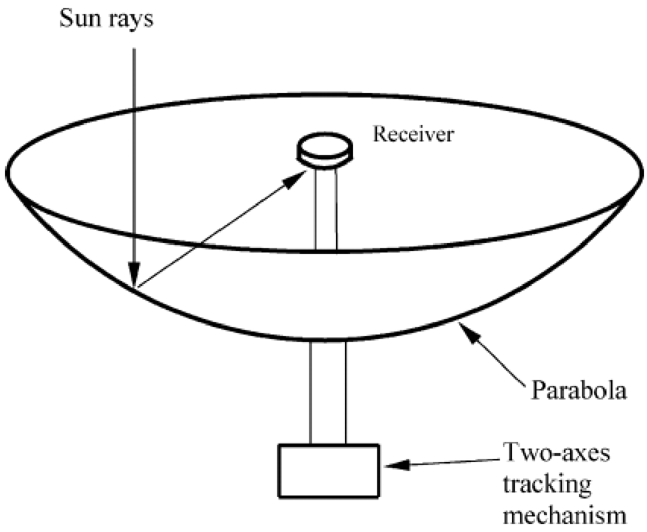

Figure 2.3 Illustation of a parabolic dish reflector for solar collection.

2.6 Double reflecting collector

A double reflector system collects the rays parallel to the principal axis of a primary parabolic dish reflector and focuses them at one focus of an ellipsoidal reflector (a Gregorian system) as shown in Figure 2.4 a), or hyperboloidal reflector (Cassegrainian system) and into a receiver as shown in Figure 2.4 b) (Kaykaty 1966).

Traditionally, concentrating solar collectors are used for power production, by converting heat to electrical power. To avoid thermal and pressure losses, the power conversion has to be close to the point of heat collection. One of the advantages with a double reflector system would be that the obstruction losses due to the rather bulky conversion system, is diminished. This does however depend on how small the secondary reflector can be made referring to the fact that it will be significantly heated by the concentrated solar light to be reflected. The main drawback is a loss of collection efficiency due to two reflections, and the increased accuracy this demands of the tracking system.

Employing the double reflector concept as a solar oven has the advantage of being able to heat a thermal storage by direct illumination from the top. If the heat storage is placed at the base of the primary reflector, and the tracking axes goes through the point of the storage, the focal point will be fixed. These factors enables the use of PCM as a heat storage medium

Keeping the receiver as small as possible will minimise the radiation losses from the storage, and keeping the secondary reflector small will minimise the obstruction loss it poses for the primary reflector.

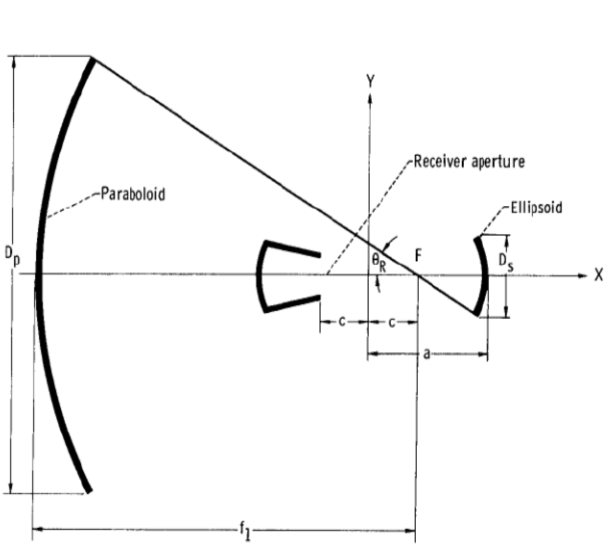

b) Ellipsodial

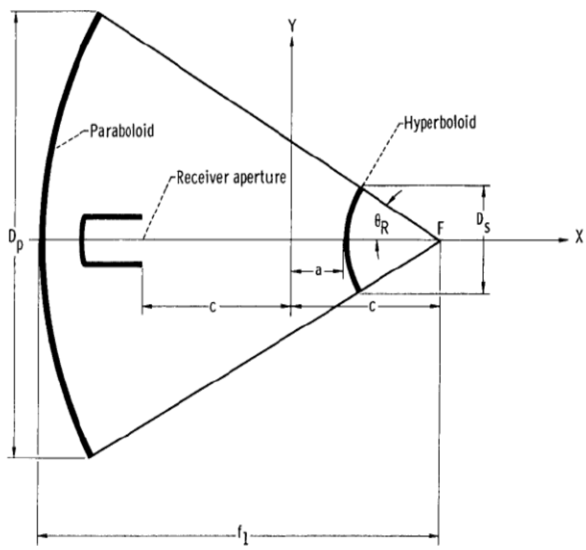

b) Hyperbolodial

Figure 2.4 Schematic diagrams of double reflector solar collection systems.

2.7 Charging of a PCM heat storage

It is important to ventilate a heat storage containing solar salt. The salt is reactive to water, and condensation should not take place inside the heat storage. When the salt is heated, it will start expanding as it starts melting. The solar salt is for that reason usually filled up to 90% of the storage's volume. This is a challenge when the heating is done from the top.

3 System description

In this chapter, the system description of the experimental set-up of the double reflector system will be presented, followed by the technical data of the different components used. The elements of the system are then described more in detail.

3.1 The experimental system

The experimental system's main components are two concentrating parabolic reflectors, a large primary reflector and a small secondary reflector. It has a two axis tracking system running on electric motors, and a heat storage filled with a solar salt mixture. The tracking is controlled by a control box with four sensors mounted in the same plane as the rim of the primary reflector. See Figure 3.1. The concept is simple enough: Focusing the rays of the primary reflector via the secondary reflector down to the heat storage through a hole at the base of the primary reflector.

Figure 3.1 Tracking axes (left), double reflector system (centre), and sensor box (right) mounted at the rim of the primary reflector.

Before any testing could be conducted, the system was completed by adding new motors and a new sensor to complete the two-axis tracking, and by ordering, and lining a secondary reflector with a self-adhesive reflective film. The system was also improved by designing and constructing a new flexible mounting system for the secondary reflector, and the insulation thickness of the existing heat storage was increased from the existing 1 cm to 5 cm. Discoveries also led to the replacement of the reflective material of the primary reflector from reflective film to reflective aluminium tiles for a better performance.

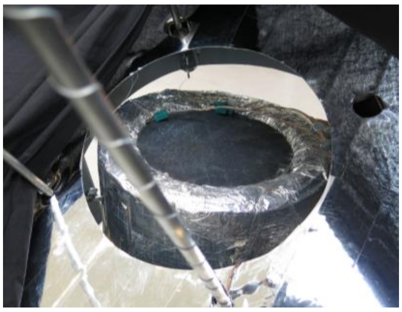

Figure 3.2 The thermal storage seen from above.

The secondary reflector was chosen to be a parabolic dish instead of an ellipsoid or a hyperboloid due to practical reasons. A parabolic dish is easier and cheaper to get a hold of, and there are more options for choosing the shape of a parabolic dish than for example an ellipsoid in general. An ellipsoidal dish would have to have had just the right diameter and focal lengths to be able to hit the absorber, while a parabolic dish only needs a certain ratio between diameter and focal length. The secondary reflector is supported by 3 or 4 legs, and the height above the base of the primary reflector is adjusted on each leg.

The system has a thermal storage placed below a hole at the base of the primary reflector, as seen in Figure 3.2. The storage is a cylindrical container filled with a PCM.

For laser characterization, a CNC milling machine is used to traverse a self-adjusting laser, pointing vertically down, in a grid over the primary reflector. The absorber plate is a circular plate of acrylic glass, with a white protective covering on one side. The camera used is the Canon G15 Powershot.

3.1.1 Technical data

These are the technical data of the components of the double reflector system:

Primary reflector	
Diameter, D_P	2 m
Measured focal length	≈ 665 mm
Calculated focal length, FL_P	≈ 662 mm
Measured height H_P	≈ 377 mm

MIRO-SUN® weatherproof. Reflective aluminium plate cut in tiles	
Reflective	90 %
Thickness	0.5 mm
Width	50 mm
Length	260−275 mm
Material	Pure hard aluminium

Secondary reflector clad with reflective film	
Diameter, D_S	12 in ≈ 304.8 mm
Focal length, FL_S	3 in ≈ 67.2 mm
Hight, H_S	3 in ≈ 67.2 mm

Kindman Reflective film w/self-adhesive model nr K−MF98	
Reflective	98 %
Thickness	0.05 mm
Width	0−50 cm
Length	Any
Base material	PET
Reflective material	Aluminium
Operation temp., wide	−30 °C − +70 °C
Max. continuous use temp	120 °C

Dot Line Laser 1002 HPV from Limit, with magnetic damping compensator:

Watt	10 mW
Wavelength	635 nm
Class	2M
Accuracy dots	± 4 mm/10 m
Self levelling range	± 4°
Operation time	7 hours
Weight	500 g

3.1.2 Primary reflector

The theoretical focal length of the primary reflector is calculated by Equation (2.2) from measurements of the height and the diameter. Since there is a hole at the base of the parabola, some iterations was done to assure a good approximation of the actual height. The holes' diameter is measured to be 290 mm. The position of the hole is assumed to be such that the centre is the principal axis of the primary reflector (the line from the vertex to the focal point). The height from the rim of the hole to a beam lying across the principal axis of the reflector was measured to be 370 mm. The same beam was used to measure the diameter of the primary reflector equal to D_P = 2000 mm.

The focal length is calculated with in an iterative process until the total height is equal to a calculated height from the base to the place of measurement (at the radius of the hole; 145 mm) plus the measured height (370mm). by keeping the diameter constant, and varying the focal length. The result is a focal length of FL_P = 662 mm, and a total height of H_P = 378 mm.

The rim angle of the primary reflector with these dimensions is the angle at which a ray is reflected at the outer rim of the dish, as illustrated in Figure 3.3. It is calculated by trigonometry to θ_R = 74.1°.

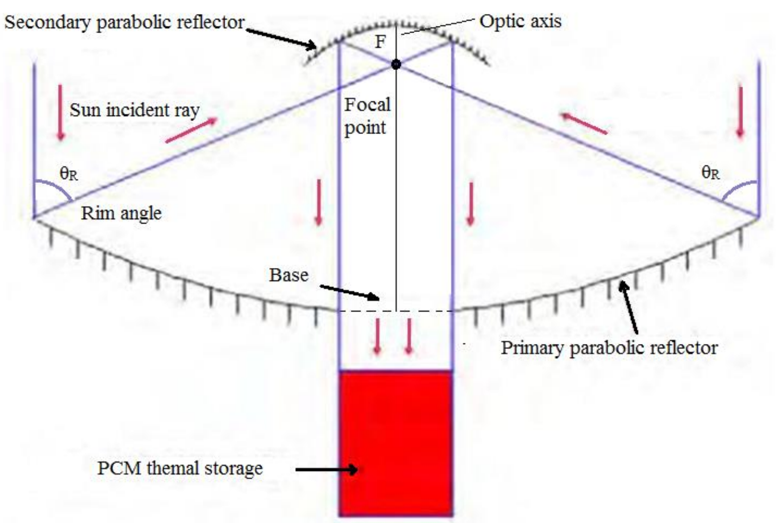

Figure 3.3. Illustration of a double reflector with two parabolic reflectors with coinciding focal points. Illustation credit to (Woh 2011)

3.1.3 Secondary reflector

To establish the theoretical height of the secondary reflector above the base of the primary reflector, the height above the vertex of the surface of the primary reflector at the location of the legs has to be calculated. The 4 legs are situated at distances of 365 and 375 mm apart, measured across the principal axis at the centre of each leg. They are assumed to be situated at an equal distance to the centre of the reflector, and directly opposite of each other. The height is calculated by Equation (2.2) to be an average of 13.3 mm for all 4 legs.

The two reflectors are positioned opposite of each other in a concentric manner, with the principal axis of the paraboloids (the line going through the centres of the reflectors) as the optic axis. When positioned such that the foci coincide, and if the reflecting surfaces and the reflection were to be perfect, the result would be a concentrated beam of parallel rays, as illustrated in Figure 3.3.

If there is a separation of the location of the two foci, the resulting beam of light will be slightly focusing or diverging. The focusing effect appears when the secondary reflector is lifted (hereby referred to as a positive separation distance). The aim is to find the position of the secondary reflector that gives the best focusing effect of the system.

From Equation (2.2) in Chapter 2.5, the relation between the dimensions of a parabolic dish is:

$$R^2 = 4 * FL * H \tag{3.1}$$

Where R is the radius, FL the focal length, and H the height of the parabolic dish. The geometrical features of a parabolic dish are thus described by these three parameters.

When choosing a secondary reflector, a ratio of focal length over diameter was used as a measure of the depth/shallowness of the dish. The wanted diameter was known as the same diameter of the hole in the base of the primary reflector, approximately equal to 30 cm. This size is chosen to utilize the same mounting system as before, and to get as little shading of the primary reflector as possible. The ratio for the primary reflector was calculated to be:

$$\frac{FL_p}{D_P} = \frac{0.662\ m}{2\ m} = 0.331 \tag{3.2}$$

Should a geometrically similar secondary parabola be chosen with the diameter of 30 cm, the focal length would be equal to:

$$0.3\ m * 0.331 = \ 0.10\ m$$

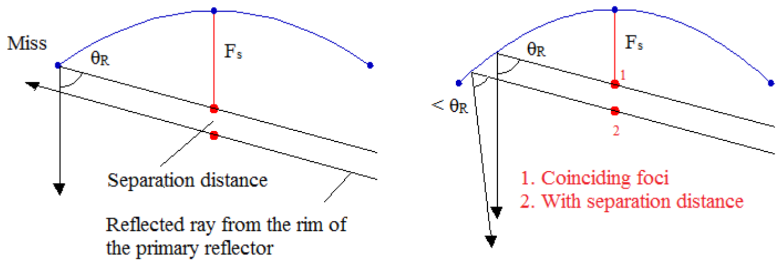

Figure 3.4. Selection of secondary reflector. The parabola to the right has a deeper parabolic shape

A secondary reflector with these characteristics would fit perfectly for the case of coinciding focal points. However, when lifted to a positive separation distance between the foci, the shape cannot be geometrically similar. This would result in rays missing the secondary reflector along the rim. This is illustrated in Figure 3.4, which shows the ray from the outmost point of the primary reflector hitting the secondary reflector with, and without a separation distance between the foci. Evidently, the secondary reflector has to have a deeper parabolic shape. For the same diameter, the focal point should be located closer to the base of the secondary parabola, and the ratio should be smaller than 0.337.

A secondary parabolic dish is selected with the dimensions: D_S = 12 in = 304.8mm and FL_S = 3 in = 67.2 mm. The new secondary reflector then has a ratio of focal length over diameter of:

$$\frac{3\ "}{12\ "} = 0.25$$

By Equation (3.3), it is shown that the height of the selected secondary reflector is equal to its' focal length:

$$R_s{}^2 = 4 * FL_s * H_s \rightarrow H_s = \frac{R_s^2}{4FL_s} = \frac{(6")^2}{(4 * 3")} = 3" \qquad (3.3)$$

Maximum separation distance can be calculated using the rim angle of the primary reflector, θ_{R},. and the radius of the secondary reflector. By trigonometry, the maximum separation distance for the double reflector can be 42 mm, before rays are lost along the rim in the ideal case.

3.1.4 Heat storage

Charging the heat storage will be done by direct illumination on the top plate from the double reflector. The heat from the top plate is conducted to the solar salt via fins welded onto the top plate.

The thermal heat storage used in experiments is from a previous Ph.D thesis, "Experimental and numerical investigations of a small scale double-reflector concentrating solar system with latent heat storage" (Woh 2011). $NaNO_3$-KNO_3 binary mixture was in this project selected as the latent heat storage medium with a suitable melting temperature around 220 °C. The mixture consists of 60:40 % mixture of $NaNO_3$ and KNO_3 respectively. The solar salt was mixed in a stainless steel container, and the salt has a determined melting point of 217.04 ± 0.19 K and phase transition in solid state observed at a temperature of 106.5 ± 0.54 K. Measurement points are located 15, 10 and 5 cm from the bottom of the heat storage, facing the wall.

A solar salt container must be ventilated to avoid a pressure build up as the salt is expanding upon melting. This makes it difficult to allow the top storage to be tilted along with the tracking of the sun. The container should be steadily placed in an upright position, which gives a horizontal top plate at a fixed position. The top plate will be illuminated at an angle similar to the solar altitude angle, changing during the day, and depending on the altitude angle of the location and seasonal declination of the sun. For this reason, it is important to ensure a small focal point of the system, to be able to hit the top plate of the storage, even at low solar altitudes occurring in the morning and evening.

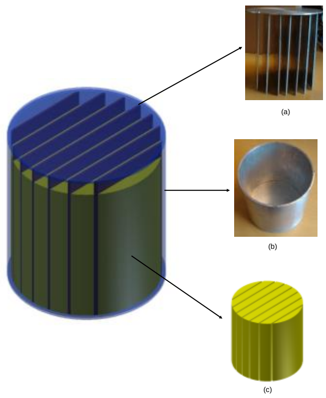

Figure 3.5 Illustration of heat storage. (Woh 2011)

3.1.5 Tracking system

The tracking system for the double reflector is the so-called altazimut mount, including a vertical and horizontal tracking axis. The vertical tracking axis is situated in the centre under the double reflector system, and the horizontal tracking axis is situated across the bearing ring of the primary and secondary reflectors. The horizontal tracking axis' placement is the key to be able to keep the focal point of the system, fixed while charging the heat storage and tracking the sun. However, this comes with the cost of having to balance the system with counter weights to be able to operate it with small electric motors. The vertical and horizontal tracking axes with chain and electrical motors and gears are shown in Figure 3.6

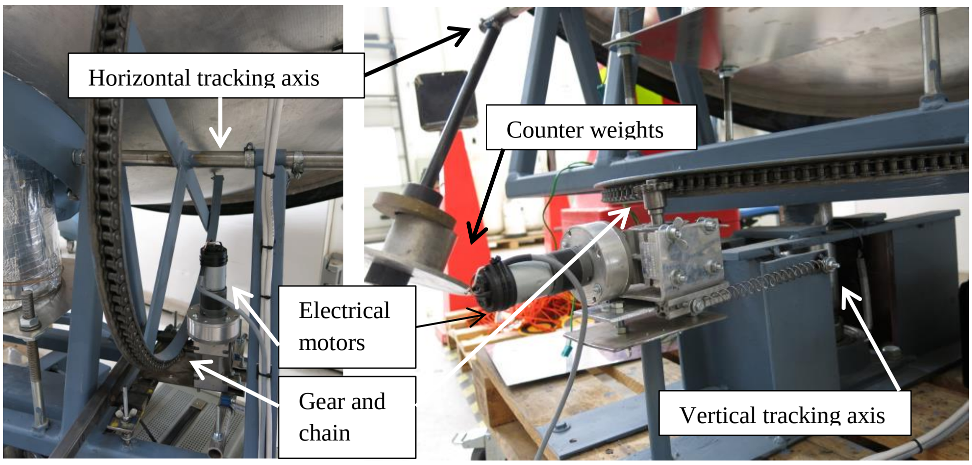

Figure 3.6 Horizontal tracking axis (left) and vertical tracking axis and counter weight (right).

3.1.6 Logging temperatures

For tests conducted in the sun, the temperatures inside the heat storage are measured at three different places using thermocouples. A thermocouple was also mounted on the surface of reflective film of the secondary reflector to monitor potential overheating of the film. A thermocouple is a sensor for measuring temperature, and it does so by measuring the voltage produced from heating or cooling a junction between two different metals (OMEGA_Engineering).

The voltage signal from the thermocouple is first transformed into a digital signal by a logging box, before it is recorded in a Labview program on a computer connected to the logging box. The Labview program used was written by the former PhD student Maxime Mussard, who did his doctoral thesis on a solar trough concentrator at NTNU.

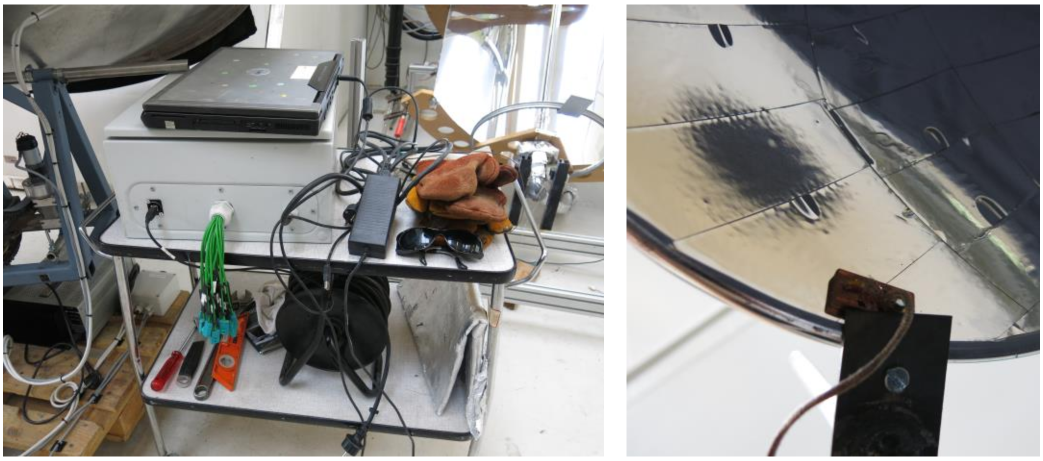

Figure 3.7 Test equipment (left) and thermocouple placement on the secondary reflector (right)

4 Tests and experimentation

In this chapter the experimental setup and methodology will be described. Two main types of experiments were conducted, namely outdoor experiments with collection of solar energy, and indoor laser characterization experiments. The outdoor experiments include tests with the heat storage and tests with a thin absorber plate placed at the focal point.

4.1 Thermal test with heat storage

The aim for the tests conducted with the thermal storage was to be able to charge the heat storage and determine the efficiency of the heat charging of the storage in the double reflective system. Two tests were executed in the sun, one with half the primary reflector revealed, and one with the full system uncovered. A risk assessment report was written before experiments could start (a simplified version is found in Appendix A).

4.1.1 Test procedure

Before the test started, the control box of the tracking system was calibrated to be situated parallel to the plane of the rim of the primary reflector. This was done by levelling the primary reflector utilizing a beam lying across the principle axis with a leveller in the middle of the beam, both in the direction of the horizontal tracking axis, and perpendicular to it. A leveller was then used to adjust the positioning of the control box.

The storage was positioned in an appropriate height such that it would be able to receive as much of the concentrated sunbeams as possible, with the top plate at the level of the base of the primary reflector. Before starting the test, the primary and secondary reflectors were cleaned with compressed air and ethanol, and the primary reflector was covered with a black fabric cover as seen in Figure 4.1.

Figure 4.1 The double reflector covered with a black fabric cover.

After bringing the reflector out in the sun, the tracking system was plugged, and the thermo couples connected to the logging box and the computer for measurements. An infrared camera was set-up to record temperatures on the top surface of the storage. The system was tracked with the cover still on until it was facing the sun. Even with the black cover, it was possible to see where the focal point of the system would be. The calibration procedure did not seem to have worked like it should, and the tracking system had to be adjusted until the focal point was hitting the thermal storage. By lifting some of the fabric away, the focal point was visualized, and the secondary reflectors height above the primary reflector was adjusted in steps.

When the desired focusing of the system was made, the test could start, and the cover was taken off.

The results from these tests suggested that something was not working well enough. The adjustment of the secondary reflector and the primary reflector was done with the greatest effort, but the temperatures in the storage did not show any evidence of a good focus. Besides the adjustment of the system, the reason could be the surface roughness of the primary reflector. The roughness is due to the way the parabolic dish was produced, which has left furrows across the radial direction of the surface. This combined with a thin layer (approx. 0.05 mm) of reflective film with overlaps makes the reflection uneven, and it was hard to get a good mirrored image from the reflective film. Another thing that was a disadvantage with the reflective film was that it was easily scratched and therefore very difficult to clean, since the dust would scratch the surface and result in a downgrading of the overall reflectivity.

The conclusion was that the reflective film of the primary reflector had to be replaced. The new reflective material to be put was a reflective aluminium plate of the type MIRO-SUN® weatherproof, with reflectivity of 90 %.

4.1.2 Replacing the reflective film

The solution for how to place tiles on a parabolic dish is not given, and the method used was tested with cardboard tiles before the reflective film was taken off, as shown in Figure 4.2. The adjustment for each tile is done by cutting along the dashed line as shown in the circle in the middle image. After the film was taken off, the primary reflector was cleaned from all glue residues. The parabolic dish was first divided in four equal sections by using two crossing aluflex beams to find the middle and four reference points at the rim. A thin aluminium strip was cut straight and was used as a ruler, and later as a guide when laying the tiles.

Figure 4.2 Test of tiling method with cardboard. Right: Paper cutter used for aluminium tiles.

The tiles were rubbed and cleaned with ethanol before gluing them on with superglue of the type LocTite 420. An instant adhesive is a quick way of permanently gluing the tiles on, which was crucial for the time frame necessary to glue small tiles on a large surface. Also, as a result of this type of glue, the possibility to remove the reflective tiles and further improve the surface is still an option for later experiments.

The tiles are laid parallel to the vertical line from the centre and in a row out to the sides as shown in the left of Figure 4.2. The first row has to follow the horizontal line dividing the quadrants, and create a new straight line following the parabolic shape under the row. The lower edge of the tiles should therefore always be cut at 90°. The tiles are angled more and more to the left (when working on the lower left quadrant) as the edge of the dish is reached, so the top side of the tiles is adjusted manually with a paper cutter, as shown by the dashed line in the circle in the image to the right. To adjust the tiles correctly, they are first placed over the horizontal line, and the cut-off line is marked. For extra precision, a sharp knife was used to cut smaller curves if needed. When placing the tiles, emphasis is put on getting as little space between tiles as possible and putting pressure on the entire tile so that it follows the shape of the reflector.

The disadvantage of this tiling method is the space created between the tiles on the long side because of the curvature of the dish. The advantage is the possibility to easily adjust each tile to fit in a way that covers the whole dish in a symmetrical manner, and that it does not require any sophisticated shapes or time consuming adjustment for each tile. A length of 275 mm was chosen for the aluminium tiles to make four rows of equal length at the starting point. The tiles were all cut with the same width, and to minimize losses due to increased cut-off sizes, the length was cut in batches of 275 mm to 260 mm.

The result is visible in Figure 4.3. One thing that was discovered after tiling was that the roughness of the furrows was visible also across the 0.5 mm thick aluminium tiles. A way this could have been avoided would have been to first rub down the furrows before starting the tiling.

Figure 4.3 Left: The primary reflector with reflective aluminum tiles. Right: The edge tiles with plastic covering during tiling.

4.2 Thermal test with thin absorber plate

In late fall experiments, it became increasingly difficult to place the thermal storage under the double reflector in a manner that would allow the focal point to hit the top plate. This was due to low sun and physical restrictions of the rig. As seen in Figure 4.4, the bearing ring at the base of the primary reflector blocks the storage from having the right position when the solar altitude angle is small, and the tilt angle for tracking becomes large. Therefore it was decided to continue experiments with the objective of getting a visualization of the focal point of the double reflector to prove the systems' ability to collect energy. This would then be supported by conducting additional tests with a laser to look at the optical characterization of the system, and its focusing ability.

Figure 4.4 The bearing ring of the primary reflector is blocking the storage's position.

For the remaining tests conducted outside, a thin plate of carbon steel of thickness 1 mm was cut to fit as the absorber plate, and placed as close to the base of the primary reflector as possible. An infrared camera of the type FLIR was used to track the temperatures, and to get a visualisation of the focal point of the system. In the last two tests conducted, a thermocouple was attached to the absorber plate at the place that was predicted to be the location of the focal point. However, changing the order of the secondary reflectors' legs made the focal point shift, so that the temperature was measured outside the focal point on the absorber plate, approximately 9.5 cm away from the centre of the focal point.

Similar techniques were used to find the focal point as for the heat storage tests. Figure 4.5 shows images of the test. To the left, the primary dish is partly uncovered, showing a focal point low on the absorber plate. In the image in the middle, the heating of the plate is visible due to oxidation of the steel. The rightmost image shows the front of the double reflector during a test.

Figure 4.5 Images from testing in the sun with a thin steel plate.

4.2.1 Tempering colours of steel

For understanding what has been going on in the steel plate, this section will describe tempering colours of steel.

Thermal treatment of steel can greatly increase the number of properties that can be obtained. When heated to certain “critical temperatures”, the iron changes from one type of crystal to another. The critical temperature for steel range between 700 °C and 870 °C (Oberg, Jones et al.). Steel above this range but below melting point has a crystalline structure known as austenite.

A heat treatment referred to as tempering is performed after hardening of iron-based alloys to reduce some of the excess hardness. The process is to heat the metal to a much lower temperature than was used in the hardening process. When heated in an oxidising atmosphere (such as air), a film of oxide forms on the surface of the metal, and it changes colour as the temperature increases. The colour displayed after a certain temperature is however affected by the composition of the metal, but the colouring chart can serve as a rough indication of the temperatures that has been reached in the absorber plate.

The manifestation of these oxides serves as a proof of the focusing power of the double reflector, and they give a physical picture of the temperatures occurring in the on the absorber plate of the double reflector. In Table 4.A, different colours linked to specific temperatures reached in plain steel are listed.

Table 4.A. Table of tempering colours of plain steel (Oberg, Jones et al.).

Degrees			Degrees		
Fahrenheit	Centigrade	Color of Steel	Fahrenheit	Centigrade	Color of Steel
430	221.1	Very pale yellow	510	265.6	Spotted red-brown
440	226.7	Light yellow	520	271.1	Brown-purple
450	232.2	Pale straw-yellow	530	276.7	Light purple
460	237.8	Straw-yellow	540	282.2	Full purple
470	243.3	Deep straw-yellow	550	287.8	Dark purple
480	248.9	Dark yellow	560	293.3	Full blue
490	254.4	Yellow-brown	570	298.9	Dark blue
500	260.0	Brown-yellow	640	337.8	Light blue

4.3 Laser characterization

For the laser experiments, the aim is to determine the real focal point of the primary reflector, the optimal placement of the secondary reflector and to develop a procedure for obtaining an intensity plot of the real focal point of the double reflector. For determining the focal length, a manual registration of laser hits is done, utilizing a Computer Numerical Control machine (CNC-machine) to traverse the laser. For determining the optimal placement of the secondary reflector, and creating the intensity plot, a procedure for automatically photographing the reflection of a laser beam using a digital camera was developed. Post processing of the images acquired was written in the Matlab programming software, as described in Chapter 4.4.

4.3.1 Experimental focal length of primary reflector

In this section, the method for determining the focal length of the primary reflector is described. The experiments were conducted using a CNC-machine, a laser diode and graph paper. The test was conducted both for the reflective film and the reflective aluminium tiles, with a laser sight and a self-adjusting laser used respectively. The procedure will be described for the laser sight first, and then the self-adjusting laser. The focal length (FL_P) was determined by the Red Laser Diode Technique (Mlatho, McPherson et al. 2010). This method was chosen due to the simplicity and low cost, and because it is a good alternative for optical characterization of a reflecting dish while solar testing outside is no longer an option.

Reflective film tests

The technique consists of a laser diode emitting a narrow beam, mounted to be parallel with the optic axis and incident to the reflective surface of the primary reflector. The laser diode emits red light in the wavelength of 630−650 nm. The reflector is placed under a CNC machine, allowing for the control of the position of the laser diode in an x-y plane above the aperture of the dish. The test setup for the reflective film is shown in Figure 4.7. A horizontal plate made of acrylic glass with an x-y grid was suspended perpendicularly about the principal axis of the dish at different heights from the base of the primary reflector. The absorber plates position was controlled by the laser placed at the centre. The coordinates of the laser reflection on the absorber plate is recorded for each point in the grid.

Figure 4.6 Left: Laser sight laser, Middle and right: Calibration of laser diode.

The laser diode of the laser sight is adjustable in 2 directions. It was calibrated with a distance of about 2.5 m by parallel mounting on to the end of a straight steel pipe, marking the distance from the pipe to the laser accurately, and adjusting the laser to hit the same spot at the opposite end of the pipe. The pipe was mounted vertically, with the laser pointing down towards a mark on the floor, as seen in the two rightmost images in Figure 4.6. The laser was then mounted vertically on the CNC-machine as shown in the leftmost image. The reflector and the laser were levelled horizontally and vertically by means of a leveller.

A table was made of 40x40 mm aluflex beams to support the double reflector, give room for a camera to take pictures of the absorber plate from underneath, and to fit the primary reflector under the CNC-machine. Because of the total height of the primary reflector with the legs for

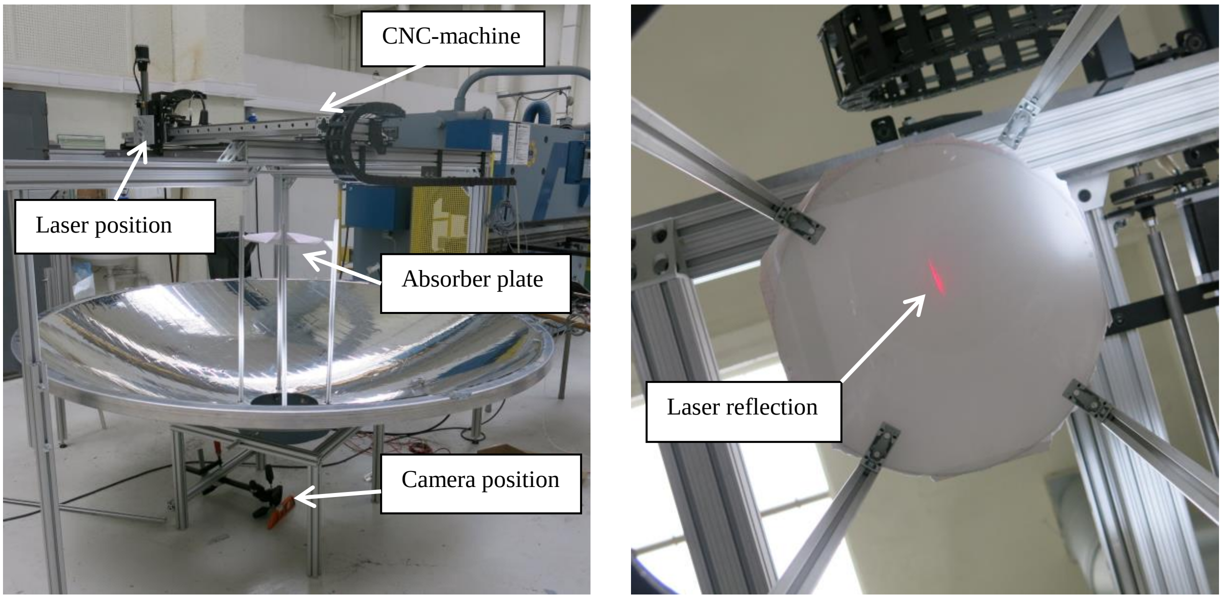

Figure 4.7 Experimental setup with primary reflector placed under CNC-machine.

holding the absorber plate and the height of the table, the legs of the CNC-machine needed to be lifted to a total of 1.40 m. These aspects are also visible in the left image in Figure 4.7.

The CNC machine was interlinked with Torchmate CNC Cutting System software, running on G-codes. A program using G-codes was to be written to automate the test procedure in moving the laser from point to point in a specified uniform grid, and automatically taking pictures of the reflected laser on the absorber plate with a digital camera connected to the CNC-machine. Unfortunately, the camera control was not possible to accomplish due to problems with the software, leading to the usage of manual registration on a grid paper instead. The positions of the laser reflections were registered with the origin at the principal axis of the primary reflector. Another problem with this setup was the increased height of the CNC machine, leading to undesired oscillations of the structure holding the CNC-machine.

The reflective film had burn marks from previous tests and it was dusty, and needed to be repaired and cleaned before a test could start. A risk assessment was submitted before tests started and a simplified version is to be found in Appendix B. The film was repaired by cutting out patches of the burnt areas, and replacing them by corresponding patches of new reflective film. To avoid scratching the film while cleaning, compressed air was used to remove dust particles before cleaning with denatured alcohol by utilizing a microfiber cloth. This was found to be the least harmful method for cleaning.

The first thing to do was to calibrate the system to be levelled. This was done by means of a leveller at the rim of the reflector. To get an idea of the whereabouts of the focal point, a sheet of paper was held vertically at the principal axis of the double reflector, and 7−8 equally spaced points along the radial direction of the primary reflector were inspected. Distances of 610 mm, 625 mm, 635 mm, 665 mm and 675 mm were tested with 20 equally spaced points along a radial line of the primary reflector. Due to little knowledge about the CNC-machine, and an unsteady setup, the traversing in the X-direction was frequently stopped, and the reflector was thus only tested in one line along the radial direction. The experiment was carried out by registering the points of the laser reflection on the grid paper at the different heights. The range of the CNC-machine was about 1.2m x 1.2m, so only the line from the edge of the primary reflector to the centre was inspected. The work was done in cooperation with Nabin Kumar Shrestha and Swati Singh during their specialization thesis at the same period.

Reflective tile tests

The Double Reflector system is tested optically by means of a self-adjusting laser diode mounted on the CNC milling machine. In the test, the self-adjusting laser is pointing vertically down onto the primary reflector. The laser is mounted on an arm fixed on the top of the supporting construction of the Z-axis of the CNC milling machine. The arm is long enough to reach over ¼ of the primary reflector. The Red Laser Diode Technique is used also here, but this time the CNC-machine was working as it should.

Due to time constraints, only 32 points were tested in a uniform grid over the reflector. The distance between the points was 150 mm. The heights to be tested were based on the calculated focal length of the primary reflector from Section 3.1.2, of 662 mm. Two heights 5 mm lower and higher were chosen, 657 and 667 mm.

Before the test could start, the reflector was calibrated to be levelled, and the placement of the absorber plate was controlled for each height. The test procedure was the same as for the reflective film, and a graph paper was used also here to record the coordinates of the laser reflection.

4.3.2 Movies

By traversing a the laser at a constant speed over a line in radial direction, it is possible to record and see how the beam is reflected onto the absorber plate, and possibly analyse the amount of time it hits the plate as opposed to not hitting the plate. Such movies were captured for the primary reflector still having the reflective film. For this to work, the traversed laser needs to be in a fixed position pointing vertically down, and the CNC-machine should not oscillate too much.

Recordings were done of 5 different radial lines within the quarter of the parabola accessible under the CNC-machine; Y-direction, X-direction, 45° angle and 45±22,5° angles. The alignment of the strips of reflective film was in this case in Y-direction, and the camera was placed at a fixed location so that it would be at normal XY-orientation with respect to the CNC-machines coordinates. The speed of the traversing was set to 1500 mm/min.

It can be seen that the laser is distorted more and less and sometimes not appearing at all, depending on roughness of the primary reflector and overlap of the reflective film. Whether the whole laser beam is reflected or split in two with only one part appearing is difficult to say. Another challenge is the intensity of the laser dot, and how much of the light sent out that reaches the absorber plate. Since the movies were taken in daylight, the laser is also hard to see, and the light conditions should have been better.

For further development of such a test, it is important to ensure stable light conditions that. A way to analyse it could be to draw a line with varying intensity following the laser movement. Another possibility is to create a composition image of the laser movement with brighter areas for a spot that has been hit multiple times. The movies are provided in the digital attachments to this thesis.

4.3.3 Optimal placement of secondary reflector

The goal of this experiment is to find the optimal placement of the secondary reflector to achieve the best focusing effect on the absorber, and to be able to produce an intensity plot of the laser point registered. A test procedure is developed for the double reflector using a CNC-machine, a self-adjusting laser, a digital camera and Mac3 Mill software for the CNC-machine.

The Double Reflector system is tested optically by means of a self-adjusting laser diode mounted on a CNC milling machine. In the test, the self-adjusting laser is pointing vertically down onto the primary reflector. The ray is reflected onto the secondary reflector, and then reflected again onto a white absorber plate located at the base of the primary reflector. A camera steadily mounted takes a picture of the absorber plate and the laser dot from underneath. A programmed G-code is used by a CNC-milling machine to move the laser in a uniform grid and trigger the camera at each point automatically. The laser is mounted on an arm fixed on the top of the supporting construction of the Z-axis of the CNC milling machine. The setup is the same as for determining the focal length of the primary reflector with the reflective tiles, and the laser can only reach one quadrant of the primary reflector area.

Since the focal point of the double reflector is not in the centre of the absorber plate (experience from outdoor testing), the assumption that it is symmetrical does not yield, and all 4 quadrants of the primary reflector has been tested. For each quadrant tested, the double reflector is levelled and calibrated, and the secondary reflector is kept at a constant position.

The laser simulates a single sunrays' path to the focal point of the double reflector system, much like a ray tracing program. As pointed out by (Mlatho, McPherson et al. 2010), it is important to use a large number of rays spaced close together to obtain information on small variations in the intensity distribution. The reflected ray of the laser diode was observed as a somewhat circular dot, a diffuse shape in different sizes, or not observed at all in which case it was considered a loss.

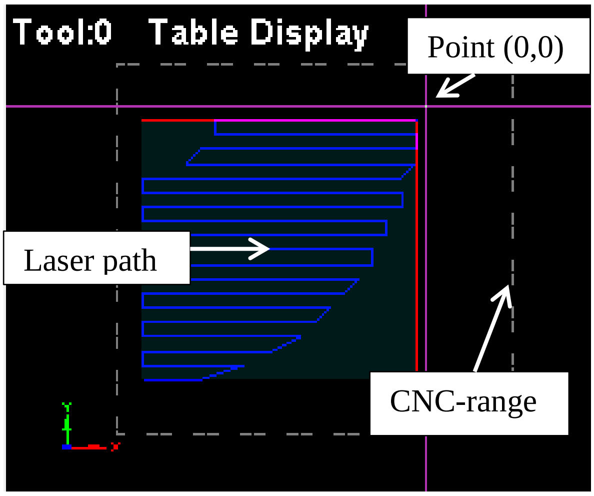

Figure 4.8 Traversing as seen in Mac3 CNC software. The dashed line marks the range for the CNC-machine.

The laser should step through all points over the reflective material in a uniform grid, with a certain step length. The traversing was done in a zigzag pattern, as seen in Figure 4.8, to minimize the traversing distance and therefore the time spent on running each test. To avoid getting data from the same coordinates twice, the first row of the zigzag pattern is skipped for each test quadrant. It is also important to not include areas outside the primary reflector to be able to know that the laser has hit the reflective surface when a loss is registered. A program for generating G-codes has been written in Matlab with inlet variables: step length, outer radius, inner radius, time in seconds required to wait for the laser to stabilize, and federate in mm/min. The Matlab code is presented in Appendix C. The outer radius to be included in the steps of the laser is made a few centimetres shorter than the real radius to assure that the laser will hit the reflective material. The inner radius has been set to 250 mm, which is larger than the secondary reflector, to avoid that the bulky laser crashes into the mounting construction. This means that the area between this limit and the secondary reflector is not included in the tests. Since the secondary reflector has a radius of 152.5 mm, this area is the circular strip area between the inner radius, 250 mm and the reflectors real radius, 152.5 mm (corresponding to an area of about 0.123 m^2).

An array of six lasers is mounted next to the self-adjusting laser. The array make it possible to adjust the double reflector by looking at the way it focuses the light of the six lasers before starting a new test, this is seen in the right image of Figure 4.9. The calibration of the additional lasers is done at a height of 170 cm above the floor, using the self-adjusting laser as a reference, as seen in the left image of Figure 4.9.

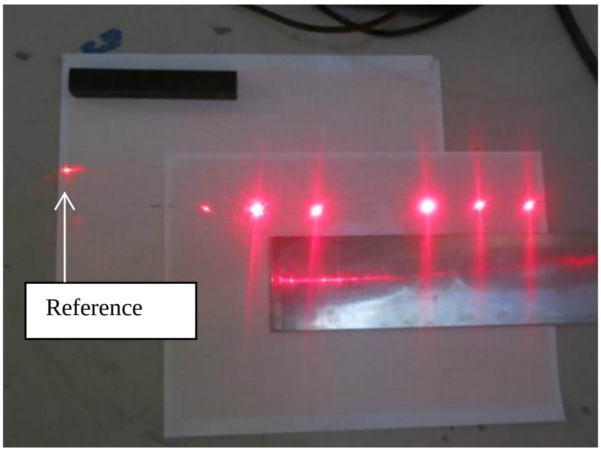

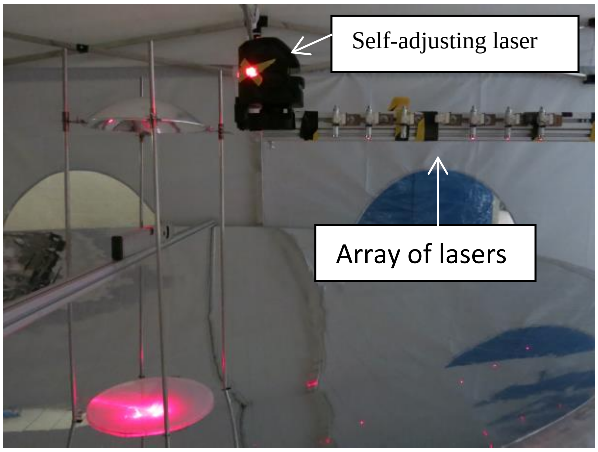

Figure 4.9 Left: Calibration of array of lasers. Right: Array used to adjust the double reflector to the best position for testing.

To be able to calibrate the positioning of the double reflector for testing, 4 reference points were made on the rim of the primary reflector. The rim is 5 cm wide, and the reference points are located in the middle of the rim (2.5 cm in from the edge of the rim). Each reference point is named after the four cardinal directions, North, South, East and West, to keep track of the position of the reflector. The camera is mounted on a plane horizontal surface, with the camera lens positioned as close to the centre of the primary reflector as possible. The camera is oriented with north direction upwards from underneath (i.e. “east” is left and “west” is right in the images), and the camera position is stationary and independent of the area being tested. When calibrating the reference points and the camera position, it was evident that the primary reflector is not perfectly round. Also, the double reflector is not mounted perfectly normal to the vertical tracking axis, nor is it perfectly centred. This means that the reflector and the CNC coordinate system have to be adjusted for every new quadrant when testing.

A row of lasers is placed in parallel with the self-adjusting laser to correctly adjust the system when starting a new test. This is to ensure that the focal point is on the absorber plate. The double reflecting system is first adjusted so that both the reflectors are levelled. The row of lasers is then traversed over the primary reflector to view the focal point. If the focal point is large, the distance from the base of the primary reflector to the rim of the secondary reflector is adjusted. If the focal point is located outside or partly outside the absorber plate, the angle of the primary reflector is adjusted (since the secondary reflector is mounted together with the primary reflector, the angle changes also here). The angle is then measured by a digital leveller.

4.3.4 Test procedure

The procedure followed for each new test is described in this section.

Start-up

1. Plug the tracking system of the double reflector.
2. Calibrate the CNC coordinate system by a start-up procedure involving the “reference all home” function. Activate the “soft-limits” switch.
3. Attach the self-adjusting laser to the overhanging arm of the CNC, and make sure that the laser has enough battery power, is set on self-adjusting mode, and that the arm is steady while traversing.
4. Make sure the camera is fully charged and has sufficient space available on the memory card.
5. Make sure the light conditions for the test is as specified. (Equal to earlier tests).

Calibration procedures

6. Calibrate the array of lasers by means of the self-adjusting laser and a millimetre paper on the floor marked with the measured distance between the lasers, including the self-adjusting laser. The direction of the millimetre paper is lined up with the direction of the CNC coordinate system.
7. Adjust the secondary reflector in the vertical direction. This is the main controllable parameter to be tested. When the secondary reflector is mounted, each leg should be placed as vertically as possible.
8. Position the double reflector so that $1/4^{th}$ of the primary reflector (test area) can be reached by the laser.
9. Calibrate the primary reflector to be levelled in North-South direction (direction of horizontal tracking axis) by using an aluflex beam[1] across the primary reflector and a

[1] Any beam that has a square cross section and is known to be fairly straight will do the job. It is an advantage that the beam is light for practical reasons.

leveller in the middle of the beam. Level the system by placing pieces of metal of known thickness under two of the wheels of the system, depending on the direction of the primary reflector.

10. Level the East-West direction by utilizing a flashlight to control the horizontal tracking axis. This is possible, and a good way to fine tune the system, because the tracking system is controlled by the side sensors for horizontal rotation and the top and bottom sensors for vertical rotation, and the motors are running on a low gear (i.e. the speed of rotation is slow). Since there is some slack in the tracking in the way the gear is mounted, a control leveller should be placed on the rim when removing the beam, to ensure the angle did not change. (Because of local variations along the rim, the two angles will not be the same.)
11. Level the secondary reflector. This is done by utilizing a small leveller and holding it against the underside of the rim. The adjustment is done directly. The position of the secondary reflector is kept the same for each of the other three quadrants to be tested.
12. Calibrate the cardinal directions to match the CNC coordinate system by traversing the self-adjusting laser over the aluflex beam placed besides two opposing reference ("cardinal") points. Start at the edge of the beam close to the secondary reflector, and move back to the reference point. The beam should be placed so that the reference points line up with the edge of the beam. The double reflector is rotated around the vertical tracking axis by utilizing a flashlight on the light sensor until the laser dot hits the reference point. The procedure is repeated until the aluflex beam, and thereby the cardinal points of the primary reflector, lines up with the corresponding axis of the CNC machine.
13. Verify the alignment with the CNC machine by traversing the laser to the other of the two reference points in the test area.
14. Use the array of lasers to verify a good focusing of the system. In case the focus does not hit the absorber plate, the system is adjusted in East-West direction until the focusing seems to hit the absorber plate. The angle around the horizontal tracking axis is measured with a digital leveller and kept the same for each of the other three quadrants to be tested.
15. Set the origin of the CNC to the reference point closest to the edge of the CNC machine.
16. The distance between the reference point and the edge between the rim and the paraboloid, and the margin distance to assure hitting the reflective material has to be accounted for, so the laser is moved to the position X = −(distance rim + margin reflector). This is set as the new origin.
17. To correctly focus the camera, the laser is moved to a position where the reflection on the absorber plate is good. The camera is set to TV, shutter speed 1/20", the display is turned off and the camera is placed in the correct position. Now the wire connecting the camera and the CNC-machine is plugged in, and the camera focuses.
18. The wanted G-codes are loaded into the program. The tool path of the G-codes is studied to avoid any collisions with the secondary reflector.
19. Push "Cycle Start" and confirm that the camera is taking pictures as it should, and that the time for the self-adjusting laser to come to rest is sufficient.

For the 3 next quadrants

20. Turn the system to test a new quadrant of the primary reflector.
21. Repeat steps 3−13.
22. Control the angle between East and West to be identical to the first quadrant.
23. Repeat steps 15−19.

Test parameters

Table 4.B describes the test parameters in each test. The distance is measured from the vertex of the primary reflector to the height of the rim of the secondary reflector along the principle axis of the reflectors. The angle is adjusted around the horizontal tracking axis (North−South), and is positive when looking north. (East is higher than West). Each angle should reflect the best focusing of the height in consideration. The step parameter is the distance between the grid points when traversing the laser with the CNC-machine, and thereby the “resolution” of the result.

Table 4.B Test parameters

Distance [mm]	683	683	688	698	703	708	708
Angle [°] ±0.2	0.9	0.9	1.4	0	1.3	0	1.7
Step [mm]	25	50	50	50	50	50	50

4.4 Image processing in Matlab

Post processing of the images of the laser reflection on the absorber plate is done in Matlab. The purpose of the image processing is to detect and analyse the incident reflection of each position of the laser, and create an intensity plot using the real intensity of the laser dot in the images. The percentage of hits is calculated. In developing the program, it is important to understand how the Matlab scripts interpret the images. A simple approach is stressed for the accomplishment of a complete program.

The test was conducted in a semi-dark room to be able to visualize the white absorber plate while the red laser reflection is captured without over-exposure. Keeping the light conditions at the same level and the camera settings constant for each test was emphasized to produce even images with little intensity variation between different tests. This was to ensure reliable test results from direct intensity analysis of the images.

Figure 4.10 shows a typical reflection captured during a test. Evidently, the laser beam is no longer a narrow dot. This is caused by a non-perfect reflection in the primary and secondary reflector. It is believed that the effect is greatest in the reflection on the secondary reflector, because of bubbles under the reflective film caused by overheating during tests in the sun. The beam is at this point already spread out due to the curved surface of the primary reflector, and this amplifies the result.

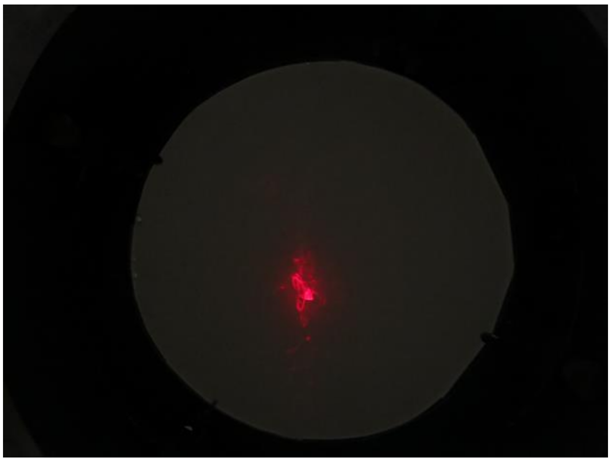

Figure 4.10 Typical image of the absorber plate (grey), showing a red dot laser reflection.

The image is a true-colour 8-bit RGB image in the jpg file format. This means that the picture has 3 different layers of pixel values for red, green and blue colour. The pixel values range from 0 to 255, where the value of 0 for all colour layers gives the colour black to the pixel, and the value of 255 gives white.

As can be seen in the image, the laser dot appears to be brighter than the absorber plate and the surroundings. It is therefore possible to use a simple method involving thresholding to detect the laser dot. Because the camera position was not held perfectly constant for the different quadrants tested however, alignment of the images from the 4 quadrants of one test needed to be done first. The different parts of the image processing were done in different programs:

- Image registration (aligning the images) (Appendix E)
- Laser do detection and extraction of data
- Creating an ordered list of the positions of the laser in the grid of the CNC-machine
- Generating intensity plots from the data collected

4.4.1 Image registration

A slight change in the camera position causes the position of the absorber in the images to deviate for different sets of images. For the purpose of adding all the registered laser dots into a composition of the total intensity pattern, the images should align. In image processing, image registration is the process of aligning images from two or more datasets.

Intensity and feature based registration are the two well-known approaches of performing automatic image registration. Intensity based registration aligns images based on their relative intensity patterns, while feature based registration utilize feature detection, extraction and matching (Sharma and Thé). Both of these methods were investigated, and intensity based registration was selected.

An image of the absorber with no laser reflection is chosen as the reference image. All the images from the remaining 3 quadrants (target images) of a complete test are to be aligned with this reference image. A for loop loads a target image, registers it, and saves it, numbered in the same order starting from one. For each new image to be registered, the optimizer object for optimizing the similarity metric, and the metric object to be optimized is created using the `imregconfig` function. The image is then registered using the `imregister` function with transformation type `'translation'`, see Appendix E for the Matlab code used.

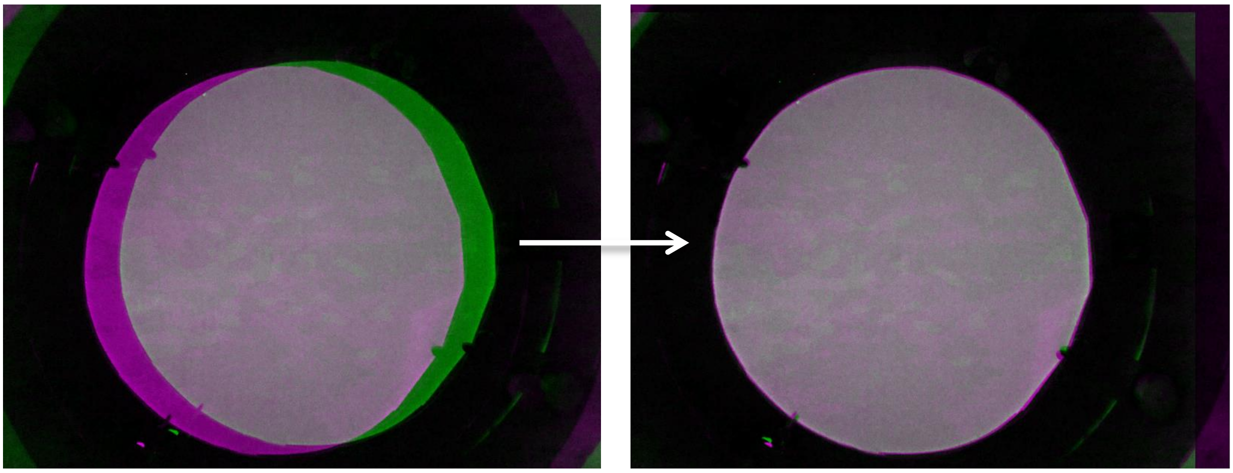

Figure 4.11 Composition images showing the reference image and the target image together before (left) and after (right) default image registration.

Figure 4.11 shows the default registration of two images of different quadrants in a test. The purple and green colour indicates the misalignment, and perfectly aligned images will appear as a greyscale. Because the reference image is slightly brighter than the target image, the composition to the right appears slightly purple in colour. The images are well-aligned, although some misalignment can be observed in two low obstructions in front of the absorber plate, and in the bright spot at the lower left corner. For the purpose of demonstration, two images from early tests that differ quite much are used. The camera has a fixed position and can only be rotated around the mounting screw, which will change the angle of view, giving an explanation of the misaligned details.

4.4.2 Detection by thresholding

A display of the three colour components next to the RGB image is shown in Figure 4.12. The colour of the laser dot is nearly purely red, but with the absence of some green, and some additional blue. Because of this, and the fact that the intensity of the laser dot is significantly brighter from the rest of the image, it is possible to use only the red pixel values to detect the dot. This simplifies the programming. For further image processing, only the greyscale image containing red colour information is considered.

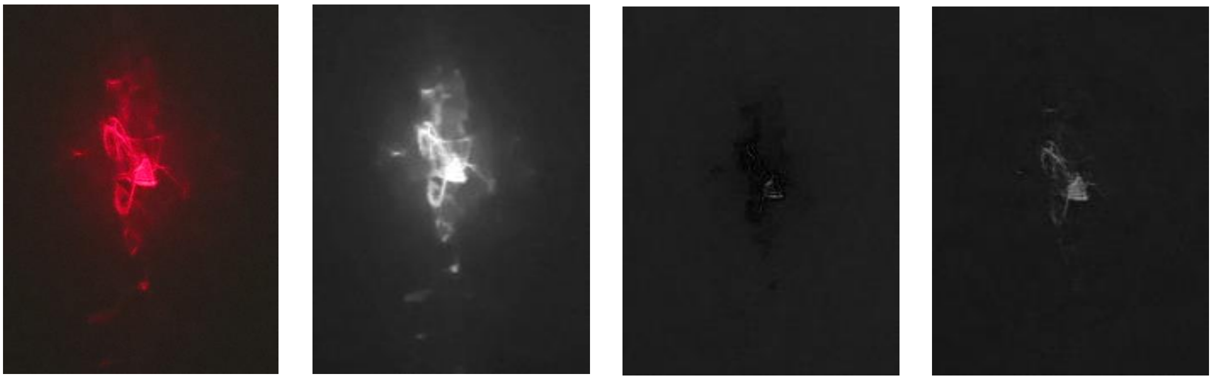

Figure 4.12 From left to right: original image, red, green, and blue colour components of the laser dot.

The light intensity increases slowly towards the centre of the laser dot. Some of the faded light around the laser dot is most likely caused by diffusion of the red light on the white cover on the absorber plate, which means that it is not crucial to manage to collect all of the dim light around the contours of the laser dot.

A threshold value is used to convert the laser dot to a binary image. The value is calculated based on the mean intensity of the absorber plate. The first step to finding the mean intensity is to segment the absorber plate by default thresholding to a binary image. Other objects detected are then removed and the border is cleared using morphological operations, as shown in Figure 4.15 and Figure 4.15. The segmentation is used to extract the mean intensity from the greyscale image. It is assumed that the light condition during the test is constant, so the threshold value for detecting the laser dot is constant for a series of photos. The value is found by multiplying the mean intensity value by a factor of 2.5. This was found to be a suitable factor.

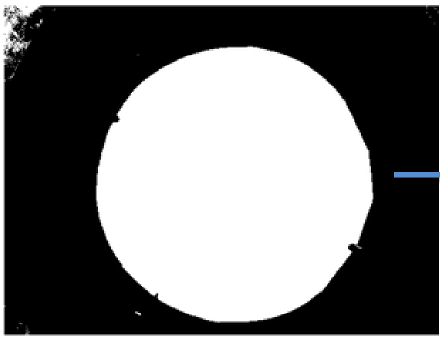

Figure 4.15 Default thresholding of grayscal image

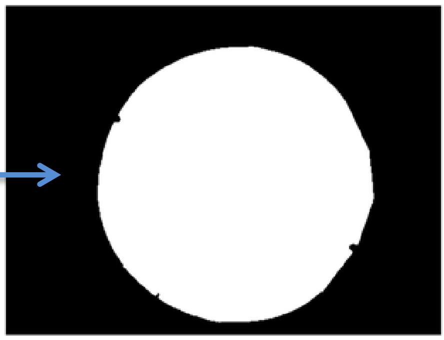

Figure 4.15 After cleanup by morphological operations

Figure 4.15 Left: Original greyscale image. Middle: Segmenting the laser dot by thresholding. Right: Added intensity to segmented laser dot

After detecting the laser dot with the calculated threshold value, the next step is to cancel out any bright spots detected outside of the absorber plate. The same procedure for segmenting the absorber plate as described above is done for every image, and the resulting binary image (as the one seen in Figure 4.15), is multiplied with the binary image of the detected laser dot, removing everything detected outside the absorber plate (not shown). Finally, the binary image is multiplied by the image of the laser dot to remove all other information. The resulting 4 quadrants that have been processed will later be added together in a compilation to show the final result.

The number of images with no detected laser dot is counted. A detected spot that is very small is likely to be outside the absorber plate, or a bright spot on the absorber plate (i.e. not the laser reflection), and a limit of 100 pixels is set for a detected dot to be registered.

The following information is collected for every laser dot detected and recorded in an ordered list: (see detailed code and description in Appendix F)

- Intensity values of the laser dot are added to a composition matrix
- Pixel area detected
- Mean intensity of the laser dot
- Pixel position of the weighted centroid for the laser dot
- Hit result (1 if there is a hit, 0 for a miss)

A way to quantify the uncertainty in the image processing has not been looked into, but is suggested as a topic for further investigation and improvement of the test procedure.

4.4.3 Compilation of results

The compilations of all detected laser dots from the 4 quadrants are put together in a final compilation, and the result is plotted as a 3D surface showing elevated levels corresponding to higher intensity of the focal point. (See appendix H for Matlab code)

5 Modelling and simulation

In this chapter, a simple analysis of the focal point of the double reflector using a Ray Tracer program is looked into. The Ray Tracer program was developed by prof. Ole Jørgen Nydal as a part of the NUFU network project. The analysis will focus on the positioning of the secondary and primary reflector to simulate the laser characterization tests.

5.1 The ray tracer program

The ray tracer program enables ray tracing of parallel rays simulating the sun. The program has built in functions for crating various shapes of reflectors and absorbers, here referred to as elements. A 3D-view of the reflector with zoom function, and a list of elements with their position enable continuous control when tracing rays. The program features are highlighted in Figure 5.1 below.

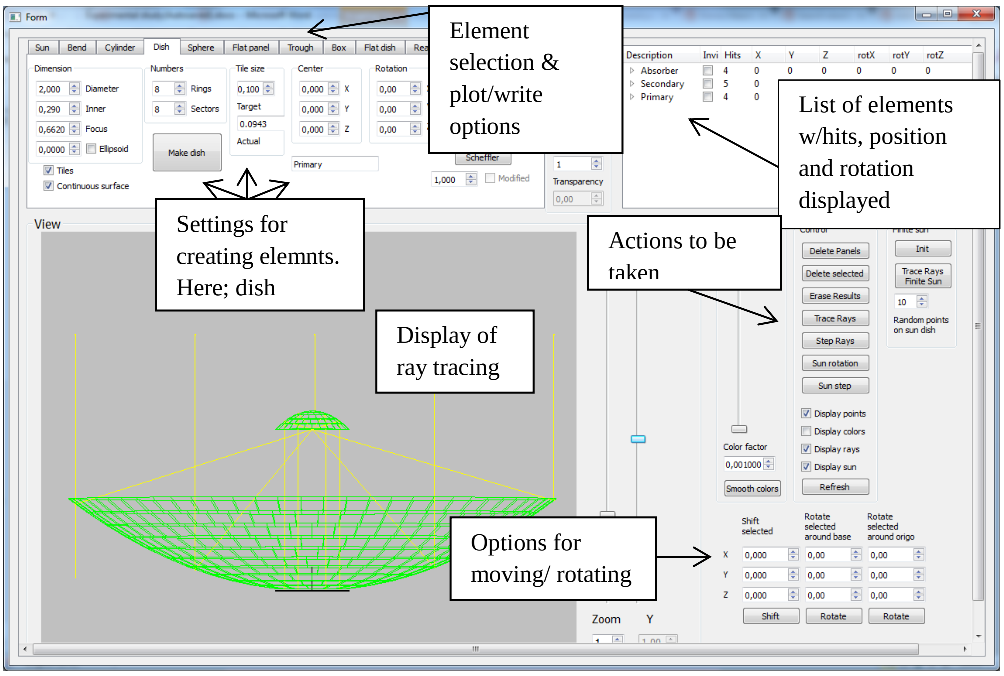

Figure 5.1 Display window of the ray tracer program with key features highlighted.

The two parabolic dishes are constructed in the ray tracer program with theoretical values.

Primary reflector:
Diameter 2 m, focal length 662 mm, inner hole 290 mm

Secondary reflector
Diameter 305 mm, focal length 76 mm

Absorber plate
Flat plate of 300 x 300 mm

5.2 Optimal separation distance

The Ray Tracer is used to investigate the optimal separation distance for the double reflector. The idea was to make intensity plots to look at the intensity variation inside the focal point at the different separation distances, but the process became too time consuming for the program to handle, and only two intensity plots were created with a poor result.

By looking at the absorber plate isolated, it is still possible to find the separation distance giving the smallest focal point. The secondary reflector was moved 1 mm up, and the focal point was looked at. Figure 5.3 shows the case of coinciding foci to the left, and a separation distance of 20 mm to the right.

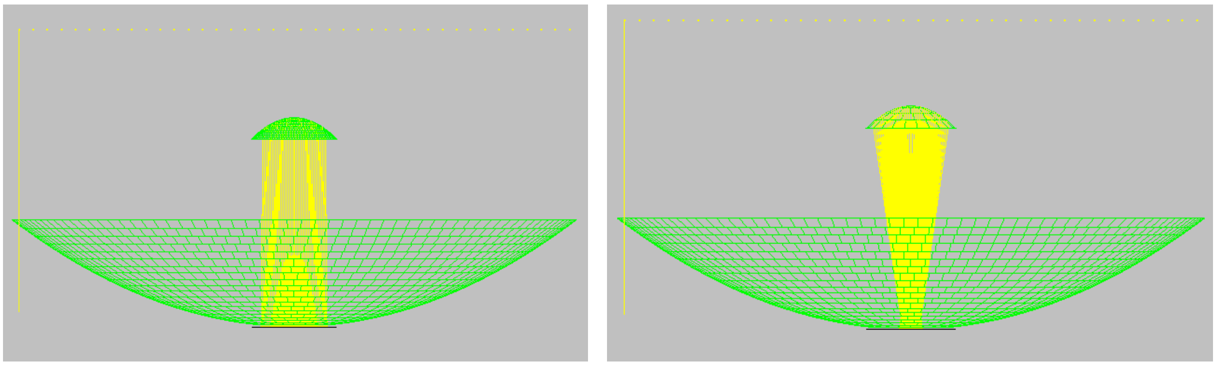

Figure 5.3 Illustration of different separation distances using a ray tracinf program

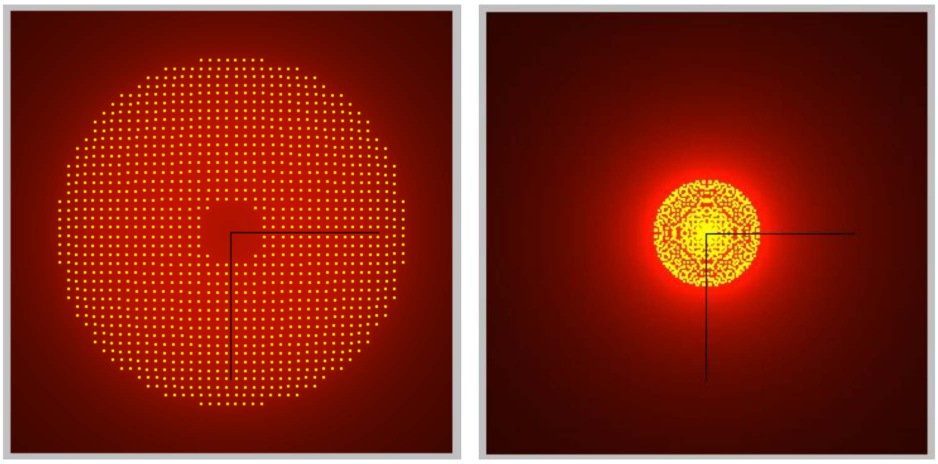

Figure 5.2 Focal point of the double reflector with coinciding foci, and with a separation distance of 2 cm.

5.3 Tracking sensitivity

The tracking sensitivity is looked into by modelling the system in the ray tracer program, and using the built-in function for changing the solar angle, and registering the percentage of hits on an absorber plate of a specific size. The absorber plates tested are a circular with a diameter of 10 cm and 20 cm. The result is shown in Figure 5.4 with varying the sunrays from -1 to 1 degree in a step of 0.1 degrees.

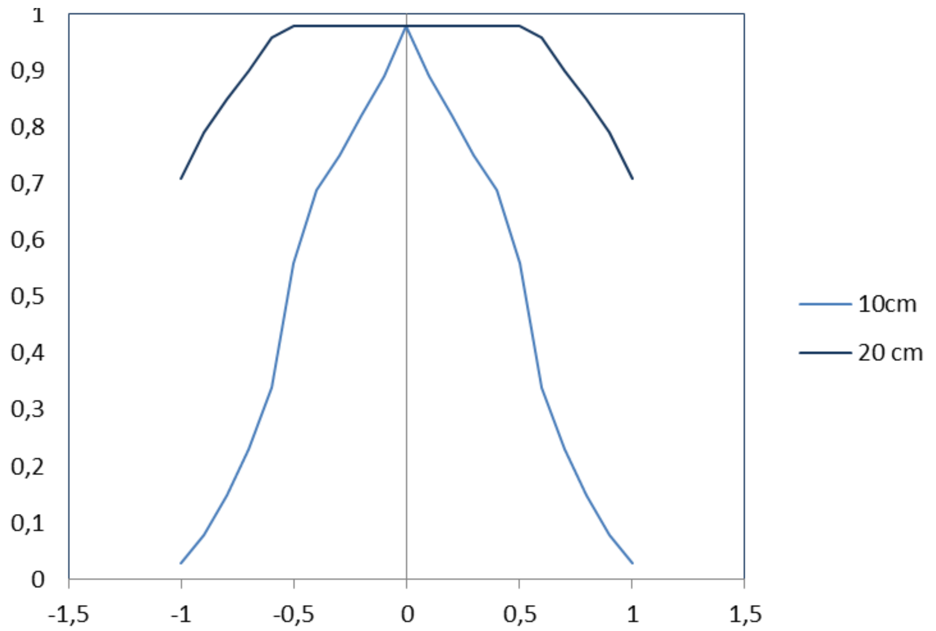

Figure 5.4. Interception ratio for sun rays reaching the absorber dish. X-axis: solar tracking error (degrees). Y-axis interception ratio

The dish of diameter 10 centimetres is sufficiently big to capture all the rays, but the tracking error is large for very small angles. By increasing the diameter of the dish to 20 cm, the tracking error is lower. The reason the intercepted rays never reach 100 %, is believed to be because of the sunrays hitting the secondary reflector above is counted as well.

5.4 Test conditions

It is useful to look at how sensitive the double reflector is to tracking error or displacement of the secondary reflector. From the laser testing, it was discovered that the system was focusing better when it has a small tilt angle, than when it was completely levelled. The tilt angle can be modelled as a tracking error. It is expected that there is some displacement in the horizontal direction of the secondary reflector that is cancelled out by the tilt of the system. This is suggested as a topic of further analysis of the system.

The Ray Tracer program is a useful tool for analysing a solar collector system, and further analysis of tracking error and intensity plots to investigate the size of the focal point when the absorber plate is tilted is suggested as the next step.

6 Results and discussion

Results and discussion will in the following sections be provided for the instrumentation and tests conducted on the double reflector.

- Instrumentation of the double reflector system
- Charging the thermal storage by the sun
- Heating a thin absorber plate made of steel
- Focal length measurement
- Optimal placement of secondary reflector
- Image processing and intensity plots of the focal point

6.1 Instrumentation

The main instrumentation change made to the existing system was the improvement of the secondary reflector mounting.

The construction of the mounting of the secondary reflector was conducted with the goal of making the adjustment easier in vertical direction while testing outside in the sun, and to minimise the obstruction of rays by making the legs narrower. The assumptions made in Section 3.1.2 and 0 for the position of the hole at the base and the position and angle of the mounting points of the legs may not have been correct. This is believed to be the reason why the double reflector focuses the rays better when the system has a small tilt angle.

When the mounting system for the secondary reflector was designed, it was also assumed that the steel pipes used as legs were sufficiently straight. To mount the legs, a solid steel cylinder was turned to a cylindrical shape that fits into the existing mounting points (made of pieces of square pipe). A cylindrical cavity with the same diameter as the leg was made. The steel cylinder is fastened with a screw going through the square pipe. For safety reasons for testing in the sun, the legs and the cylinders were not welded together. This results in an unwanted wobbliness. These two factors may have made it difficult to obtain a fixed position of the secondary reflector during laser testing of the 4 quadrants, as a beam lying across the principle axis had to be placed several times, and avoiding collision was difficult.

6.2 Charging the thermal storage

The results from the tests for charging the thermal storage will here be looked at and discussed. The temperatures reached in the storage for the two tests reached a maximum of 58 °C in the first test with only half the primary reflector uncovered, and 108 °C. with the full system uncovered. The duration of the tests was a little less than 2 hours for both the tests. The solar radiation conditions were variable caused by small clouds passing by.

Measurements for the first and second test are plotted in Figure 6.1 and Figure 6.2. The storage’s temperature is measured at three different positions, with number 1 being closest to the top plate. The solar radiation data was recorded at the Department of physics at NTNU, and was provided by prof. Partick J. Espy. The solar radiation data is measured by two measurement devices for both direct beam radiation and global horizontal radiation. The direct beam radiation is the only one that is collected by a reflecting solar collector such as the double reflector. Showing both these in the graph provides information on the conditions of the sky.

In the first test it was a concern that the reflective film of the secondary reflector could melt if it became too hot, as it had done in previous attempts. This was the reason for uncovering only half the primary reflector. However, the placement of the thermocouple on the secondary reflector was not considered at the time, so the reason for the low temperatures measured from the secondary reflector is that it was placed on the opposite side of the incoming rays from the primary reflector. In Figure 6.1, the gaps of data are due to a bad connection with the thermocouple. From observing the fluctuations, the thermocouple measuring storage temperature number 1 was proven faulty, and had to be fixed for the next test.

The temperatures of the three points in the storage are in both tests close together, indicating good heat conduction within the storage. In the second test, the surface temperature of the top plate on the heat storage is recorded using a thermal camera. The surface temperature achievable is crucial for the heat transfer into the storage. Figure 6.2 show the temperature of the secondary reflector plotted for the same points as the registered temperature of the surface of the storage for comparison. The two temperatures follow the same trend, in spite of being recorded on different devices with a possible timing error. (ref. fluctuations in temperature of the secondary reflector as seen in Figure 0.2, Appendix C). The thermal camera was set to measure a spot temperature, resulting in measurements being done on different spots of the heat storage surface. A graph with the complete temperature plot of the secondary reflector, and a larger version of the two graphs provided here is listed in Appendix C. The surface temperature of the storage and the secondary reflector temperature both mainly depend on the instantaneous illumination from direct solar radiation, and the wind speed for cooling.

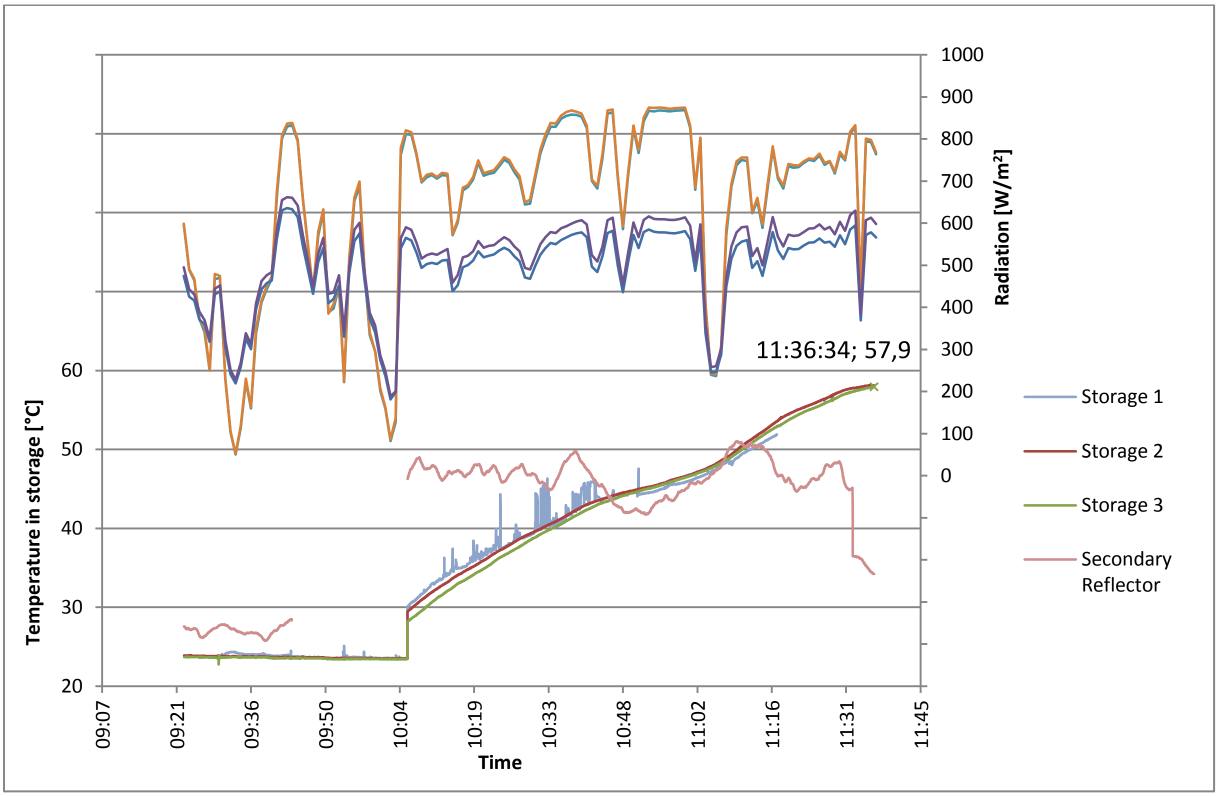

Figure 6.1 Temperature and radiation measurements for the first test of charging the heat storage.

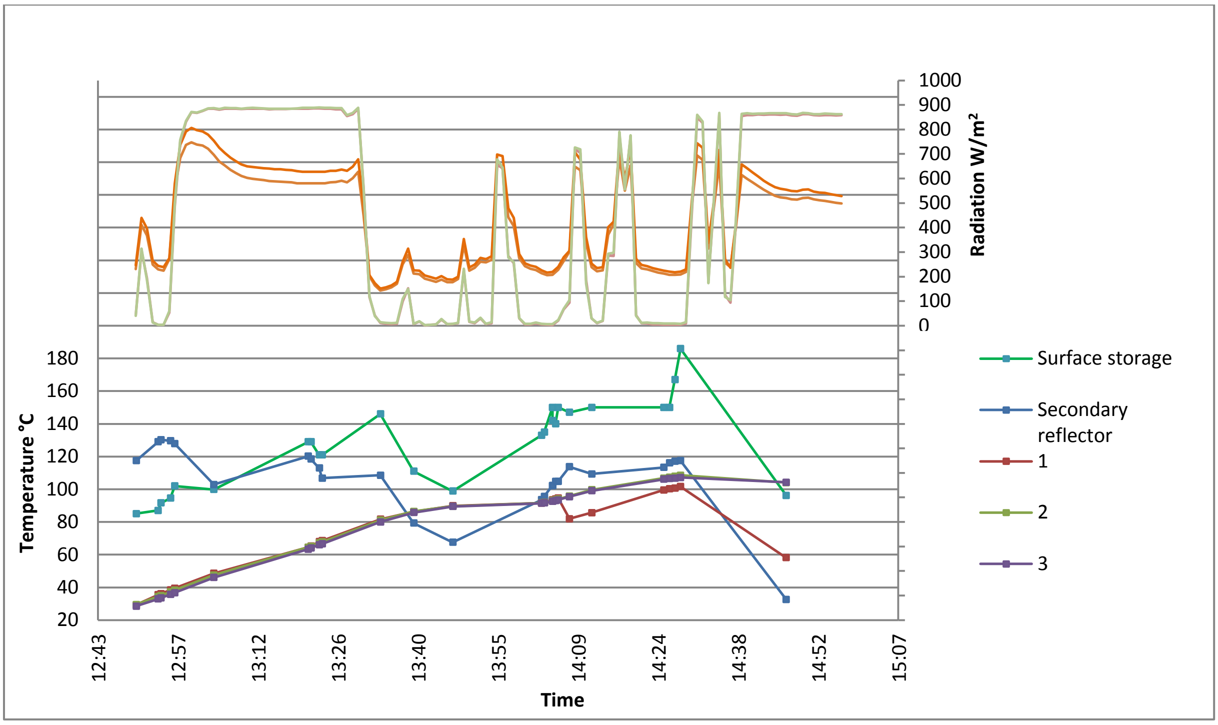

Figure 6.2 Temperature and radiation measurements for the second test of charging the heat storage.

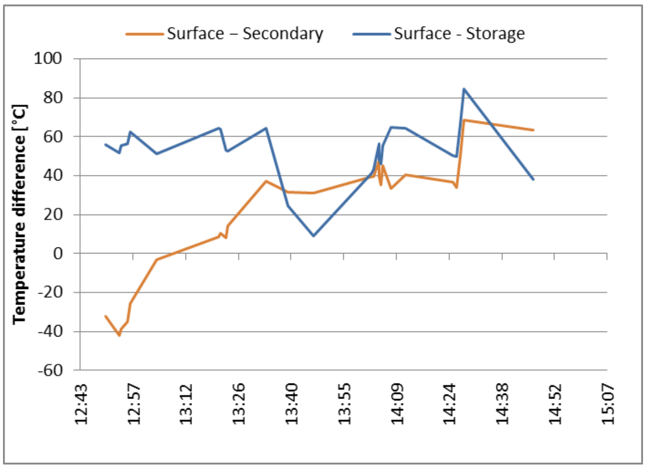

Figure 6.3 The difference in temperature of the surface of the heat storage and the secondary reflector, and the surface of the heat storage and inside the storage plotted according to the time the measurements were taken.

The focal point of the system determines the magnitude of the temperature achievable on the surface of the storge, and thus the rate at which the storage can be heated. The thermal images provide a visualization of the focal point on the heat storage (Appendix J). The surface temperature of the storage was lower than expected. The temperature difference between the surface of the storage and the points inside the storage tended to remain at a relatively constant level, represented by the blue line Figure 6.3 (the dip in the line at the middle is due to clouds). This suggests good heat conduction between the surface and the fins heating the salt in the storage, and that the temperature of the surface would continue to rise as the temperature in the storage is rising. However, the heating of the storage for these tests proved slow, despite numerous attempts on achieving a better focal point. The orange line in Figure 6.3 represents the difference in temperature of the surface of the storage and the secondary reflector. The experience from the movies of the laser on the reflective film supports the decision of replacing the reflective film with reflective tiles.

6.3 Heating a thin absorber plate

The four tests with thermal images serve as a visualisation of the focal point of the double reflective system with reflective aluminium tiles. A thermocouple provided measurements of the absorber plate temperature in the last two tests. A complete list of thermal images from the tests is provided in Appendix L.

The first test did not achieve high temperatures. This was most likely because of cloudy conditions, or a poor adjustment of the secondary reflector to get good focal point. Measurements of the temperature by the thermal camera proved to be lower than the experienced temperature of the plate. The thermal images can however serve as a visualisation of the distribution of an off-focus focal point. Unreliable measurements with the thermal camera was most probably due to a combination of a poor set-up and the fact that it is difficult to measure temperatures on a reflective materiel such as steel, which also has a low emissivity. The measurements of the top plate of the storage coated with black lacquer appeared to be much more reliable.

The second test achieved temperatures in the focal point around 200−400°C shown by the oxidation of the metal taking place at the focal point. Table 6.A shows a visual comparison of the focal point with infrared images and digital images taken simultaneously by the infrared camera during the second test. The parameters of the infrared camera was again not properly set, as the temperature rose much higher than stated maximum temperature measured of 108 °C (seen from the thermal images). The emissivity ε should have been set to around 0.5 for carbon steel instead of 0.98, and the ambient temperature was not 23 °C, as it was in

Trondheim in the end of September, but closer to 10 °C. As seen in the infrared images, the size of the focal point does not seem to change with intensity during this short test, but the conduction through the metal can be seen as a larger size of the hot areas in the last image. The reason for choosing steel as the material for the plate was that it has a low thermal conductivity giving room to visualize the focal point of the system. This does however make it harder to perform a thermal analysis on the plate to find the incoming radiation for an efficiency measurement.

Table 6.A Visual comparison of metal tempering colours and infrared images from the second test of heating the thin absorber plate.

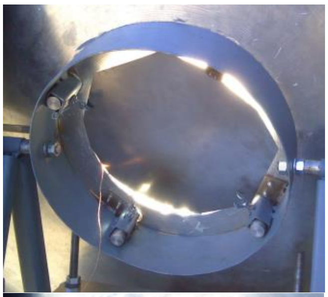	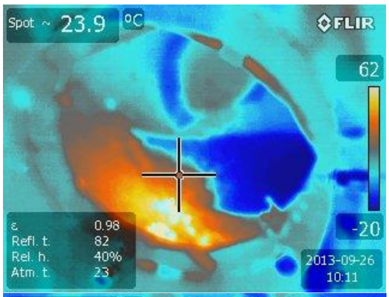	*The focal point is starting to show due to oxidation of the metal.*
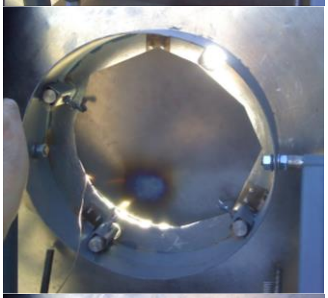	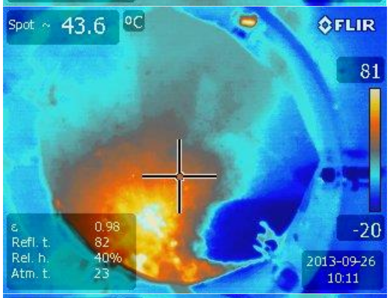	*24 seconds after the initial picture.*
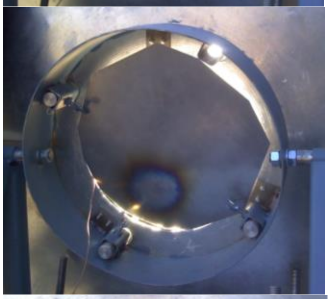	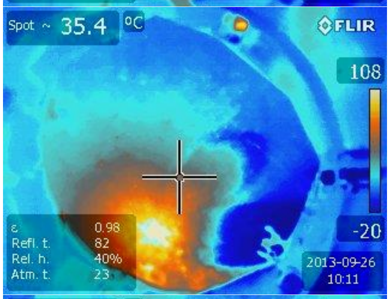	*36 seconds after the initial picture.*
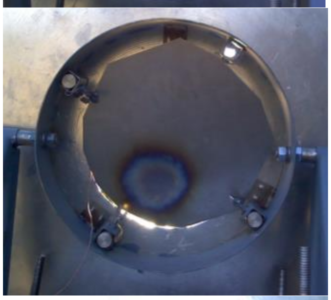	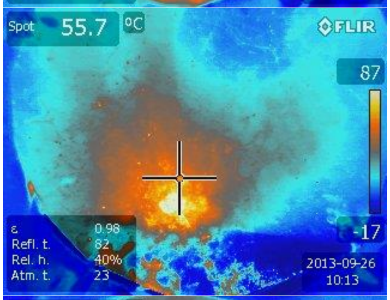	*112 seconds after the initial picture.*
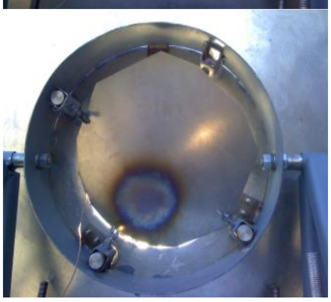	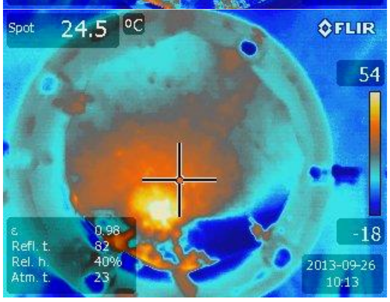	*128 seconds after the initial picture.*

In the third and fourth test the temperature was measured outside the highest intensity of the focal point by 9.5 cm as mentioned previously. The plate reached a maximum temperature around 300 °C at the point of measurement in the third test. The plate reached a steady state after being heated for about 136 seconds from a temperature of 15 °C to 260 °C, as illustrated by the graph in Figure 6.4 by the two first points marked. The average temperature at the point of measurement between the two points in the graph at steady condition is 265 °C. The ambient temperature at both the third and fourth test was about 8 °C, and the wind speed is listed by the Norwegian meteorological institute to be 2 m/s.

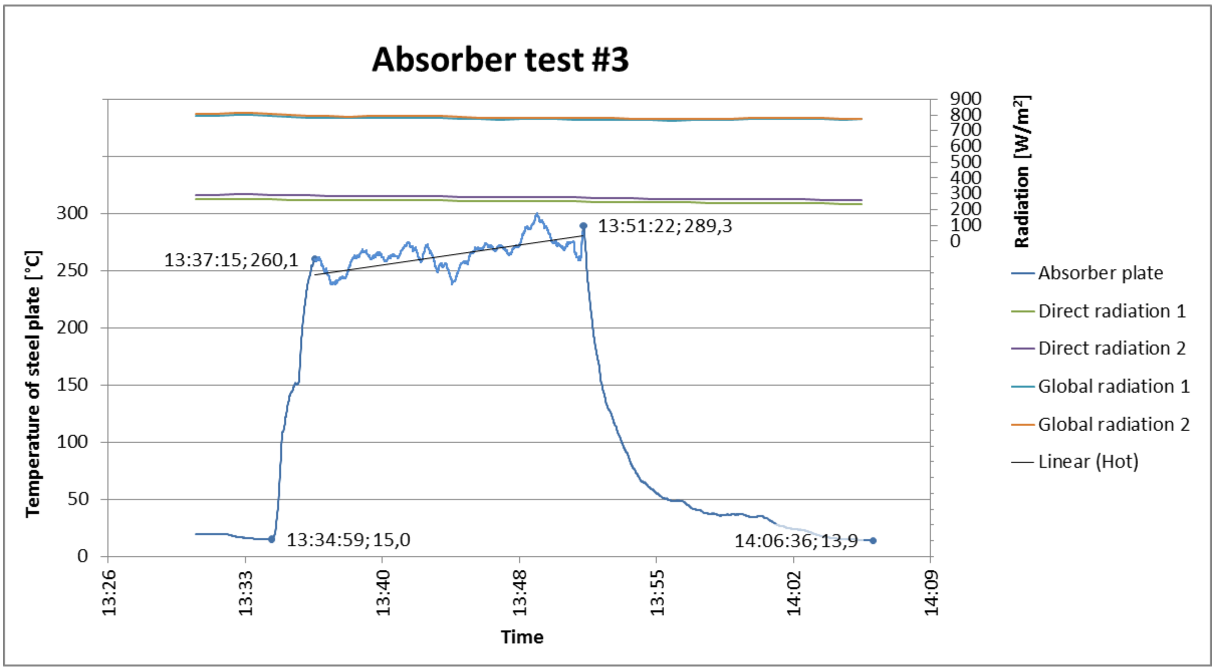

Figure 6.4 Plot of the temperature measurements of the thin steel plate and radiation measurements of global and direct solar radiation in the third test.

In the fourth test, absorber plate also reaches a maxim of about 300 °C. The heating at this test seems to correspond to the first test until a certain point where it slows down. Figure 6.5**Error! Reference source not found.** shows a plot of the temperatures of the absorber plate and the secondary reflector, and the solar radiation in the fourth test. The solar radiation is kept on a constant level. The slow heating also occurs on the secondary reflector, suggesting that there might have been some shading of the primary reflector or wind cooling. In the end of the test, a tracking error appears to have happened, since the temperature of the absorber plate decreases, whilst the secondary reflectors temperature seems to increase. More of the rays is likely to have hit the thermocouple on the secondary reflector, while missing the absorber plate. This was most likely caused by the control box for tracking being shaded. After a while, the absorber plate seems to reach a steady state condition, as seen between the fourth and fifth points, and the average temperature of this region is 293 °C, which is a higher level than for the third test.

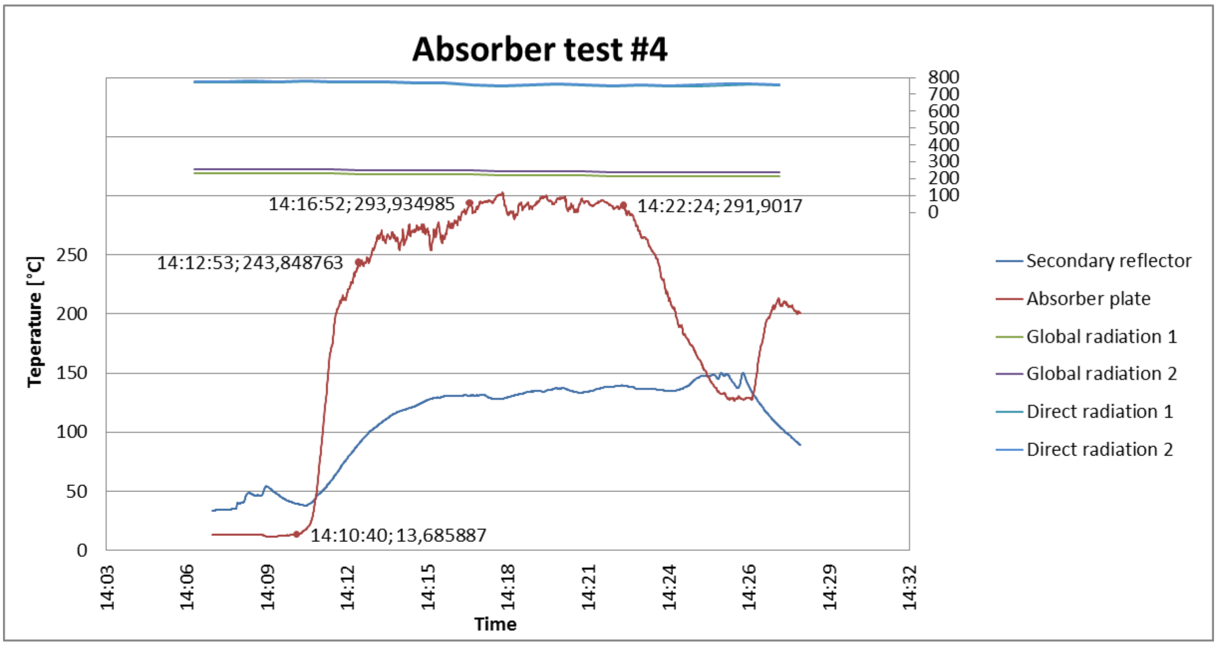

Figure 6.5 Plot of the temperature measurements of the thin steel plate and secondary reflector, and radiation measurements of global and direct solar radiation in the fourth test. Critical points of the plate's temperature are labeled with time and temperature values.

Both the third and fourth tests lasted around 15 minutes with different positioning of the secondary reflector. The thermal couple was as described in section 4.2 mounted outside the focal point by approximately 9.5 cm. This is measureable because the highest intensity of the focal point has resulted in an area coloured black. It is unknown what causes the black colouring, and the oxidation table in section 4.2.1 does not mention anything about a black colour.

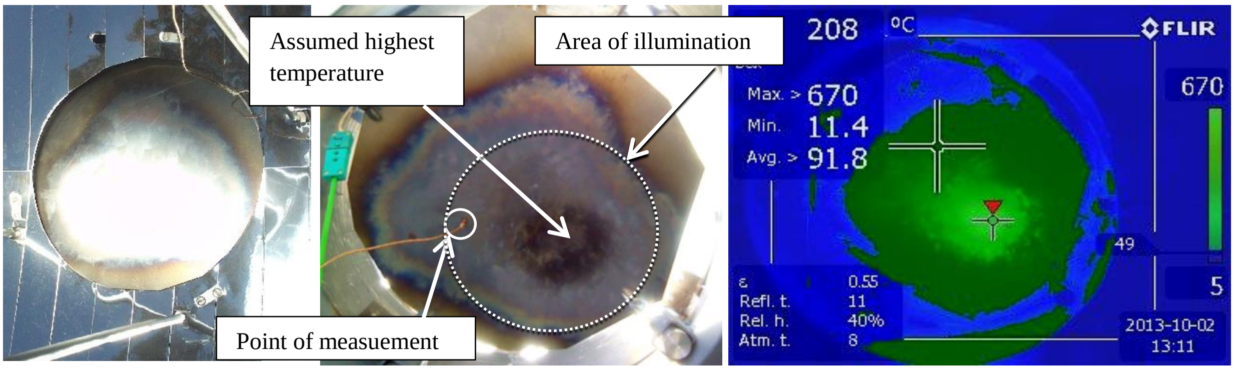

Figure 6.6 Comparison of illumination, oxidation and thermal image of the flat absorber plate during testing.

Figure 6.6 shows the absorber plate during testing. The left and middle images show the absorber plate seen from above and behind during testing. The right shows a thermal image of the absorber plate from behind. Because of the oxidation formed on the surface of the steel, and the information from the infrared image, it is possible to roughly determine the size of the focal point of the double reflector at the specific test, and calculate a concentration ratio.

From the left image, it seems like most of the illuminated part of the absorber plate stays within the oxidation lines. (The reason for the uneven shape of the oxidation is previous testing done on the same absorber plate). Because the thermal camera was not set-up correctly, the readings are uncertain, and show a jump in temperatures from the blue to the green area in the image to the right. But the shape seems to correspond well to the shape of the oxidation as illustrated by the dashed circle in the image in the middle, though the shape is a little larger in the thermal images. For calculating the concentration ratio, the focal point is determined to be 20 cm in diameter giving receiver aperture area of A_a = 0.0314 m^2. The aperture area of the solar collector is A_c = 2.849 m^2, giving a concentration ratio of 90.7. The average direct solar radiation for both the measurements is calculated to be 264.9 W/m^2 for the third test and 235.4 W/m^2 for the fourth test. In comparison, the direct beam radiation on a typical summer day with a cloudless atmosphere and with the sun at zenith position (directly overhead), the direct beam radiation is about 1000 W/m^2 (UO-SRML). Since the surface of the absorber plate at the tests have a much poorer ability to collect radiation energy than a heat storage with a black coating suited to absorb radiation, the double reflecting system is believed to have an acceptable concentration for collecting high temperature heat in a thermal storage. This is provided that the system can be adjusted so that the focal point will manage to hit the top plate of the storage, and that the incident angle of the focussed sun beams is not too small. Further testing of heating a storage is recommended.

6.4 Focal length of primary reflector

The results from the laser diode test for determining the focal length of the primary reflector for the reflective film and the reflective aluminium tiles are plotted in Figure 6.7 and Figure 6.8.

For the test with the reflective film, the results are varying, and the measurement of the focal length is done with a relative uncertainty. The calibration of the laser sight was only done once, and it is assumed to hold for the testing period. It is not easy to level the laser sight because of the shape, and the fact that is it very small. The coordinates of the laser reflections on the absorber plate are also registered with an uncertainty since the laser reflections were rather large in some points because of overlaps of the reflective film, and sometimes the ray was even split in two.

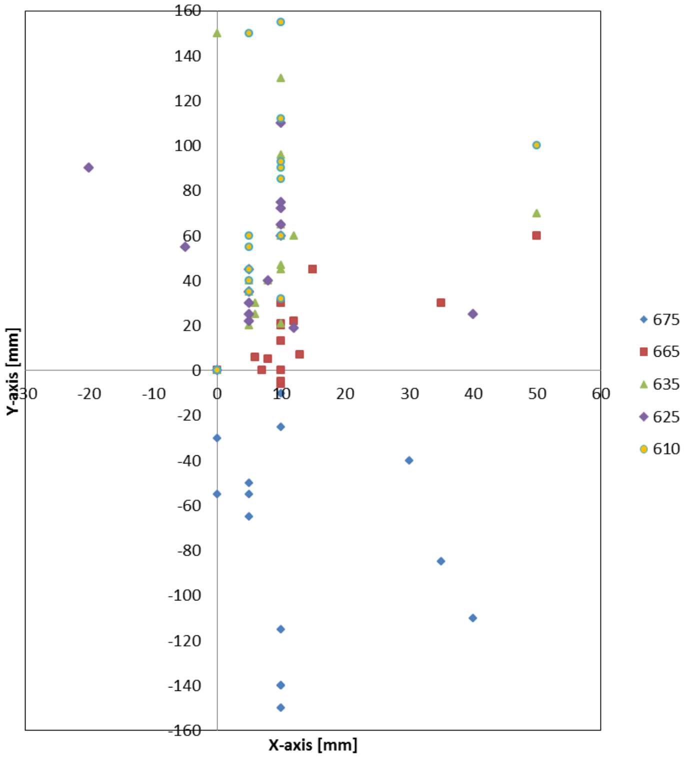

Figure 6.7 Scatter plot of laser rays on the absorber plate with focal lengths 675, 665, 635, 625 and 610 mm. Laser diode test on reflective film.

It is evident from the plot in Figure 6.7 that the test was done for only the y-axis, as the variation in x-direction is much smaller than the variation in y-direction. It is expected that the rays will hit in the positive y-direction when the absorber plate is placed at a height lower than the focal point and in the negative y-axis when placed above the focal point. This is because the rays will pass the focal point or not reach the focal point with heights over and under the focal point respectively. It is also expected that the points will be more spread out the further the absorber is from the focal point. All these expectations are met in the test, with negative values for the focal length of 675 mm, and increasingly spread points from 665 to 610 mm focal lengths. The focal length of the primary reflector is from these test results closest to 665 mm, represented by the red and square markers in the plot.

For the test with the reflective tiles, the CNC-machine set-up had been improved, and was functioning like it should. As mentioned, only one quadrant of the reflector was considered with 32 different laser positions in each test. The low number of points was chosen due to time constraints.

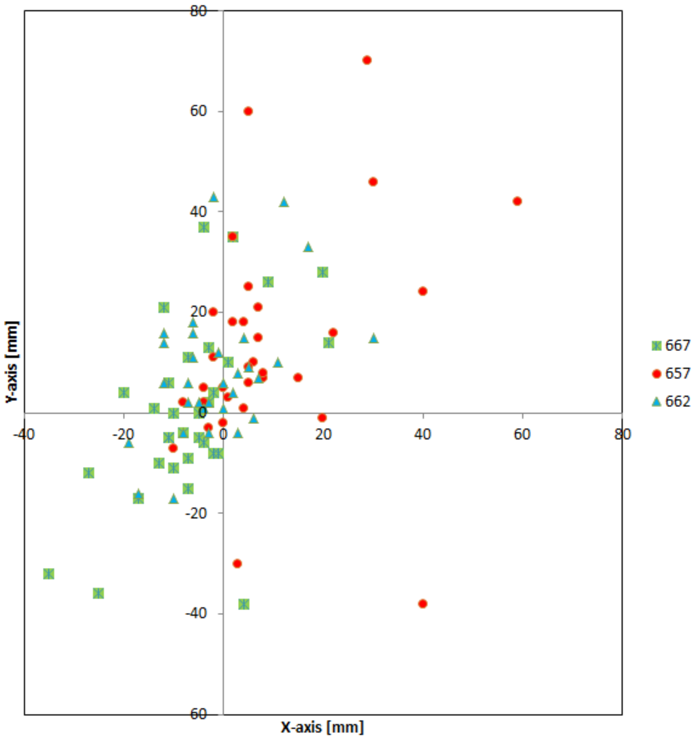

Figure 6.8. Scatter plot of laser rays on the absorber plate with focal lengths 657, 662 and 667 mm. Laser diode test on aluminium tiles

Since the test was only conducted for one quarter of the primary reflector, it is expected that most rays will hit in the first quadrant of the absorber plate if it is placed below the focal point and in the third quadrant if it is placed above the focal point, as for the tests with the reflective film. As can be seen from the plot, the absorber plate at a focal length 667 mm has the highest number of rays in the first quadrant, and the plate at a focal length of 657 mm has the highest number of rays in the third quadrant as expected. The different points of the tests were traversed with the CNC-machine, and the primary reflector was calibrated once, so the conditions for each test are similar.

In Figure 6.9, the total intensity of rays per cm^2 within a certain radius of the principal axis is plotted. The plot does not consider whether the points are mainly in the first or third quadrant, only the absolute length form the principal axis. Central points weigh more, since the area increases faster than the radius. Therefore, it is hard to see the difference further away from the centre of the absorber plate in these plots. It is also the reason why one hit less than 2 mm from the centre gets an intensity of 8 rays per cm^2 in plot B. The intensity peaks further away from the principal axis in plot C, and the peak is more spread out with a lower intensity. This indicates that the focal point at 667 mm is more widespread than the other two heights.

Plots A and B are hard to tell apart, and one “lucky” hit very close to the principal axis in plot B cannot be conclusive. Considering that the intensity peak is slightly wider for a focal length of 662 mm, and that the extreme points are clearly further away from the centre in Figure 6.9, the conclusion is that the focal length is somewhere around 662 mm.

The results from the two tests are presented in Table 6.B, and the results agree with the calculated theoretical value for the focal length very well. The calculated value was the basis for choosing the heights to test for the reflective tiles, and the results suggest this to be closer than the other two values tested with the amount of points considered.

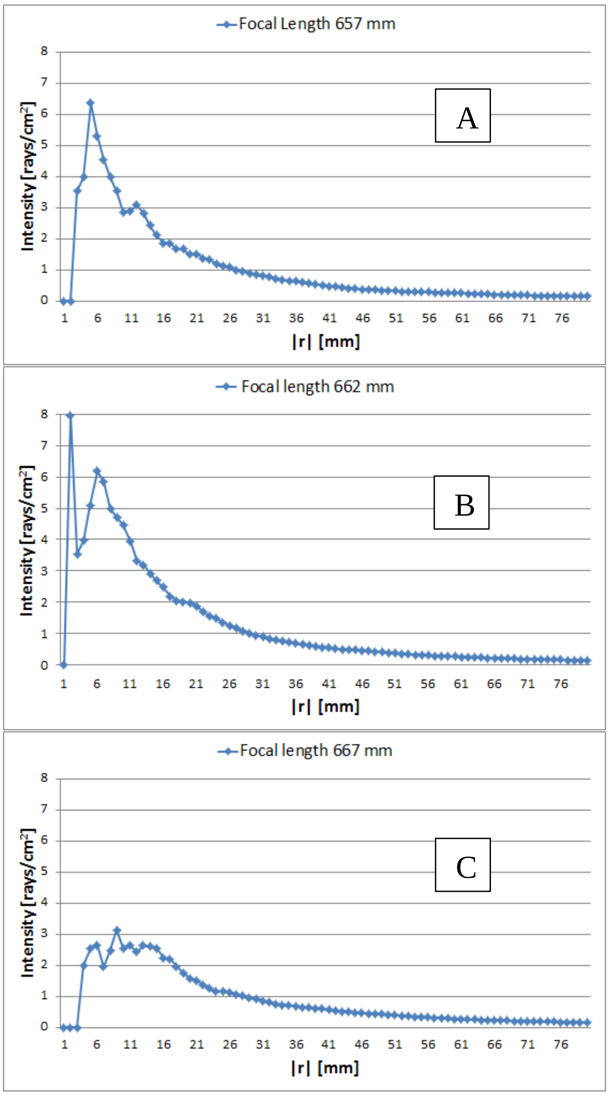

Figure 6.9 Intensity plots with different focal lengths, A 657 mm, B 662 mm, and C 667 mm.

Table 6.B Comparison of theoretical and experimental focal point of the primary reflector

	Reflective film	Reflective tiles	Theoretical
Focal length [mm]	≈ 665	≈ 662	662

6.5 Optimal placement of secondary reflector

The findings from the laser characterisation of the focal point of the double reflector system is presented in this section. The quality of the test procedure and image processing will be discussed.

6.5.1 Test procedure

The quality of the calibration of the different parts of the double reflector during testing is difficult to demonstrate. The most uncertain aspect of the double reflector is the mounting of the secondary reflector, specifically the position in the horizontal direction. This is believed to be the reason why the double reflector performed better when the system was tilted. The secondary reflector was not levelled after the tilting. By knowing the tilt angle distance from the base of the primary reflector to the rim of the secondary reflector for each test, the displacement can be calculated. For a tilt angle of 1.7°, the displacement in X-direction is 21 mm, and 3 mm in Z-direction. The situation of tilting the whole system can be compared to that of a mistake in the tracking by the same angle. It is likely that the initial displacement of the secondary reflector is cancelled out by the displacement caused by tilting the system.

The position of the secondary reflector should maintain at a fixed position while testing the 4 quadrants of the reflector. Different aspects can cause a shift in the position. As mentioned, the beam that has to be placed across the principal axis is easy to accidentally crash into the legs, as the space around the double reflector is small. The wobbliness of the legs themselves can cause a change in the position when the reflector is turned or lifted to level the system in the direction of the horizontal tracking axis.

The position of the absorber plate when finding the focal length of the primary reflector was possible to measure because the laser could move over the absorber plate and the middle could be placed at the principal axis. The absorber plate is also easier to level since it is flat. The levelling of the secondary reflector was done with a short leveller along the rim, and the placement was only assessed through maintaining as vertical legs as possible. Since the legs were known to not be the same, they were marked with the cardinal direction they were placed close to in order to keep track of them. The same was done to the mounting place along the rim of the secondary reflector. This way the tests for the different focal lengths would be as

6.5.2 Image processing uncertainty

There are many sources of uncertainty in the image processing of the laser reflection. They will be discussed in this section

Bright spots on the absorber plate sometimes appeared due to scratches in the white cover of the absorber plate. These spots were getting registered for every image on the same spot, resulting in a maximum value for the focal point of that test. The value is larger for this spot since the values are added together in the same spot every time, which is not the case for the laser dot. This could be solved by developing a different way of detecting the dots. This problem only occurred at for certain tests. As long as the peak is isolated from the rest of the focal point of the double reflector, it is removed by the condition checking if the region having the maximum concentration value also has the largest area. If it does not, this region is removed all together. The problem is when the focal point of the system is close to the point where the bright spot is detected. For every plot, this is checked and where the problem remains, the peak is removed by locating the maximum value, and creating an area of a certain pixel size where the value is set to zero.

Because the laser dot is significantly different than the rest of the image, there are still other ways to obtain a result without having to correct the result afterwards. One way could be to analyse all 3 colour matrices, and select the data on the condition that the red pixel values should be a certain amount larger than the blue and green pixel values. A bright spot typically has the same values for red, green and blue pixel values in the RGB colour space, and thus appears light grey. Another possibility is to convert the images to the Lab colour space, a three-dimensional space where L describes the lightness, and a and b the colour component dimensions. This was looked into, but not selected when developing the image processing.

6.5.3 Compilation of results

The compilations of all detected laser dots from the 4 quadrants are put together in a final compilation, and the result is plotted as a 3D surface showing elevated levels corresponding to higher intensity of the focal point. (See appendix H). The best efficiency, 91.0% of hits was obtained with the secondary reflector placed at the height of 683 mm over the base of the primary reflector, with a tilt angle of 1.7°. This height also obtained the best focussing power of 11.62. Assuming a focal length of 662 mm, this gives a separation distance of 21 mm between the foci, which corresponds well to the optimal separation distance found in the ray tracing of 20 mm. Because of time constraints, no tests below this distance has been conducted, and it is unknown if a shorter distance could have made a better result.

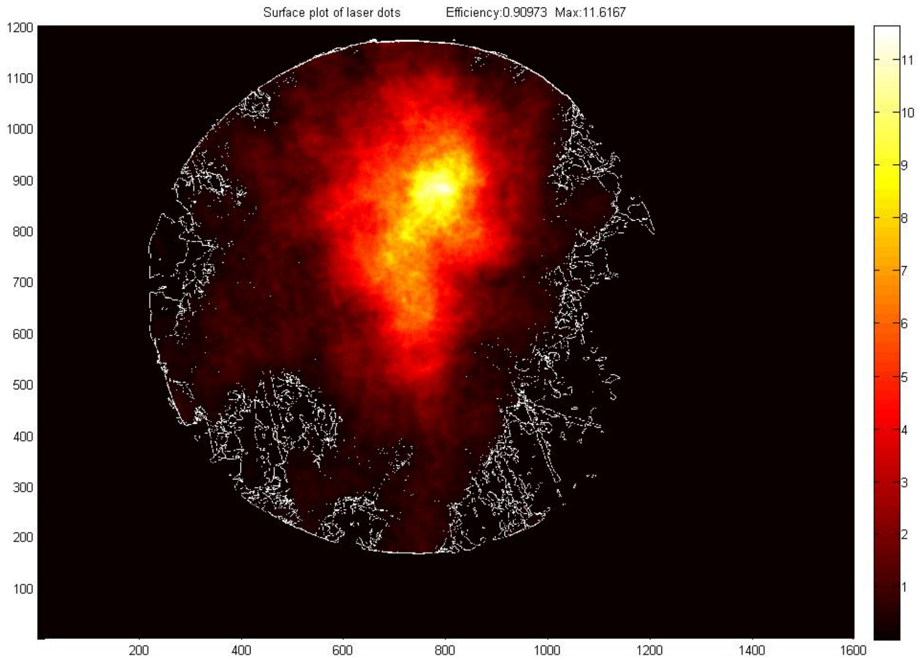

Figure 6.10 Intensity plot of the laser dots detected with a separation distance of 21 mm.

The results for the tests are presented in , and the intensity plots can be found in Appendix M. The pixel values of the laser dots are added as raw data to the composition matrix. To get an intensity value that is independent of the number of hits on the absorber, the added values are divided by the number of hits. (The average of all the mean values divided by the number of hits will then correspond to a concentration of 1.)

Table 6.C Results from the laser testing of optimal placement of secondary reflector.

Distance [mm]	683	683	688	698	703	708	708
Angle [°] ±0.2	0.9	0.9	1.4	0	1.3	0	1.7
Step [mm]	25	50	50	50	50	50	50
Max intensity	9.93	11.61	10.2	6.15	10.1	7.4	9.1
Hit efficiency	0.874	0.910	0.828	0.747	0.845	0.440	0.553
Separation distance [mm]	21	21	26	36	41	46	46

The tests were as mentioned very time consuming, and time only allowed the 7 tests presented to be conducted. One test was conducted with a smaller step distance between the laser positions. This was done for the best result, with a distance of 683 mm, and the same tilt angle of the double reflector. The step distance in this test was 25 mm, giving 4 times the amount of rays detected. Shape of the focal point corresponds well with the two tests. The intensity plot

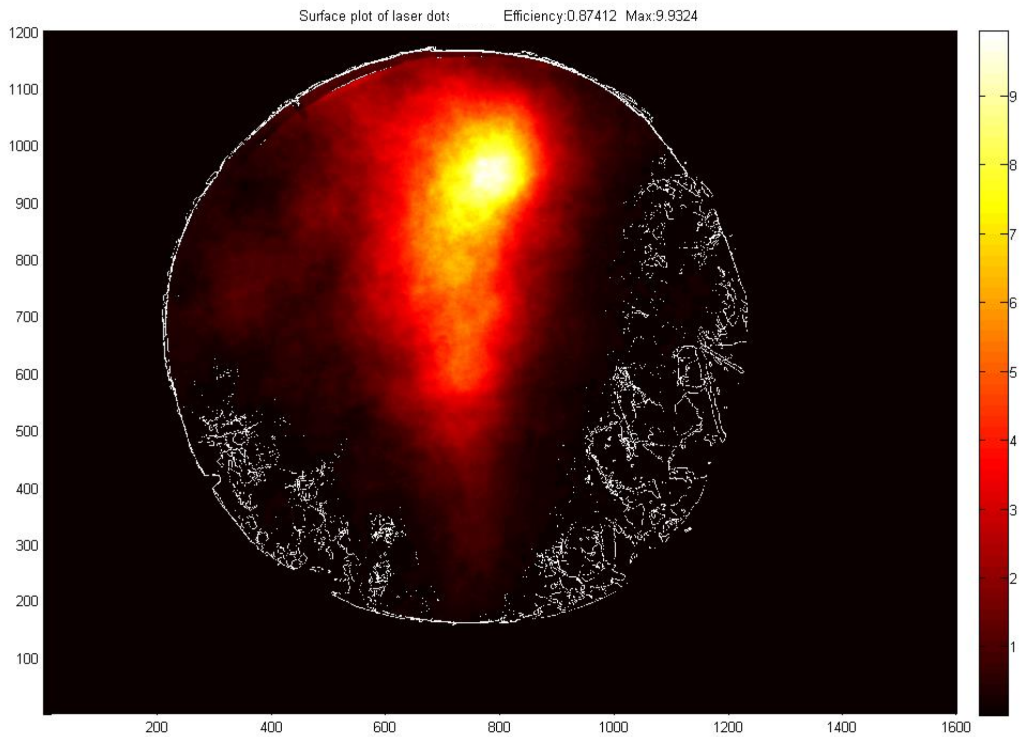

Figure 6.11Intensity plot for distance 683 with a step distance of 25 mm.

for the final test is shown in Figure 6.11.

6.6 Further testing

In this section some thoughts and considerations about further testing of the double reflector is provided.

Heating of the secondary reflector will occur due to incident radiation from the primary reflector and directly from the sun above being absorbed. This is because no surface can be 100 % reflective, and it also depends on the production method. If the secondary parabola has been made with tiles or strips of reflective material, the space between the tiles will serve as an area that is more absorbing than the surface of the tiles/strips. Depending on the quality of the reflective surface and the size of the secondary reflector, the secondary reflector will be heated due to incident radiation from the primary reflector, and from the direct sun from the top. Depending on the size of the reflectors, the concentration ratio hitting the secondary reflector from the primary reflector will vary. With a larger secondary reflector with respect to the primary reflector, the concentration factor will be lower, but this will cause more of the primary reflector being shaded. So there is a trade-off between size of the secondary reflector and the effective aperture area utilized.

The secondary reflectors reflective material in the tests conducted can withstand a maximum operating temperature of 120 °C. This limit was exceeded, and it is therefore suggested to consider a different material or a type of cooling for the secondary reflector. An identical reflector covered in reflective aluminium tiles was made, but not tested in the sun. A heat resistant glue was used to attach the tiles. Another solution could be to increase the size of the secondary reflector.

The secondary reflector is prone to damage of reflective material from burn marks caused by the heating. It is therefore important that the mounting of the secondary reflector allows for regular cleaning and inspection. The primary reflector is easily covered in dust, especially outside where pollution and dust particles come with the wind. It is also important to be able to clean the primary reflector in order to maintain it in a good way. A primary reflector of diameter 2 m is just on the limit to what is manageable for one (quite tall) person.

The secondary reflectors mounting should be improved or changed to allow a better control of the position of the secondary reflector. A way of better levelling the secondary reflector is recommended to be developed.

For more laser tests to be done, it is recommended to get a laser with a power supply. It is difficult to know how long the laser will last, and a lot of batteries were used. For the array of lasers, this is essential for an efficient use of resources, since the lasers use a lot of energy, and the expensive small batteries does not last long. A camera with a power supply is also recommended. This way a test could be conducted over night with a small step size.

Conclusion and recommendation

Conclusion

Charging of a thermal battery in the sun with a double reflective solar collector did not succeed for various reasons. By improving the reflective material on the collector, the system has proved to be able to collect high temperature heat on a thin absorber plate even with low radiation values. An efficiency measurement of the system could not be conducted because of too few tests conducted in the sun.

The automatic procedure for using a red laser diode technique together with a CNC-machine and post processing of images provides an accurate collection of data for making an intensity plot of the focal point. The test procedure seems to be working well, but there are still improvements to be made. The intensity of the focal point seems to be much higher in a small area, which makes it attractive for further testing and improvement

Recommendation

The double reflector is recommended to be tested further. These points are important to consider:

- The design specifications of a solar cooker has to take into account a number of practicalities that make it as user-friendly, robust, safe, efficient and durable as possible.
- The secondary reflector must be able to withstand high temperatures without getting damaged
- An optimization of the size of a larger secondary reflector should be looked into
- The mounting system of the secondary reflector must be more robust.

Appendix

NTNU SINTEF

A. Simplified risk assessment report on solar testing of double reflector

Risk Assessment Report

Double reflector

Prosjektnavn	Direct charging of a solar thermal battery
Apparatur	Double reflector
Enhet	NTNU
Apparaturansvarlig	Victoria Sivertsen
Prosjektleder	Ole Jørgen Nydal
HMS-koordinator	Morten Grønli
HMS-ansvarlig (linjeleder)	Olav Bolland
Plassering	Varmeteknisk Lab
Romnummer	C163
Risikovurdering utført av	Victoria Sivertsen

Approval:

	Navn	Dato	Signatur
Prosjektleder	Ole Jørgen Nydal		
HMS koordinator	Morten Grønli		
HMS ansvarlig (linjeleder)	Olav Bolland		

1. INTRODUCTION

The rig setup consists of a double reflector readily mounted on a tracking system with a small heat storage underneath. The system directly illuminates the heat storage that contains a salt mixture of KNO3 and NaNO3, and is to be tested in the sun with the heat storage to determine the efficiency. The aim is to be able to melt the salt in the storage, which melts around 220 degrees C. The double reflector is located in the refrigeration laboratory. Testing in the sun will mostly be done near the gate at the south side of the lab (Refrigeration part).

2. CONCLUSION

The experimental setup is approved

Apparaturkort (UNIT CARD) is valid for **XX months**
Forsøk pågår kort (EXPERIMENT IN PROGRESS) is valid for **XX months**

3. ORGANISATION

Rolle	
Prosjektleder	Ole Jørgen Nydal
Apparaturansvarlig	Victoria Sivertsen
Romansvarlig	
HMS koordinator	Morten Grønli
HMS ansvarlig (linjeleder):	(Erik Langørgen)

4. RISK MANAGEMENT IN THE PROJECT

Hovedaktiviteter risikostyring	Nødvendige tiltak, dokumentasjon	DATE
Prosjekt initiering	Prosjekt initiering mal	04.04.13
Veiledningsmøte Guidance Meeting	Skjema for Veiledningsmøte med pre-risikovurdering	04.04.13
Innledende risikovurdering Initial Assessment	Fareidentifikasjon – HAZID Skjema grovanalyse	29.08.13
Vurdering av teknisk sikkerhet Evaluation of technical security	Prosess-HAZOP Tekniske dokumentasjoner	29.08.13
Vurdering av operasjonell sikkerhet Evaluation of operational safety	Prosedyre-HAZOP Opplæringsplan for operatører	29.08.13
Sluttvurdering, kvalitetssikring Final assessment, quality assurance	Uavhengig kontroll Utstedelse av apparaturkort Utstedelse av forsøk pågår kort	29.08.13

5. DESCRIPTIONS OF EXPERIMENTAL SETUP

The experimental setup consists of a large primary parabolic reflector of D=2m, FL around 65 cm, mounted on an electrical tracking system in two axes with a weight adjustment for balance. The primary reflector has a hole in the middle of Ø29cm and a thermal storage containing nitrate salts underneath (60:40 $NaNO_3$ and KNO_3). The thermal storage is cylinder shaped with D=20 cm and height H=21 cm. The top plate has flat fins going down into the salt mix to transfer the heat. 10% of the volume is kept free from salt on the top to allow the salt to expand when melting, and there are holes for air to enter to avoid a pressure build-up. A secondary reflector with specifications D=12" (30,5 cm) and FL=3" (7,62 cm) is mounted above a little above the coinciding of the reflectors focal points to reflect the concentrated solar beams from the primary reflector down to the thermal storage. The mounting provides some vertical and little horizontal adjustment possibilities. Both the primary and the secondary reflector are clad with a reflective film. The test will consist of:

- Tracking the sun using the electrical tracking system.
- Measurements of the charging process using thermo elements readily installed in the heat storage, on the reflective film of the secondary reflector and on the top surface of the heat storage.
- Measurements for monitoring purposes of surface temperatures using a thermal camera, and a thermal couple to determine the temperature of the reflective film on the secondary reflector.

Component list with specifications:

- Primary parabolic reflector clad with reflective film, with a diameter of D_P = 2 m, and a focal length of FL_P around 67.5 cm
- Secondary parabolic reflector clad with reflective film D_S = 30.5 cm, FL_S = 7.62 cm.
- Mounting system with electrical tracking device, 2 electrical motors and a tracking control system. A calibration device is located next to the control system to check if the control is correct.
- Computer for recording of data from temperature measurements.
- Insulated heat storage with fins filled with a solar salt mix with attached thermal couples for temperature measurement. D = 20 cm, H = 21 cm. Insulation layer of 5 cm on sides and bottom, exposed top plate for charging.
- Logging box.
- Extendable power cord.
- Control box for the tracking system, with an emergency off switch.
- Dark safety goggles, thermal safety gloves, fire blanket and safety barriers – 4 cones with a security band (not displayed in pictures).
- Tools to make adjustments, including: wrench, leveller with adjustable angle, flat screw driver and utility knife.
- A piece of cardboard and a steel plate to use when looking at focal points.

See pictures a)-i) below with descriptions.

Attachments:

- Process and Instrumentation Diagram (PID)

a) PR mounted on tracking system

b) Thermal heat storage, side view

c) Weight balance and steel plate

d) PR covered with black sheet

e) Control system and calibration

f) Horizontal tracking axis

g) Mounting of secondary parabola with thermal couple

h) Computer with logging box, safety gloves, safety goggles, rig tools, power cord and fire blanket.

i) Thermal heat storage seen from above.

6. ASSESSMENT OF TECHNICAL SAFETY

○ HAZOP

See Chapter 13 "Guide to the report template".

The experiment set up is divided into the following nodes:

Node 1	Double reflector system with all parts assembled; primary reflector, tracking system and secondary reflector.
Node 2	Thermal heat storage placed under the primary reflector/attached to the primary reflector containing a solar salt mix.

Attachments: Form: Hazop_mal
Conclusion: (Safety taken care of)

○ Radiation

See Chapter 13 "Guide to the report template".

YES	Radiation source need to have an own risk assessment
NO	

Radiation source: the sun

Attachments:
Conclusion: Safety taken care of by putting barriers so that passers-by cannot get close enough to take damage from the concentrated beams.

○ Chemicals

YES	Do a risk assessment of the use
NO	

Attachments: MSDS Safety sheet for the two salts and the thermal insulation is attached.
Conclusion:

The salts should be stored in the thermal heat storage, and no water should be allowed to go inside. The storage should be places steadily during tests and cool-down and not be tilted when the salts are melted. The insulation material should be handled with care since it emits a dangerous dust by even a light touch. Always cover up the skin, use gloves and a face mask, and work over an exhaust chamber when cutting and working with it. Cover it up with heat resisting material so that it is sealed when the insulating is completed.

7. QUANTIFYING OF RISK - RISK MATRIX

See Chapter 13 "Guide to the report template".
The risk matrix will provide visualization and an overview of activity risks so that management and users get the most complete picture of risk factors.

IDnr	Aktivitet-hendelse	Frekv-Sans	Kons	RV
1	*Some concentrated radiation escaping the secondary reflector -> put barriers so this area cannot be reached*	3	A	A3
2	*Getting in touch with the concentrated solar beams in the focal point -> put waring signs (and barriers)*	1	D	D1
3	Tilting the heat storage with melted salt inside -> fix the storage to the system. Serious consequences since it will very soon solidify when in contact with the skin and be hard to get off. The same problem on the floor.	1	E	E1
4	Damage eyes by looking directly into the focal point on the heat storage or by looking into the parabola without safety goggles	2	B	B2
5	Setting fire to objects who fall into the focal area -> do not put flammable objects in this area	1	C	C1
6	Getting mted reflective film dripping on skin -> this will only happened if the parabola is tilted to a bad angle while attempting to abort the experiment -> operators should be aware of the risk	1	D	D1

Conclusion : *Participants will make a comprehensive assessment to determine whether the remaining risks of the activity / process is acceptable. Barriers and driving outside working hours e.g.*

8. DOCUMENTATION

- Tegninger, foto, beskrivelser av forsøksoppsetningen
- Hazop_mal
- Sertifikat for trykkpåkjent utstyr
- Håndtering avfall i NTNU
- Sikker bruk av LASERE, retningslinje
- HAZOP_MAL_Prosedyre
- Forsøksprosedyre
- Opplæringsplan for operatører
- Skjema for sikker jobb analyse, (SJA)
- Apparaturkortet
- Forsøk pågår kort

9. GUIDANCE TO RISK ASSESSMENT TEMPLATE

Chapter 9 Quantifying of RISK

Quantifying of the residue hazards, Risk matrix
To illustrate the overall risk, compared to the risk assessment, each activity is plotted with values for the probability and consequence into the matrix. Use task IDnr.
Example: If activity IDnr. 1 has been given a probability 3 and D for consequence the risk value become D3, red. This is done for all activities giving them risk values.
In the matrix are different degrees of risk highlighted in red, yellow or green. When an activity ends up on a red risk (= unacceptable risk), risk reducing action has to be taken

CONSEQUENSES	Svært alvorlig	E1	E2	E3	E4	E5
	Alvorlig	D1	D2	D3	D4	D5
	Moderat	C1	C2	C3	C4	C5
	Liten	B1	B2	B3	B4	B5
	Svært liten	A1	A2	A3	A4	A5
		Svært liten	Liten	Middels	Stor	Svært Stor
		PROBABILITY				

The principle of the acceptance criterion. Explanation of the colors used in the matrix

Colour		Description
Red		Unacceptable risk Action has to be taken to reduce risk
Yellow		Assessment area. Actions has to be considered
Green		Acceptable risk. Action can be taken based on other criteria

Attachment to Risk Assessment report

Double reflector

Prosjektnavn	Direct Charging of a solar thermal battery
Apparatur	Double reflector
Enhet	NTNU
Apparaturansvarlig	Victoria Sivertsen
Prosjektleder	Ole Jørgen Nydal
HMS-koordinator	Morten Grønli
HMS-ansvarlig (linjeleder)	Olav Bolland
Plassering	Varmetekninsk Lab, Fellesverksted
Romnummer	
Risikovurdering utført av	Victoria Sivertsen

ATTACHMENT B: HAZOP TEMPLATE

Project: Node: 1						Page	
Ref	**Guideword**	**Causes**	**Consequences**	**Safeguards**	**Recommendations**	**Action**	**Date/Sign**
	More pressure	Pressure building up in the thermal storage due to something ceiling the opening.	Danger of blow-out; might cause scatters of what are ceiling/small metal parts to blow out of the heat storage, in addition to hot air.	Do not stay too close to the heat storage.	Always be sure that there is room for air exiting the system before starting to run the experiment, and entering after (while cooling down).	Check the passage of air before running experiments.	
	More temperature/ Abnormal Operation of the secondary reflector	Overheating of secondary reflector due to scratches of reflective film, dirt/finger-marks or too high concentration factor from primary reflector.	The film may start to melt and drip down to the primary reflector. It is dangerous to touch the secondary reflector at this state. Also damaging to get the melt on you.	Avoid touching the secondary reflector, use gloves when adjusting it.	Keep track of the temperature of the secondary reflector by using a thermal camera.	Turn the parabola away from the sun by using the mounted lever as quickly as possible, while assuring that the melting film does not	
	More temperature/ Abnormal Operation	Overheating of thermal battery, or insulation material.	The insulation material should not be able to catch fire (former experiment done with coal charging of a heat storage next to	Always know where the fire extinguisher is located, and assure that there will be no chemical reaction between	Use a thermal camera to keep track of the surface temperature of the heat storage, (or install a thermal couple to the surface) and the thermal	Turn the parabola away from the sun by using the mounted lever as quickly as possible if there is something	

Project: Node: 1						Page	
Ref	**Guideword**	**Causes**	**Consequences**	**Safeguards**	**Recommendations**	**Action**	**Date/Sign**
			insulation material was fire proof). Objects landing on/too close to an overheated storage might catch fire.	the chemicals of the fire extinguisher and the nitrate salts, since the storage is not completely ceiled. If in doubt, use a thermal blanket to put the fire out, or activate the fire alarm if it gets out of hand.	couples to keep track of the temperatures inside the heat storage.	catching fire, and cover the parabola up after putting the fire out.	
	Less temperature	Temperature increase slows down, or starts decreasing due to bad tracking or wrong positioning of the secondary reflector.	Non optimum test data and/or focus moving off the heat storage and onto the material covering the insulation.	When adjusting the secondary parabola, the primary should be completely covered, or turning away from the sum, safety gloves when adjusting the hot secondary dish should be used.	Make sure the focus is good by observing it on the heat storage, using dark eye-protection. (Glasses used for light welding).	Adjusting the secondary parabola. Observing the focal point on the heat storage through safety goggles.	
	Composition change/Chemical	Water entering the heat storage might	Development of boiling	Use the heat blanket and cover	Be sure not to flush the system with water	Keep a heat blanket with the	

Project: Node: 1						Page	
Ref	**Guideword**	**Causes**	**Consequences**	**Safeguards**	**Recommendations**	**Action**	**Date/Sign**
	reaction	cause a chemical reaction with the melted salt mixture.	water/chemical substance coming out from the heat storage through the openings for air.	the heat storage up, and turn the double reflector away from the sun using the emergency lever. At the same time, keep a safe distance from the heat storage. If it gets too messy, step away and let the reaction finish.	while experiments are running, or let any water get into the system at any time.	rig equipment while the experiment is running.	
	Instrumentation	The wires of the thermal couples are old and may short cicuit. One of them is fixed with electrical insulating tape going some way into the thermal insulation. This may melt if the temperatures get too high.	Disrupting test results and melting rubber tape may drip out from the heat storage .	Make sure the melting tape stays on the plate carrying the heat storage.	Stop the test if one thermal couple stops working and/or melting rubber tape is dripping out from the heat storage an on the ground.	Turn the double reflector away from the sun and cover it up. Let the heat storage cool down completely and find a better solution to the wire problem.	
	Safety, heat	Safety can be at risk	Due to required	If a person tips the	The storage must be	Make an	

Project: Node: 1						Page	
Ref	**Guideword**	**Causes**	**Consequences**	**Safeguards**	**Recommendations**	**Action**	**Date/Sign**
	storage with melted salt	if the heat storage is tipped when the salts are melted. A person can tip it, or it can tip if the tray carrying it tips.	openings for air, the hot salt (over 220 C) can be spilled on the floor, or at the person who made the storage tip over.	heat storage he/she should move away as quickly as possible to avoid getting salt on themselves.	securely placed on the centre of the plate, and not too close to the edge.	arrangement to secure the heat storage to the rig, to make it steady.	
	Reflection/danger of concentrated radiation on passersby	Secondary reflector not big enough to cover the beams from the primary reflector when adjusted to the best focal area at the heat storage. (Size problem). If big enough, there might still be beams hutting outside the area due to surface roughness.	Passers-by passing to close might be endangered by the concentrated light, depending on how close they go. Curious people might get the urge to stick their head closer to see underneath the secondary reflector /hand under to feel the heat and get burned.	A security barrier needs to be put up to hinder passers-by by getting too close to the double reflector and hurting themselves.	Place the barriers at least one focal length away from the parabola, be sure no concentrated sunbeams can hit passers-by, and keep in mind the tracking after the sun.	Place barriers around the test rig when running the experiment. 4 cones with a connecting safety band have been stored for experiments.	
	Bright focal point on the heat storage.	A good focal point causes a bright light on the heat storage.	This might be damaging for the eyes to look directly into.	Do not look directly at the focus point (if bright) without	Wear dark safety goggles (same as mentioned above) if adjusting or	Put a warning sign directed to passers-by, and keep it in mind	

Project: **Node: 1**						**Page**	
Ref	**Guideword**	**Causes**	**Consequences**	**Safeguards**	**Recommendations**	**Action**	**Date/Sign**
				safety goggles.	monitoring the focal point.	when they come to talk to you at the rig.	

ATTACHMENT D: HAZOP PROCEDURE (TEMPLATE)

Project: **Node: 1**						**Page**	
Ref#	**Guideword**	**Causes**	**Consequences**	**Safeguards**	**Recommendations**	**Action**	**Date/Sign**
	Not clear procedure	Procedure is to ambitious, or confusingly	N/A	N/A	N/A	N/A	
	Step in the wrong place	The procedure can lead to actions done in the wrong pattern or sequence	N/A	N/A	N/A	N/A	
	Wrong actions	Procedure improperly specified	N/A	N/A	N/A	N/A	
	Incorrect information	Information provided in advance of the specified action is wrong	N/A	N/A	N/A	N/A	
	Step missing	Missing step, or step requires too much of operator	If there is a step missing in the program, the test could be left running for too long.	Test the programmes before setting up a large and time consuming test.	Stop the program, correct the mistake.	Start over.	
	Step unsucessful	Step has a high probability of failure	N/A	N/A	N/A	N/A	
	Influence and effects from other	Procedure's performance can be affected by other sources	It the lights are off, the picture quality will change, and it might be hard to analyze it afterwards.	Try to run the tests during the daytime when there are people in the lab.	Test if the picture quality is not acceptable while the lights are off.	Leave the lights on if necessary, or adjust the camera to handle the lighting conditions.	

B. Simplified risk assessment report on laser testing of double reflector

Risk Assessment Report

Double Reflector

Prosjektnavn	Direct charging of a solar thermal battery/ Optical evaluation of a double reflector solar system
Apparatur	Double reflector and XY-table
Enhet	NTNU
Apparaturansvarlig	Victoria Sivertsen, Swati Singh, Nabin Kumar Shrestha
Prosjektleder	Ole Jørgen Nydal
HMS-koordinator	Morten Grønli
HMS-ansvarlig (linjeleder)	Olav Bolland
Plassering	Varmeteknisk Lab
Romnummer	
Risikovurdering utført av	Victoria Sivertsen, Swati Singh, Nabin Kumar Shrestha

Approval:

	Navn	Dato	Signatur
Prosjektleder	Ole Jørgen Nydal		
HMS koordinator	Morten Grønli		
HMS ansvarlig (linjeleder)	Olav Bolland		

1. INTRODUCTION

The rig setup consist of a double reflector readily mounted on a tracking system with a small thermal heat storage underneath. The system is to be tested in the sun to determine the efficiency. The reflectors should also be tested with laser mapping under an XY-table. In this case the system is mounted horizontally under the XY-table. Testing will consist of an optical laser hitting an absorber plate both with the primary reflector and with the two reflectors working together. The laser will be of low radiation intensity, and the absorber plate will be a white transparent material. The double reflector is located in the VVS lab (HVAC lab) in the solar section in room C163, and the XY-table is located……………………. Testing in the sun will mostly be done near the gate at the south side of the lab (Refrigeration part).

2. CONCLUSION

The experimental setup is approved

Apparaturkort (UNIT CARD) is valid for **XX months**
Forsøk pågår kort (EXPERIMENT IN PROGRESS) is valid for **XX months**

3. ORGANISATION

Rolle	
Prosjektleder	Ole Jørgen Nydal
Apparaturansvarlig	Victoria Sivertsen
Romansvarlig	
HMS koordinator	Morten Grønli
HMS ansvarlig (linjeleder):	Erik Langørgen

4. RISK MANAGEMENT IN THE PROJECT

Hovedaktiviteter risikostyring	Nødvendige tiltak, dokumentasjon	DATE
Prosjekt initiering	Prosjekt initiering mal	04.04.13
Veiledningsmøte Guidance Meeting	Skjema for Veiledningsmøte med pre-risikovurdering	04.04.13
Innledende risikovurdering Initial Assessment	Fareidentifikasjon – HAZID Skjema grovanalyse	
Vurdering av teknisk sikkerhet Evaluation of technical security	Prosess-HAZOP Tekniske dokumentasjoner	
Vurdering av operasjonell sikkerhet Evaluation of operational safety	Prosedyre-HAZOP Opplæringsplan for operatører	

Sluttvurdering, kvalitetssikring Final assessment, quality assurance	Uavhengig kontroll Utstedelse av apparaturkort Utstedelse av forsøk pågår kort	

5. DESCRIPTIONS OF EXPERIMENTAL SETUP

The experimental setup consists of a large primary parabolic reflector of 2m diameter, with a hole in the centre of 29 cm, and a secondary reflector. The secondary reflector is to be mounted to reflect the laser beams from the primary reflector down to an absorber plate in the centre of the primary reflector. The testing consists of:

- Characterizing the optical properties of the reflector, to find the optimal placement of the secondary reflector and to estimate the efficiency of both the primary- and the secondary reflector and both together. This is to be done with means of an XY-table setup with a camera, a laser and a partly transparent absorber material. For the purpose of this test, the primary reflector will be detached from its tracking system and mounted horizontally under the XY-table with the possibility to move it to be able to cover the whole parabola.

Component list with specifications:

- Primary parabolic reflector clad with reflective film, with a diameter of D_p = 2 m, complete with mounting system for camera and secondary reflector.
- Secondary parabolic reflector (clad with reflective film/polished/fixed with aluminium reflector material) D_S = 0,3 m.
- Mounting system with easy measurement when moving the reflector under the XY-table, made out of AluFlex components.
- XY-table setup: the setup will consist if a low radiation level laser (used as a laser sight for an air rifle) fixed on the moving part and a computer to handle the programming of the XY-table and triggering the camera.

Table 0.A: Pictures of the test rig setup for outdoor testing with tracking system.

6. ASSESSMENT OF TECHNICAL SAFETY

a. HAZOP

See Chapter 13 "Guide to the report template".

The experiment set up is divided into the following nodes:

Node 1	Double reflector system with all parts assembled; primary reflector, secondary reflector, camera, absorber plate.
Node 2	XY-table with laser mounted, connected to a computer.

Attachments: Form: Hazop_mal
Conclusion: Safety taken care of

b. Radiation

See Chapter 13 "Guide to the report template".

YES	Radiation source need to have an own risk assessment
~~NO~~	

Attachments: 03 Attachment Risk Assessment Report_Template (ENG)
Conclusion: Safety taken care of

7. QUANTIFYING OF RISK - RISK MATRIX

The risk matrix will provide visualization and an overview of activity risks so that management and users get the most complete picture of risk factors.

IDnr	Aktivitet-hendelse	Frekv-Sans	Kons	RV
1	Laser reflects from an uneven part of the double reflector into operators or bypasses' eyes, and this person stares into the laser	1	B1	B1
2	Melting the plastic reflective film	1	A1	A1

Conclusion: Acceptable risk, a warning sign will be placed to not stare into the laser should this happened.

8. DOCUMENTATION

- Tegninger, foto, beskrivelser av forsøksoppsetningen
- Hazop_mal
- Sertifikat for trykkpåkjent utstyr
- Håndtering avfall i NTNU
- Sikker bruk av LASERE, retningslinje

- HAZOP_MAL_Prosedyre
- Forsøksprosedyre
- Opplæringsplan for operatører
- Skjema for sikker jobb analyse, (SJA)
- Apparaturkortet
- Forsøk pågår kort

9. GUIDANCE TO RISK ASSESSMENT TEMPLATE

Chapter 9 Quantifying of RISK

Quantifying of the residue hazards, Risk matrix
To illustrate the overall risk, compared to the risk assessment, each activity is plotted with values for the probability and consequence into the matrix. Use task IDnr.
Example: If activity IDnr. 1 has been given a probability 3 and D for consequence the risk value become D3, red. This is done for all activities giving them risk values.
In the matrix are different degrees of risk highlighted in red, yellow or green. When an activity ends up on a red risk (= unacceptable risk), risk reducing action has to be taken

CONSEQUENSES	Svært alvorlig	E1	E2	E3	E4	E5
	Alvorlig	D1	D2	D3	D4	D5
	Moderat	C1	C2	C3	C4	C5
	Liten	B1	B2	B3	B4	B5
	Svært liten	A1	A2	A3	A4	A5
		Svært liten	Liten	Middels	Stor	Svært Stor
		PROBABILITY				

The principle of the acceptance criterion. Explanation of the colors used in the matrix

Colour		Description
Red		Unacceptable risk Action has to be taken to reduce risk
Yellow		Assessment area. Actions has to be considered
Green		Acceptable risk. Action can be taken based on other criteria

NTNU SINTEF

Attachment to Risk Assessment report

Double Reflector

Prosjektnavn	Direct Charging of a thermal storage/Optical evaluation of a double reflector solar system
Apparatur	Double reflector and XY-table
Enhet	NTNU
Apparaturansvarlig	Victoria Sivertsen, Swati Singh, Nabin Kumar Shrestha
Prosjektleder	Ole Jørgen Nydal
HMS-koordinator	Morten Grønli
HMS-ansvarlig (linjeleder)	Olav Bolland
Plassering	Varmetekninsk Lab
Romnummer	
Risikovurdering utført av	Victoria Sivertsen, Swati Singh, Nabin Kumar Shrestha

- **ATTACHMENT B: HAZOP TEMPLATE**

Project: **Node: 1**						**Page**	
Ref	**Guideword**	**Causes**	**Consequences**	**Safeguards**	**Recommendations**	**Action**	**Date/Sign**
	More temperature/ Abnormal Operation	The program getting stuck, causing the laser to maintain at one point.	Heat might develop very locally where the laser is pointed due to damages in the reflective film affecting the reflectivity.	Always check that the program works as it should the first time a test is run, be careful when touching or cleaning the reflective film.	It this happens more than once, and the burn on the reflective film is extensive, the procedure should not be run at night, or for very long periods without monitoring.	Make a safety feature to the computer to turn off after a time approximately corresponding to the expected length of the test.	
	Reflection	Roughness of material under and overlapping of the reflective film.	Might cause passing people or operator to get the laser beam reflected into their eyes.	Avoid looking for the reflection of the laser beam on the primary- and secondary reflector.	Do not stare into the laser beam.	Put up a warning sign that says that you should not stare into the laser.	

- **ATTACHMENT D: HAZOP PROCEDURE (TEMPLATE)**

Project: **Node: 1**						**Page**	
Ref#	**Guideword**	**Causes**	**Consequences**	**Safeguards**	**Recommendations**	**Action**	**Date/Sign**
	Step missing	Missing step, or step requires too much of operator	If there is a step missing in the program, the test could be left running for too long.	Test the programmes before setting up a large and time consuming test.	Stop the program, correct the mistake.	Start over.	
	Step unsucessful	Step has a high probability of failure	N/A	N/A	N/A	N/A	
	Influence and effects from other	Procedure's performance can be affected by other sources	It the lights are off, the picture quality will change, and it might be hard to analyze it afterwards.	Try to run the tests during the daytime when there are people in the lab.	Test if the picture quality is not acceptable while the lights are off.	Leave the lights on if necessary, or adjust the camera to handle the lighting conditions.	

C. Matlab codes for G-code generation

The code for generating G-codes in Matlab is provided here.

```
clc
clear

step=100;                %mm step
radius=980;              %outer radius to stay whitin
iradius=250;             %inner radius to stay whithout

margin=1000-radius       %margin we have to concider to stay whithin the
                         %reflecting surface. Plus the 25 mm from the edge.

a=(floor(radius/step))+1;

t=13;
%seconds needed to wait for the laser to stabilize
p=0.5;                   %seconds needed between taking a picture
                         %(turning on and off "cooling")
f=3000;                  %Feedrate in mm/min

for R=1:a
    for C=1:a
        A(R,C)=sqrt(((R-1)*step)^2+((C-1)*step)^2);
    end

end

D= A < radius;
E= A >= iradius;
logical= E.*D;
logical1=logical>0;

filename='gcodes.txt';
fid=fopen(filename,'w');

gridcount=0;
oddcount=0;
evencount=0;
count=0;

for r=2:a;
    if rem(r, 2) == 0
            for c=a:-1:1;
                if logical1(r,c)==1;
                %produce  G-codes
                B=zeros(5,7);
                G=num2cell(B);
                Z=A(1,c);
                X=Z-radius;
                Q=A(r,1);
                Y=Q*(-1);

                G{1,1}='G01';
                G{1,2}='F';
                G{1,3}=f;
                G{1,4}='X';
```

```
            G{1,5}=X;

            G{1,6}='Y';
            G{1,7}=Y;

            G{2,1}='G04';
            G{2,2}='P';
            G{2,3}=t;
            G{2,4}=' ';
            G{2,5}=' ';
            G{2,6}=' ';
            G{2,7}=' ';

            G{3,1}='M07';
            G{3,2}=' ';
            G{3,3}=' ';
            G{3,4}=' ';
            G{3,5}=' ';
            G{3,6}=' ';
            G{3,7}=' ';

            G{4,1}='G04';
            G{4,2}='P';
            G{4,3}=p;
            G{4,4}=' ';
            G{4,5}=' ';
            G{4,6}=' ';
            G{4,7}=' ';

            G{5,1}='M09';
            G{5,2}=' ';
            G{5,3}=' ';
            G{5,4}=' ';
            G{5,5}=' ';
            G{5,6}=' ';
            G{5,7}=' ';

            fprintf(fid, '%s %s %d %s %d %s %d\r\n', G{1,:});
            fprintf(fid, '%s %s %.1f %s %s %s %s\r\n', G{2,:});
            fprintf(fid, '%s %s %s %s %s %s %s\r\n', G{3,:});
            fprintf(fid, '%s %s %.1f %s %s %s %s\r\n', G{4,:});
            fprintf(fid, '%s %s %s %s %s %s %s\r\n', G{5,:});

            gridcount=gridcount+1;
            else
                evencount=evencount +1;
            end
        end
elseif rem(r,2)~=0;
        for c=1:a;
            if logical1(r,c)==1;
            %produce G-codes:
            B=zeros(5,7);
            G=num2cell(B);
            Z=A(1,c);
            X=Z-radius;
            Q=A(r,1);
            Y=Q*(-1);
```

```
            G{1,1}='G01';
            G{1,2}='F';
            G{1,3}=f;
            G{1,4}='X';
            G{1,5}=X;
            G{1,6}='Y';
            G{1,7}=Y;

            G{2,1}='G04';
            G{2,2}='P';
            G{2,3}=t;
            G{2,4}=' ';
            G{2,5}=' ';
            G{2,6}=' ';
            G{2,7}=' ';

            G{3,1}='M07';
            G{3,2}=' ';
            G{3,3}=' ';
            G{3,4}=' ';
            G{3,5}=' ';
            G{3,6}=' ';
            G{3,7}=' ';

            G{4,1}='G04';
            G{4,2}='P';
            G{4,3}=p;
            G{4,4}=' ';
            G{4,5}=' ';
            G{4,6}=' ';
            G{4,7}=' ';

            G{5,1}='M09';
            G{5,2}=' ';
            G{5,3}=' ';
            G{5,4}=' ';
            G{5,5}=' ';
            G{5,6}=' ';
            G{5,7}=' ';

            fprintf(fid, '%s %s %d %s %d %s %d\r\n', G{1,:});
            fprintf(fid, '%s %s %.1f %s %s %s %s\r\n', G{2,:});
            fprintf(fid, '%s %s %s %s %s %s %s\r\n', G{3,:});
            fprintf(fid, '%s %s %.1f %s %s %s %s\r\n', G{4,:});
            fprintf(fid, '%s %s %s %s %s %s %s\r\n', G{5,:});

            gridcount=gridcount+1;
            else
                oddcount=oddcount+1;
            end
        end
    else
        count = count + 1;
    end
end

fclose(fid);
```

E. Matlab codes for image registration

```
%% Image registration
% To allign the images from each image aquisition set, an image
% registration has to be done.

clc
clear

FirstNumber = 9498;
LastNumber = 9594;

cd('C:\NTNU_Data\Pictures\dist670not_levelled25\N-W');

Fixed=imread('fixed.jpg');
Fixed=Fixed(:,:,1);
imwrite(Fixed,'fixed.jpg');

%% Calculate metric and optimization values before loop

cd('C:\NTNU_Data\Pictures\dist670not_levelled25\N-W');

Moving = imread('moving.jpg');
Moving = Moving(:,:,1);

[optimizer,metric] = imregconfig('monomodal');


%% Parallel Loop images
tic
parfor i = 1:LastNumber - FirstNumber + 1      % Matlabpool needs to be run
                                          work with multiple cores.
    cd('C:\NTNU_Data\Pictures\dist670not_levelled25\N-W');
    Moving = imread(strcat('IMG_', num2str(i+FirstNumber-1),'.JPG'));
    Moving=Moving(:,:,1);

%% Default registration
registered = imregister(Moving,Fixed,'translation',optimizer,metric);

%% Save registered images counting from one
cd('C:\NTNU_Data\Pictures\dist670not_levelled25\N-W registered');
Filename = strcat('Reg_',num2str(i+1033),'.jpg');
imwrite(registered,Filename);

end
time = toc
```

F. Laser dot detection

This section of the image processing program will detect the laser dot on the absorber.

Input variables and directory

Input variables of the test are specified; the number of photos to be processed in `NumPhotos` (known from the image registration process) and the number of a representative image with no hits in `NumNoHit`. In this example, only one image is shown.

```
clc
clear
Test = 'N-E';
Dir = 'C:\NTNU_Data\Pictures\dist675not_levelled\';
Reg = ' registered';
Dot = ' dot';

NumPhotos = 1;
NumNoHit = 48;
```

Load RGB image

The truecolour RGB image from the test is converted to a Matlab variable `RGB`.

```
cd(horzcat(Dir,Test));
RGB = imread('IMG_8906.jpg');
figure(1);imshow(RGB,'InitialMagnification','fit');title('RGB image')
```

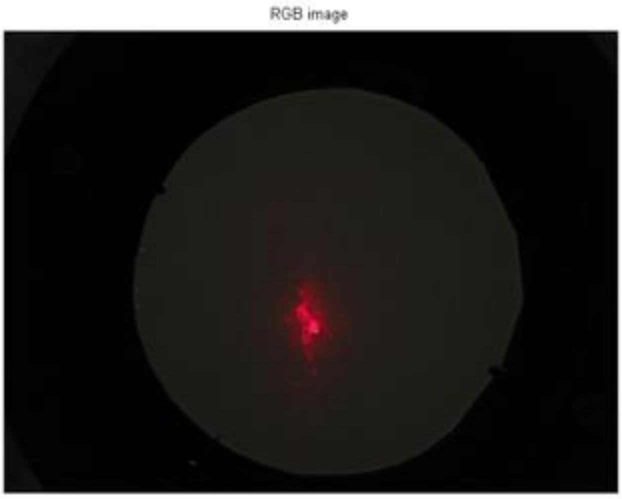

`RGB` contains pixel values in an m-by-n-by-k matrix, where m-by-n is the size of the image (the pixel height and width of the picture), and k is the three colour components, for red, green and blue colour values.

Red colour space

This will create a grayscale image showing only the information from the red colour component. (From the RGB colour space).

```
Im = RGB(:,:,1);
figure(1); imshow(Im,'InitialMagnification','fit');title('Gray scale image of red color
information')
```

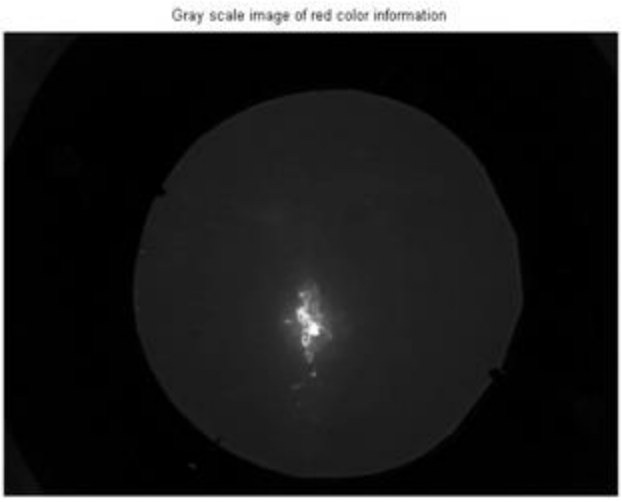

Counters

Counters are started to count the number of detected dots and the number of pictures processed.

```
Picturecount = 0;
IsEmpty = 0;
```

Composition and data matrix

The m-by-n size of the image is taken from one of the images to create a matrix containing only zeroes for the composition of all detected laser dots to be added together. Another matrix, data, is created to store the data registered from each image

```
Composition = zeros(size(Im));
data = zeros(NumPhotos,1,7, 'double');
```

Average intensity of the absorber plate

An image from the same dataset as the Test being analysed with no laser dot is used as a measure of the background intensity of the absorber plate as a base value for thresholding the laser dot.

This method requires an input value of one of the images with no hits. It also required the lighting conditions to be very stable to achieve good results. The absorber plate is detected from the rest of the image by default thresholding, and the mean intensity is extracted from

```
cd(horzcat(Dir,Test,Reg));
NoHit = imread(strcat('Reg_', num2str(NumNoHit),'.jpg'));
level = graythresh(NoHit);
bwabsorber = im2bw(NoHit,level);
bwabsorber = bwareaopen(bwabsorber,1000);   % removes objects smaller than 1000 pixels
```

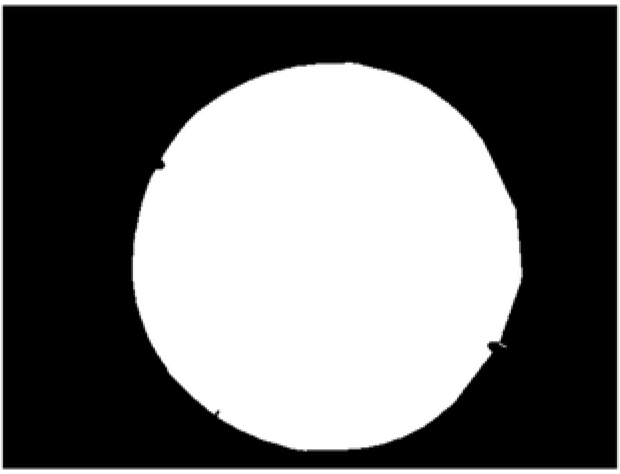

```
bwabsorber=imfill(bwabsorber,'holes'); % Fills in small holes in at the border
bwabsorber=imclearborder(bwabsorber);     % Clears the border by supressing border structures
figure(1); imshow(bwabsorber,'InitialMagnification','fit')

STATS = regionprops(bwabsorber,NoHit,'MeanIntensity');
AbsIntensity = STATS.MeanIntensity;
STATS = regionprops(bwabsorber,NoHit,'MaxIntensity');
AbsMaxInt = STATS.MaxIntensity;
```

Further the `for` loop of the images is presented showing one of the images being processed as an example.

```
i = NumPhotos;
```

Segmenting the laser dot by thresholding

The threshold for detecting the laser dot is calculated by multiplying the mean intensity of the absorber plate with a factor of 2.5 (experienced as a good value). The result is a binary image with values of 1 and 0. The pixels with the value of 1 are represented by white and show the laser dot, and pixels of 0 are represented by black.

```
thresh = AbsIntensity*2.5;
bw = im2bw(Im, thresh/255);
figure(1); imshow(bw,'InitialMagnification','fit')
title('Detection of laser dot');
```

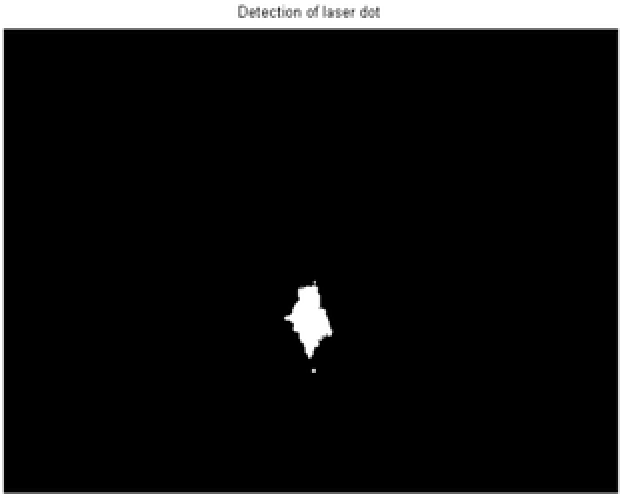

Segmenting of the absorber plate

As a way to cancel out everything around the absorber plate, the automatically calculated threshold function is used to separate the absorber from the rest of the image.

```
level = graythresh(Im);
bwabsorber = im2bw(Im,level);
figure(1); imshow(bwabsorber,'InitialMagnification','fit')
title('Detection of absorber plate');
```

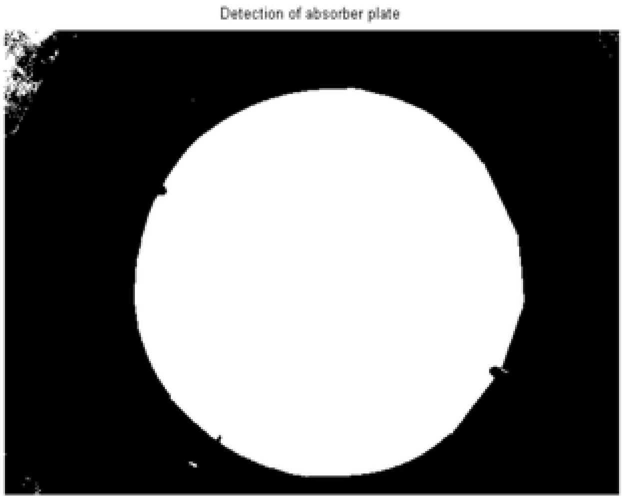

Removing small blobs

Morphology can assist segmentation. This function removes all objects smaller than a number of pixels

```
bwabsorber = bwareaopen(bwabsorber,1000);   % removes objects smaller than 1000 pixels
```

Clean up image

- `imfill` fills in small holes at the border and
- `imclearboarder` clears the border by supressing border structures

```
bwClear=imfill(bwabsorber,'holes');
bwClear=imclearborder(bwClear);
figure(1); imshow(bwClear,'InitialMagnification','fit');
title('Absorber plate cleaned up');
```

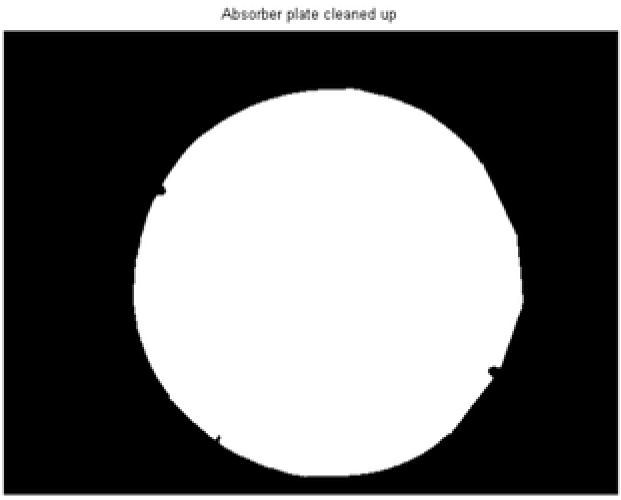

Add image to bwClean

```
bwClear=im2double(bwClear);
bw=bwClear.*bw;
figure(1); imshow(bw,'InitialMagnification','fit')
title('Background subtracted from binary image of laser dot');
```

Find remaining regions

Finding all connected regions in the binary image of the laser dot is important to see how many objects we are dealing with. No objects found indicates a miss.

```
[B,L] = bwboundaries(bw,'noholes');
```

The variable `L` is the image with all connected regions saved as a number (1,2,3 etc.)

```
numRegions = max(L(:));
figure(1); imshow(label2rgb(L),'InitialMagnification','fit')
title('Connected regions represented by RGB colours');
```

Area

The area of the detected laser dot is extracted to be able to exclude hits that are too small to be

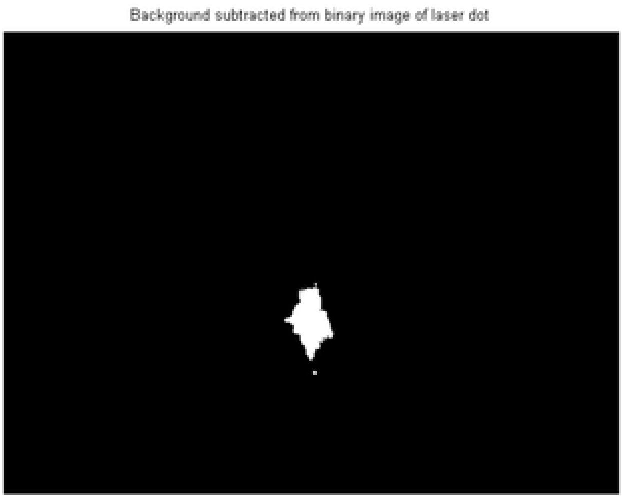

considered a good hit, and detected areas of small bright spots on the absorber plate not caused by the laser.

```
STATS = regionprops(bw, 'Area');
 Areavector=[STATS.Area];
 AreaDetected = sum(Areavector);
```

Detect the images with no laser dot

The limit for an area being approved as a detected laser dot is set to 100 pixels. Total area of a spot detected fewer than 100 pixels counts as a miss. Only images with a hit will be processed

```
if AreaDetected < 100;
    IsEmpty=IsEmpty+1;
else
   data(i,1,5) = 1;
```

Hits are registered as 1, and misses remain as 0 in `data(:,1,5)`.

Measure total area of the detected laser dot

The area of each laser dot is recorded in `data(:,1,3)`.

```
STATS = regionprops(bw, 'Area');
Areavector=[STATS.Area];
Area = sum(Areavector);
data(i,1,3) = Area;
```

Measure the Mean Intensity of the detected dot

The mean intensity of the laser dot is recorded in `data(:,1,4)`.

```
stats = regionprops(bw,Im,'MeanIntensity');
MeanIntensity = stats.MeanIntensity;
data(i,1,4) = MeanIntensity;
```

Record the pixel value of the detected laser dot

The central position of the laser dot is detected as the weighted centroid of the grayscale image of the laser dot. This is a good measure for clearly identifiable dots, but not very reprisentable for scattered reflections with no primary point of reflection.

```
stats = regionprops(bw,Im,'WeightedCentroid');
[LaserCoord] = stats.WeightedCentroid;
```

The horizontal value of the position in the image (the x-value) is recorded in data(:,1,6) and the vertical pixel value (the y-value) is recorded in `data(:,1,7)`.

```
data(i,1,6) = LaserCoord(1);
data(i,1,7) = LaserCoord(2);
```

Final laser dot

By multiplying the binary image values of the laser dot with the original greyscale image values, the intensity of the laser dot is visible.

```
Im = im2double(Im);
LaserDot=bw.*Im;
figure(1); imshow(LaserDot,'InitialMagnification','fit');
title('LaserDot with intensity');
```

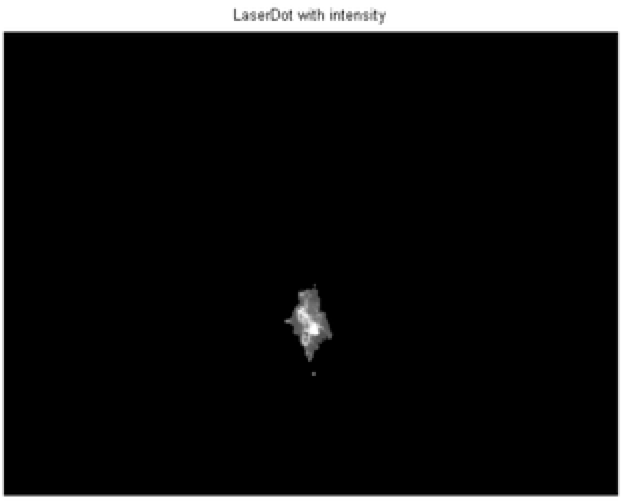

The final result of the laser dot detection is saved for later review.

```
cd(horzcat(Dir,Test,Dot));
imwrite(LaserDot,strcat('Dot_',num2str(i),'.jpg'));
```

Background

The isolated laser dot is subtracted from the original greyscale image `Im` to see what the thresholding had left out.

```
ImageRest = Im - LaserDot;
figure(1); imshow(ImageRest,'InitialMagnification','fit')
title('Information left out');
```

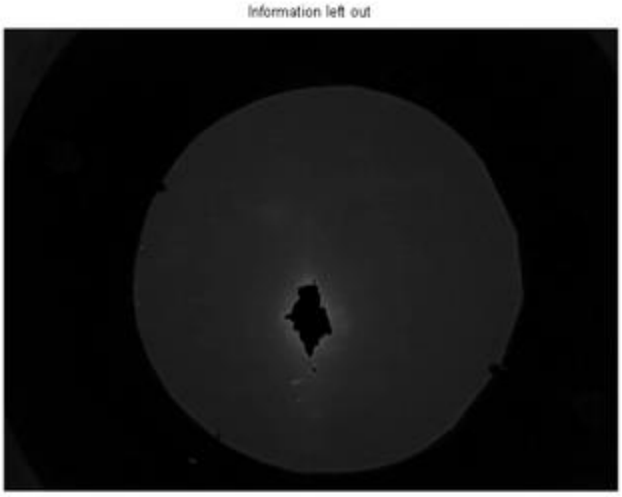

Adding the dot to the composition matrix.

The final step is to add the laser dot intensity to the composition matrix. This is done for every picture to be analysed, and it will result in the intensity distribution of the total test range.

```
Composition = Composition+LaserDot;
```

G. Matlab code for laser dot detection

```
%% Specify directory and the number of images to be processed
clc
clear

% Copy into directory if not in the right one.
% C:\NTNU_Data\Dropbox\Victoria\Skole\Master\Double Reflector -
Copy\Pictures to play with

Test = 'N-W';
Dir = 'C:\NTNU_Data\Pictures\dist670not_levelled25\';
Reg = ' registered';
Dot = ' dot';

NumPhotos = 1130;  % Number of photos to be processed
NumNoHit = 2;  % Number of a photo in cd with no hits

%% Directory
cd(horzcat(Dir,Test,Reg));   % Change directory

%% Counters
Picturecount=0;
IsEmpty=0;

%% Open one of the images
% The m-by-n size of the image (the pixel heigth and width of the picture)
% is taken from one of the images to be able to add laser dot fractions
% in the loop of the picture processing.

Compositions=imread('Reg_1.jpg');
Composition=zeros(size(Compositions(:,:,1)));
data=zeros(NumPhotos,1,7, 'double');

%% Average intensity of the absorber plate
% An image from the same dataset as the Test being analyzed with no
% laser dot is used as a measure of the background intensity of
% the absorber plate as a base value for thresholding the laser dot.
% This method requires an input value of one of the images with noe hits.
% It also required the lighting conditions to be very stable to et good
% results.

% Another way of getting an automated procedure would be to calculate this
% mean for every image in an iterative manner where the first threshold
% value is set at a low value, and a binary image of the absorber plate is
% created based on this value. And the wanted thresholding value is then
% calculated based on the mean intensity of og the absorber plate on each

Im = imread(strcat('Reg_', num2str(NumNoHit),'.jpg'));
level = graythresh(Im);
bwabsorber = im2bw(Im,level);
bwabsorber = bwareaopen(bwabsorber,1000);   % removes objects smaller than
1000 pixels
bwabsorber=imfill(bwabsorber,'holes'); % Fills in small holes in at the
border
bwabsorber=imclearborder(bwabsorber);    % Clears the border by supressing
border structures
figure(1); imshow(bwabsorber,'InitialMagnification','fit')
```

```
STATS = regionprops(bwabsorber,Im,'MeanIntensity');
AbsIntensity = STATS.MeanIntensity;
STATS = regionprops(bwabsorber,Im,'MaxIntensity');
AbsMaxInt = STATS.MaxIntensity;

%% Loop for processing images
tic
for i = 1:NumPhotos;
    cd(horzcat(Dir,Test,Reg));
    Im = imread(strcat('Reg_', num2str(i),'.jpg'));
    Picturecount=Picturecount+1;

    %% Segmenting the laser dot by threshholding
    % The level of the thresholding is calculated based on the mean
    % intensity value of the absorberplate from one image representing all
    % the images.
    thresh = AbsIntensity*2.5;  % 250% higher valu than the absorbeplate
    bw = im2bw(Im, thresh/255);

    %% Greythresh:
    % As a way to cancle out everything around the absorber plate, we use
    % the automatically calculated threshold function to separate the
absorber from
    % the rest of the picture.
    level = graythresh(Im);
    bwabsorber = im2bw(Im,level);

    %% Removing small blobs
    % Morphology can assist segmentation. This function removes all objects
    % smaller than a number of pixels
    bwabsorber = bwareaopen(bwabsorber,1000);   % removes objects smaller
than 1000 pixels
    % figure(1); imshow(bwabsorber,'InitialMagnification','fit')
    %% Clean up image
    bwClear=imfill(bwabsorber,'holes'); % Fills in small holes in at the
border
    bwClear=imclearborder(bwClear);     % Clears the border by supressing
border structures
    %% Add image to bwClean
    bwClear=im2double(bwClear);
    bw=bwClear.*bw;
    %% Find remaining regions
    % This is a way to count all connected objects in a binary image to see
how
    % many objects we are dealing with.
    [B,L] = bwboundaries(bw,'noholes'); % L is the image with all connected
regions
                                               % saved as a number (1,2,3
etc.)
    numRegions = max(L(:));

   %% Need to cancle out small bright objects that are not the laser dot
    STATS = regionprops(bw, 'Area');
    Areavector=[STATS.Area];
    AreaDetected = sum(Areavector);

        %% Detect the images with no laser dot
    if AreaDetected < 100;
        IsEmpty=IsEmpty+1;
    else
```

```
        data(i,1,5) = 1;         % Meaningless for data that has wrong
input.
    %% Measure total area of the detected laser dot
    STATS = regionprops(bw, 'Area');
    Areavector=[STATS.Area];
    Area = sum(Areavector);

    % Here the area should be saved in the row corrsponding to the number
    % the picture is
    data(i,1,3) = Area;

    %% Measure the Mean Intensity of the detected dot
    stats = regionprops(bw,Im,'MeanIntensity');
    MeanIntensity = stats.MeanIntensity;

    % Here the mean intensity should be saved in the row corresponding to
the number
    % the picture is
    data(i,1,4) = MeanIntensity;

    %% Record the pixel value of the detected laser dot
    stats = regionprops(bw,Im,'WeightedCentroid');
    [LaserCoord] = stats.WeightedCentroid;
    data(i,1,6) = LaserCoord(1);
    data(i,1,7) = LaserCoord(2);

    %% Add the intensity to LaserDot
    Im = im2double(Im);
    LaserDot=bw.*Im;
    figure(1);
    imshow(LaserDot,'InitialMagnification','fit'),title('LaserDot');
    cd(horzcat(Dir,Test,Dot));
    imwrite(LaserDot,strcat('Dot_',num2str(i),'.jpg'));
    %% Subtract the isolated laser dot to see what we are missing
    ImageRest=Im-LaserDot;
    %% Adding the dot to a new picture.
    Composition = Composition+LaserDot;

    end
end
toc
%% Calculate number of hits
% To get an idea of efficiency

Hits=Picturecount-IsEmpty;
Efficiency_hits=(Picturecount-IsEmpty)/Picturecount;

figure(1);
surf(Composition)
shading('interp');
colormap('hot');
colorbar;
view(90,0);

%% Find and exclude the wrong data
% In this section, the wrongly collected data will be removed. By wrong
data, I mean
% the data that is collected that is not the red dots on the absorber,
% but bright spots that caused by tares/scratches in the absorber plate
```

```matlab
% A better solution would be to design a better detection
% be to not detect this data (bright spots on the absorber plate), but the
% time constraints made it difficult to come up with a better code

bwComposition=Composition>0;
CC = bwconncomp(bwComposition);
[B,L] = bwboundaries(bwComposition,'noholes');

STATSmean = regionprops(L,Composition,'MeanIntensity');
Mean = [STATSmean.MeanIntensity];

STATSmax = regionprops(L,Composition,'MaxIntensity');
Max = [STATSmax.MaxIntensity];

STATS = regionprops(L,'Area');
Areavector=[STATS.Area];

STATSmin = regionprops(L,Composition,'MinIntensity');
Min = [STATSmin.MinIntensity];

% Need a way to find out whether or not there is wrong data in the result.
% It can be that there is not, so before this part of the script is used,
% this should be investigated.

%% Remove wrongly detected spots from variable Composition
% this is a so called "quick fix" to the problem of detecting the

[maxArea,A] = max(Areavector(:));
[maxInt,Int] = max(Max(:));

while A~=Int;

    Exclude = true(size(bwComposition));
    Exclude(CC.PixelIdxList{Int}) = false;
    bwExcluded = im2double(Exclude);

    % Claculate the new composition matrix, and the properties to evaluate
    % the while loop

    Composition = bwExcluded.*Composition;

    bwComposition=Composition>0;
    CC = bwconncomp(bwComposition);
    [B,L] = bwboundaries(bwComposition,'noholes');

    STATSmax = regionprops(L,Composition,'MaxIntensity');
    Max = [STATSmax.MaxIntensity];

    STATS = regionprops(L,'Area');
    Areavector=[STATS.Area];

    [maxArea,A] = max(Areavector(:))
    [maxInt,Int] = max(Max(:))
end

figure(1);
surf(Composition)
shading('interp');
```

```
colormap('hot');
colorbar;
view(90,0);

%% If this does not work, remove data in 3-by-3 matrices around the maximum
% This assures that no part of the right data is lost.

%MeanValue = Mean(A);
%critpoint = MeanValue*10;        % NB! This needs to match the graph
%[maxPoint,P] = max(Composition(:));
%Remove = 4;      % How many pixels to remove in each direction around
maximum. In a square matrix.

%[ii,jj] = ind2sub(size(Composition),P);

%while maxPoint > critpoint
%    [ii,jj] = ind2sub(size(Composition),P);
%    Composition([ii-Remove:ii+Remove],[jj-Remove:jj+Remove]) = 0;
%    [maxPoint,P] = max(Composition(:));
%end

%figure;
%surf(Composition)
%shading('interp');
%colormap('hot');
%colorbar;
%view(90,0);

%% Total area of the laser dot
Area = sum(Areavector);

%% Extract the weighted centroid of the composition of laser dots
STATS = regionprops(bwComposition,Composition,'WeightedCentroid');
Centroid = STATS.WeightedCentroid;

%% Convert composition to uint8, and calculate the real, mean pixel values
Composition8 = zeros(size(Composition),'uint8');
Composition8 = (Composition.*255)./Hits;

%% Find mean intensity of all the laser dots together
STATS = regionprops(bwComposition,Composition8,'MeanIntensity');
MeanIntensity = STATS.MeanIntensity;

%% Find minimum intensity of all the laser dots together
STATS = regionprops(bwComposition,Composition8,'MinIntensity');
MinIntensity = STATS.MinIntensity;

%% Max intensity of all the laser dots together
MaxIntensity = max(Composition8(:));

%% Locate the center of the absorber plate
cd(horzcat(Dir,Test,Reg));
Im = imread(horzcat('Reg_',num2str(NumNoHit),'.jpg'));
level = graythresh(Im);
bwabsorber = im2bw(Im,level);
bwabsorber = bwareaopen(bwabsorber,1000);    % removes objects smaller than
1000 pixels
bwabsorber=imfill(bwabsorber,'holes'); % Fills in small holes in at the
border
```

```
bwabsorber=imclearborder(bwabsorber);      % Clears the border by supressing
border structures
STATS = regionprops(bwabsorber,'Centroid');
Centroid=STATS(1);       % First value x-value (horizontal), second value y-
value (vertical)

%% Save the composition data
cd(horzcat(Dir));
save(horzcat('CompositionData',Test,'.mat'),'Composition8','Composition','H
its'...
    ,'Picturecount','Efficiency_hits','IsEmpty','Centroid','Area','data'...
   ,'Centroid','AbsIntensity','AbsMaxInt','MeanIntensity','MinIntensity'...
    ,'NumPhotos','MaxIntensity');
imwrite(Composition8,horzcat('composition',Test,'.jpg'));

%% Plot composition data
figure(1);
surf(Composition8);
title(horzcat('Surface plot of laser dots in ',Test,'
Max:',num2str(MaxIntensity)...
    ,' Min:',num2str(MinIntensity),' Mean:',num2str(MeanIntensity)));
axis('equal');
axis('tight');
shading('interp');
colormap('hot');
colorbar
view(2);

%% Plot sideways
figure(2);
surf(Composition8)
shading('interp');
colormap('hot');
colorbar;
view(0,0);
title(horzcat('Surface plot of laser dots in ',Test,'
Max:',num2str(MaxIntensity)...
    ,' Min:',num2str(MinIntensity),' Mean:',num2str(MeanIntensity)));

%% Plot countours
%figure
%axis equal
%contourf(Composition);
%colormap cool
%colorbar('location','southoutside')
```

H. Matlab code for compilation of results from the 4 quadrants tested

```
%% Composition of the 4 tests

% Copy into directory
% C:\NTNU_Data\Dropbox\Victoria\Skole\Master\Double Reflector -
Copy\Pictures to play with
clc
clear
Test = '675';
Lev = 'not_levelled';
Dir = 'C:\NTNU_Data\Pictures\dist';
cd(horzcat(Dir,Test,Lev));

%% Load N-E data
load('CompositionDataN-E.mat');
S = size(Composition);
CompositionAll = zeros(S,'double');
AreaAll = [0 0 0 0];
MeanAll = [0 0 0 0];
MaxAll = [0 0 0 0];
PicturecountAll = [0 0 0 0];
CompositionAll = CompositionAll+Composition;
AreaAll(1) = Area;
MeanAll(1) = MeanIntensity;
MaxAll(1) = MaxIntensity;
HitsAll(1) = Hits;
PicturecountAll(1) = Picturecount;

%% Load S-E data
load('CompositionDataS-E.mat');
CompositionAll = CompositionAll+Composition;
AreaAll(2) = Area;
MeanAll(2) = MeanIntensity;
MaxAll(2) = MaxIntensity;
HitsAll(2) = Hits;
PicturecountAll(2) = Picturecount;

%% Load S-W data
load('CompositionDataS-W.mat');
CompositionAll = CompositionAll+Composition;
AreaAll(3) = Area;
MeanAll(3) = MeanIntensity;
MaxAll(3) = MaxIntensity;
HitsAll(3) = Hits;
PicturecountAll(3) = Picturecount;

%% Load N-W data
load('CompositionDataN-W.mat');
CompositionAll = CompositionAll+Composition;
AreaAll(4) = Area;
MeanAll(4) = MeanIntensity;
MaxAll(4) = MaxIntensity;
HitsAll(4) = Hits;
PicturecountAll(4) = Picturecount;
%% Calculate mean
MeanTot = sum(MeanAll.*AreaAll)/sum(AreaAll);
Efficiency_hits = sum(HitsAll)/sum(PicturecountAll);
CompositionAll8 = zeros(size(CompositionAll),'uint8');
CompositionAll8 = (CompositionAll*255)/sum(HitsAll);
```

```
%% Calculate properties
bwCompositionAll = CompositionAll > 0;
bwCompositionAll = im2double(bwCompositionAll);
CC = bwconncomp(bwCompositionAll);
[B,L] = bwboundaries(bwCompositionAll,'noholes');

%STATS = regionprops(bwCompositionAll,CompositionAll8,'MeanIntensity');
%MeanIntensity = STATS.MeanIntensity;

%STATS = regionprops(bwCompositionAll,CompositionAll8,'MaxIntensity');
%MaxIntensity = STATS.MaxIntensity;

%STATS = regionprops(bwCompositionAll,'MaxIntensity');
%Areavecotr = [STATS.Area];
%AreaTotal = sum(Areavector);

%% Plot surfaces

Max = max(CompositionAll8(:));
figure(2);
surf(CompositionAll8);
title(horzcat('Surface plot of laser dots in ',Test,'  Efficiency:'...
    ,num2str(Efficiency_hits),'  Max:',num2str(Max)));
%axis('equal');
axis('tight');
shading('interp');
colormap('hot');
colorbar
view(90,0);       %view(2)
```

I. Temperature measurements from charging the heat storage by the sun

Figure 0.1 Temperature and radiation measurements of the first test of charging the heat storage. Gaps in the measurement is due to a bad connection of the thermal couples.

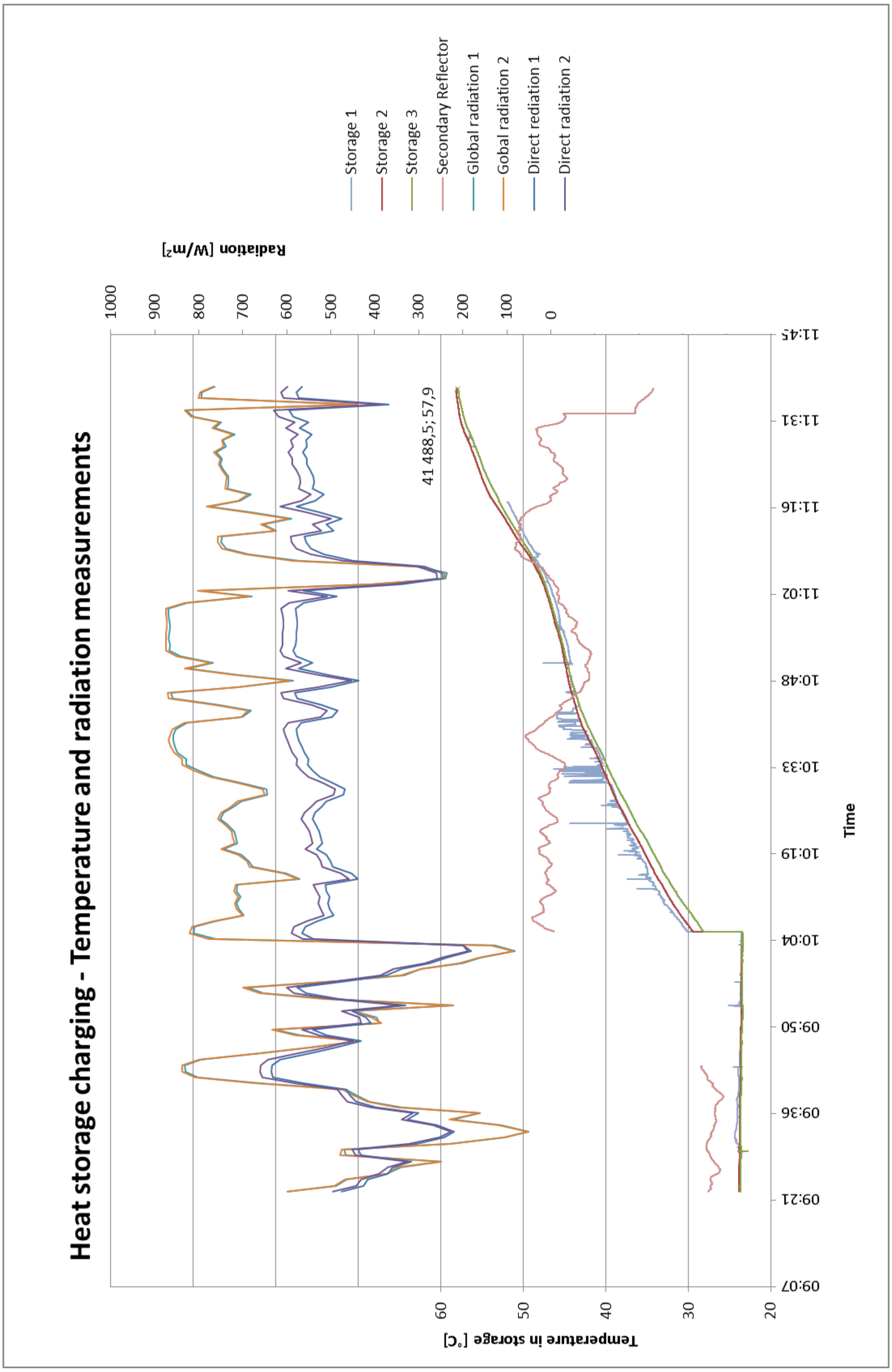

Figure 0.2 Test number 2, including all 3 temperature measurements from the heat storage, and radiation measurements of global and direct radiation. Measurments from the thermal camera is included at the points measured.

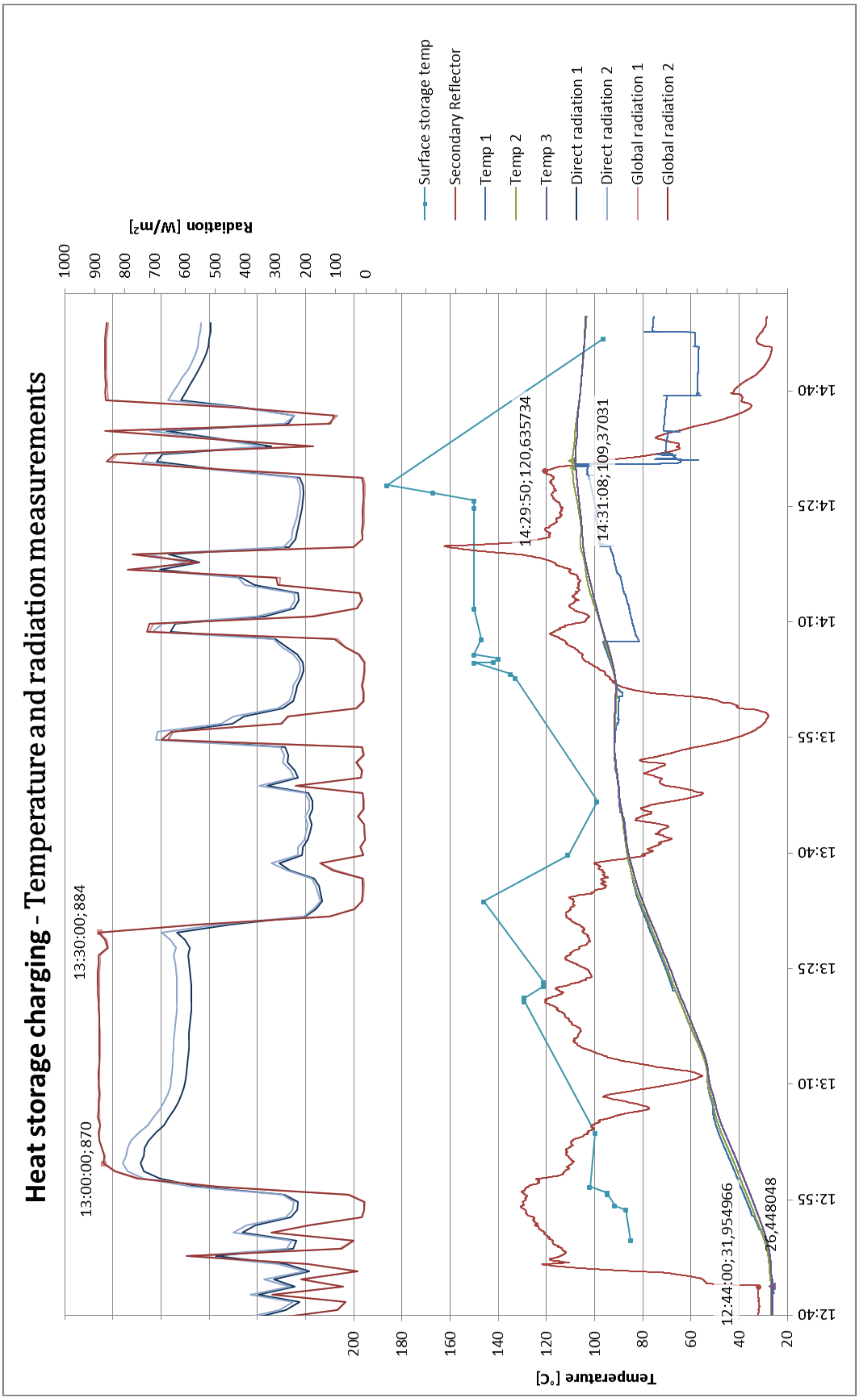

Figure 0.3 Test number 2. Secondary reflector temperature is plotted only for the points where the surface temperature of the storage is also recorded for comparing purposes.

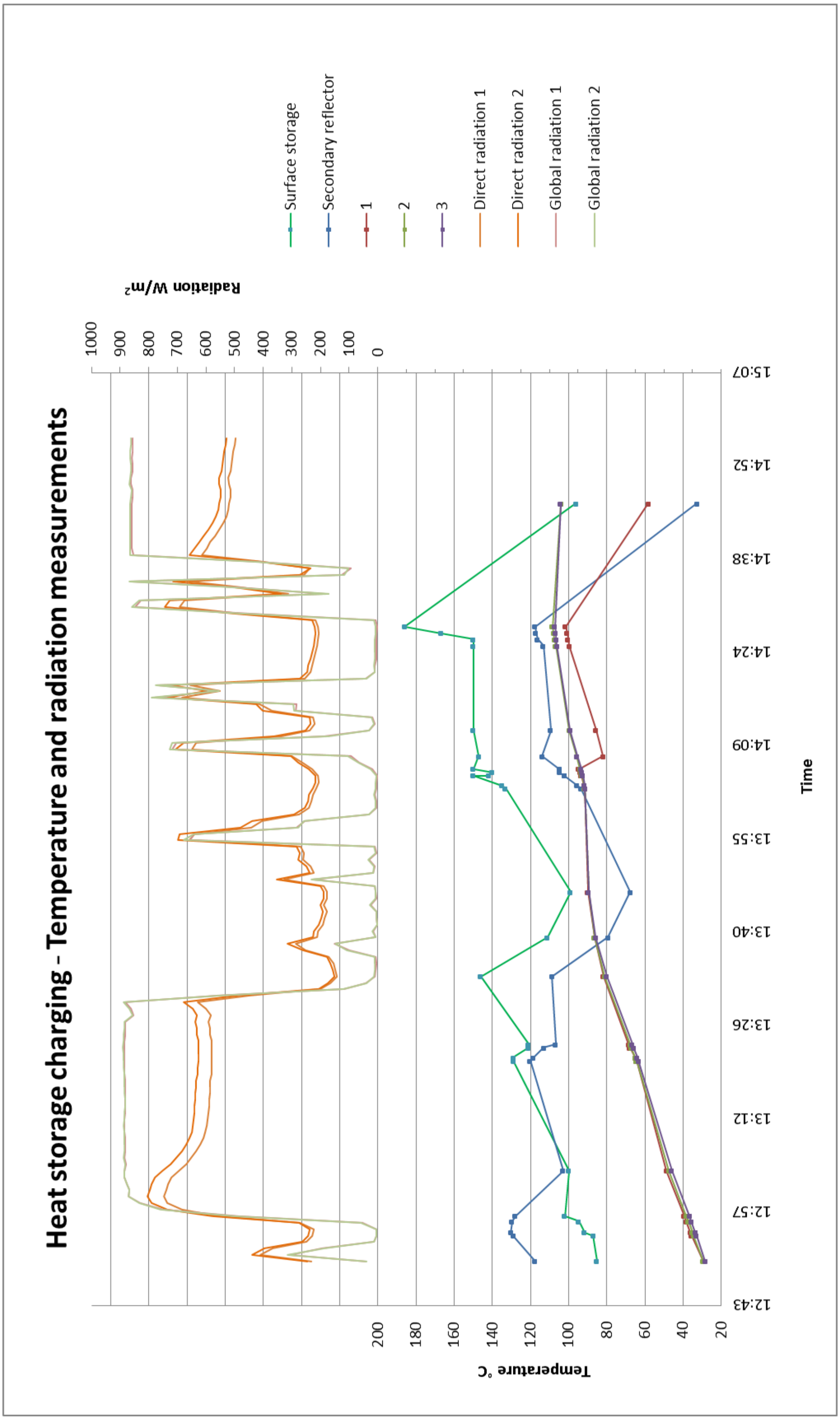

J. Thermal images of the surface temperature of the heat storage

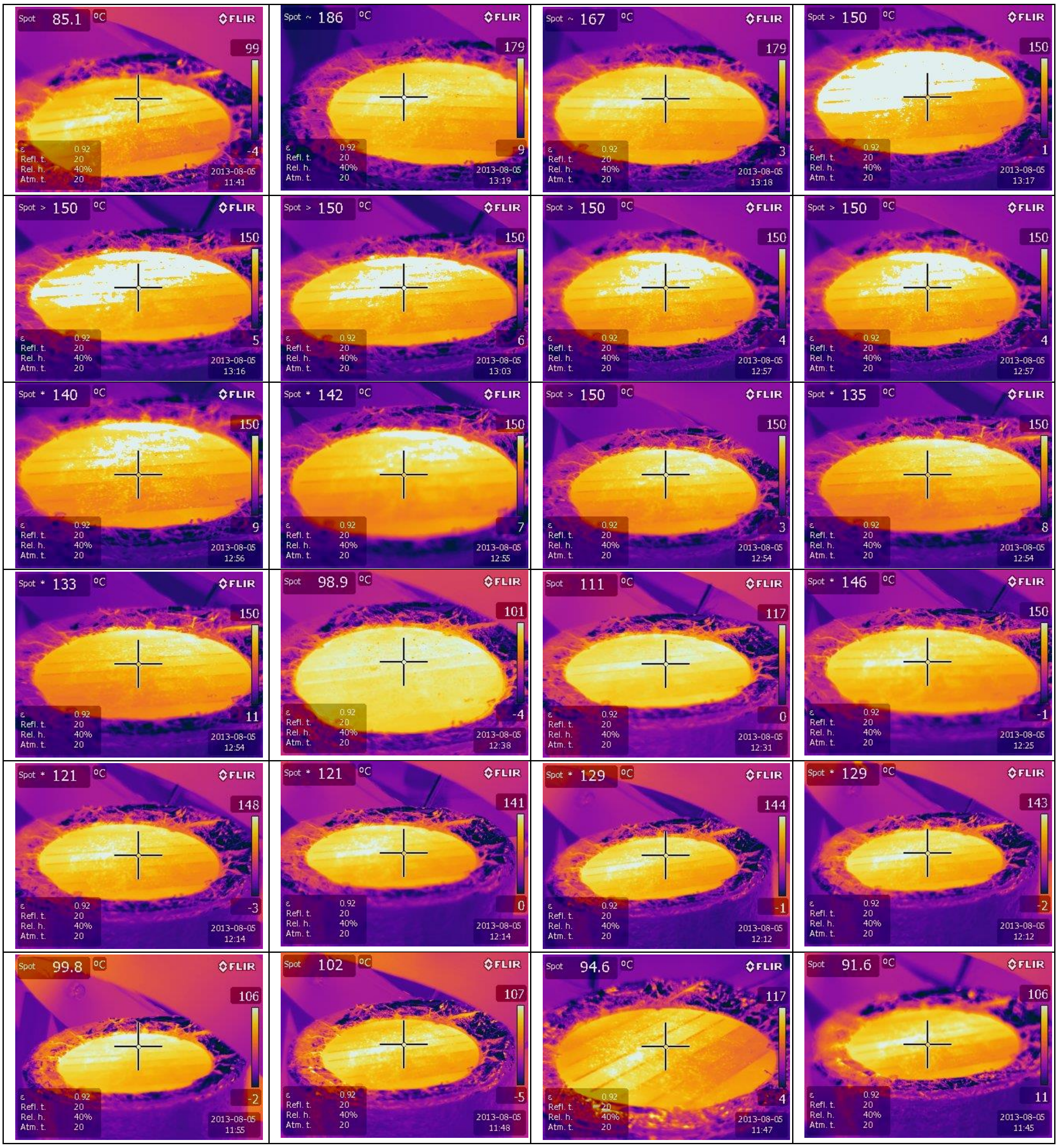

Figure 0.4 A table of the thermal images used to measure the temperature of the heat storage during the second test. The images are listed chronologically on each row from left to right. The emissivity was set to the value for black heat resistant lacquer listed by the thermal cameras book of emissivity values, and the measurement is expected to give reliable results.

L. Thermal images from flat plate tests

Figure 0.5 Thermal images from the first test conducted with the steel absorber plate. The images in the left column show a poor focusing, while the images in the right column seem to be properly focused. The time the pictures were captured is included.

<table>
<tr><td>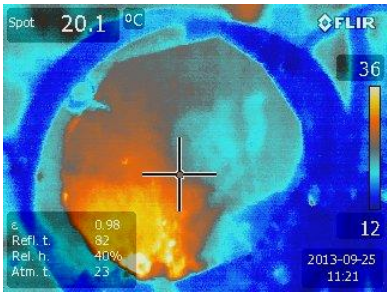</td><td>11:21:10

The focusing of the system is not satis-factory</td><td>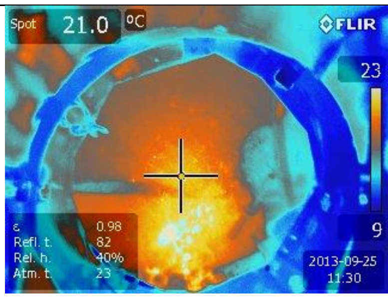</td><td>11:30:36

Focusing improved with the highest intensity hitting the absorber plate.</td></tr>
<tr><td>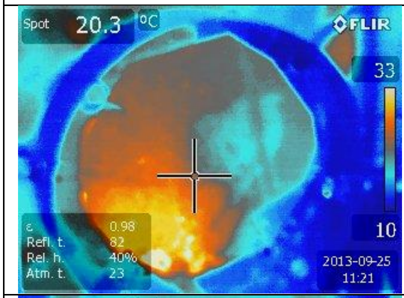</td><td>11:21:42</td><td>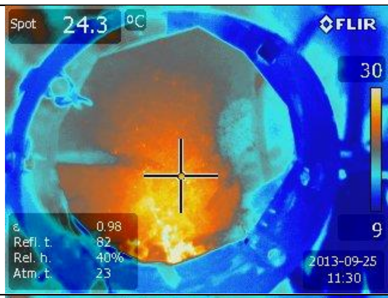</td><td>11:30:56</td></tr>
<tr><td>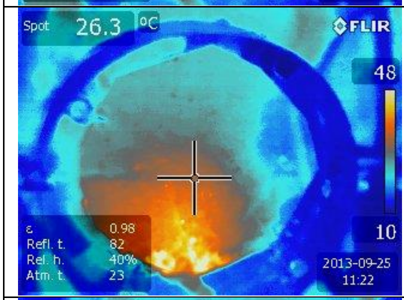</td><td>11:22:38</td><td>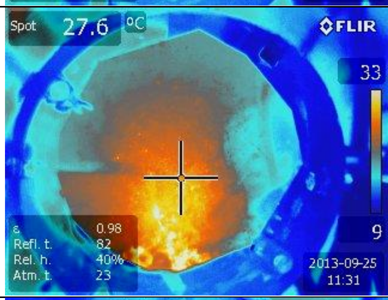</td><td>11:31:24</td></tr>
<tr><td>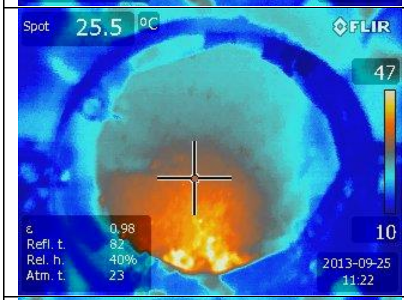</td><td>11:22:52</td><td>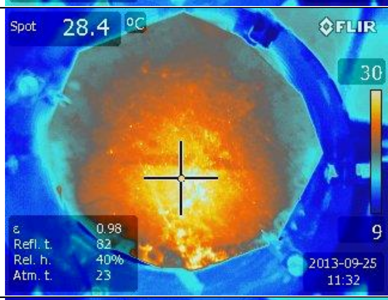</td><td>11:33:00</td></tr>
<tr><td>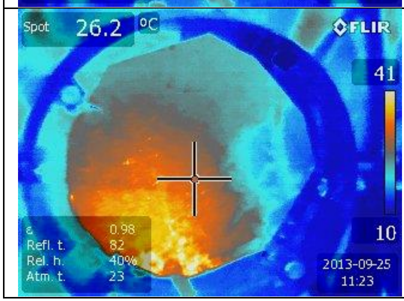</td><td>11:23:18</td><td>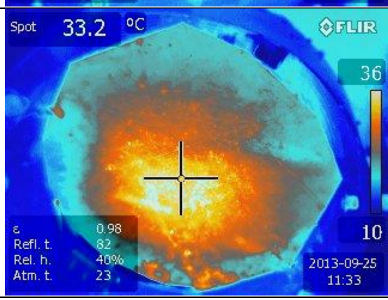</td><td>11:34:04</td></tr>
</table>

Figure 0. Thermal and digital images from the second test conducted with the steel absorber plate. The steel plate reached temperatures high enough for oxidation of the metal to take place. The images presented are shown from the first signs of oxidation takes place, with the time in seconds after this image was captured included.

	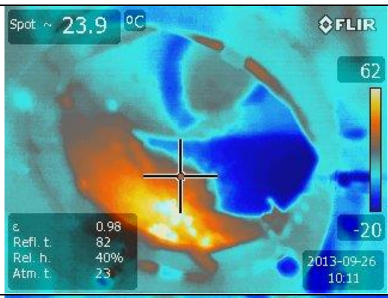	*The focal point is starting to show due to oxidation of the metal.*
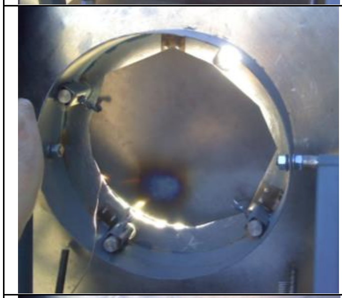	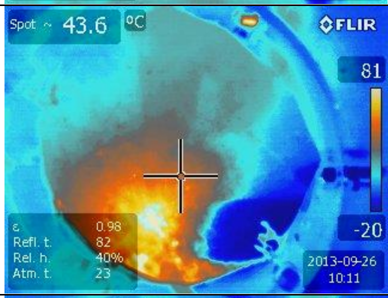	*24 seconds*
	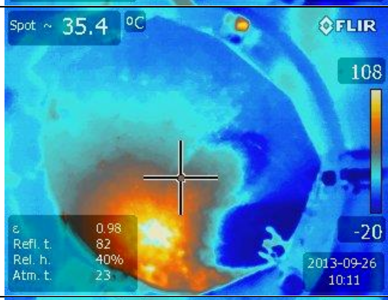	*36 seconds*
	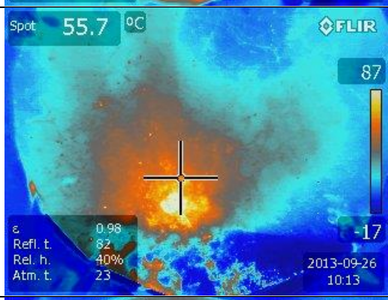	*112 seconds*
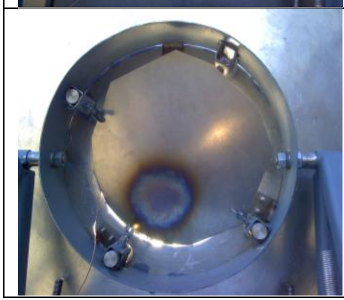	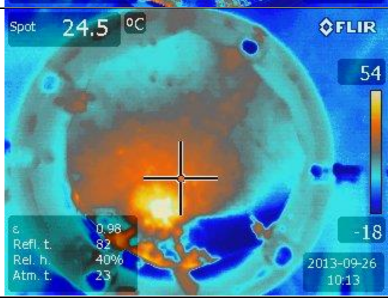	*128 seconds*

Figure 0.6 Thermal images from the third test conducted with the steel plate

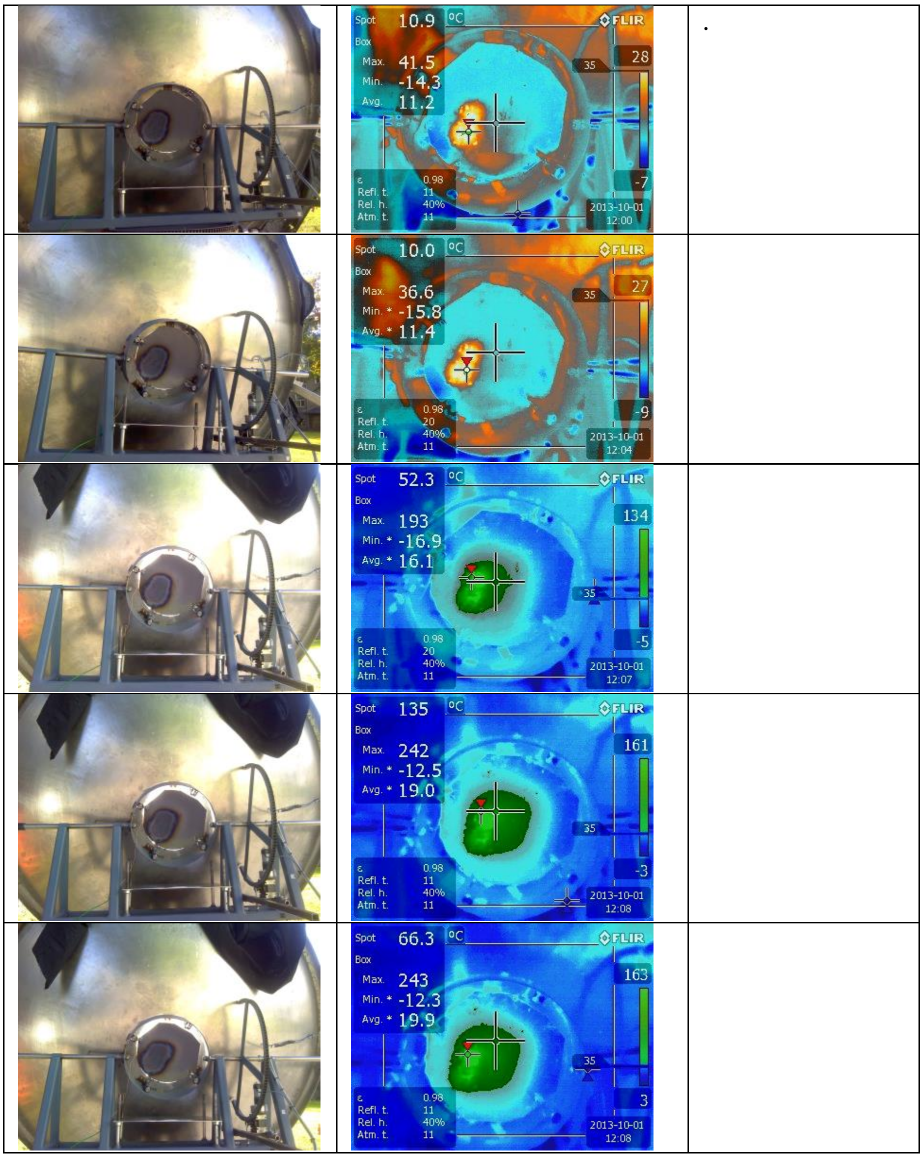

M. Intensity plots from the laser test

Table 0.B Intensity plots from the laser test of the double reflector with a graph displaying a plot as seen from the side.

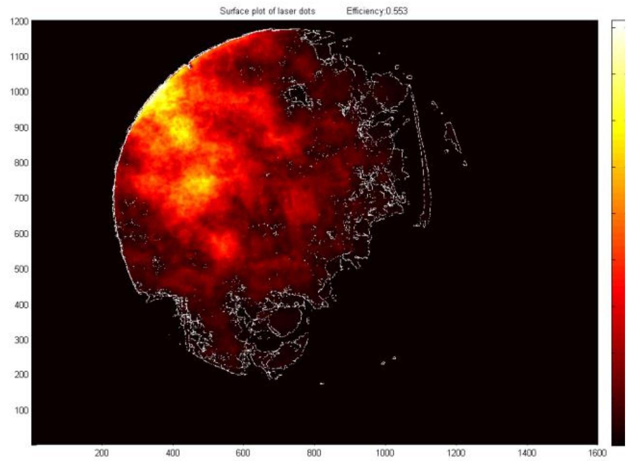

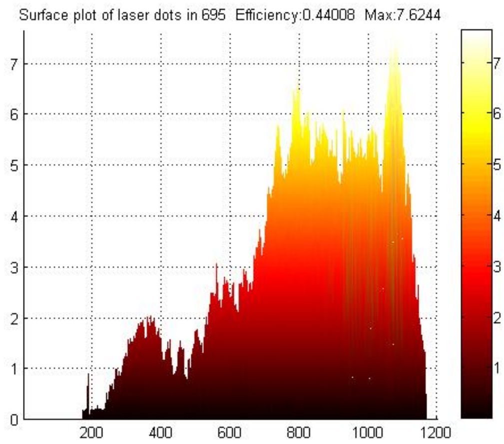

a Dist: 708 mm, Eff. 0.44, Intensity 7.4, Angle 0

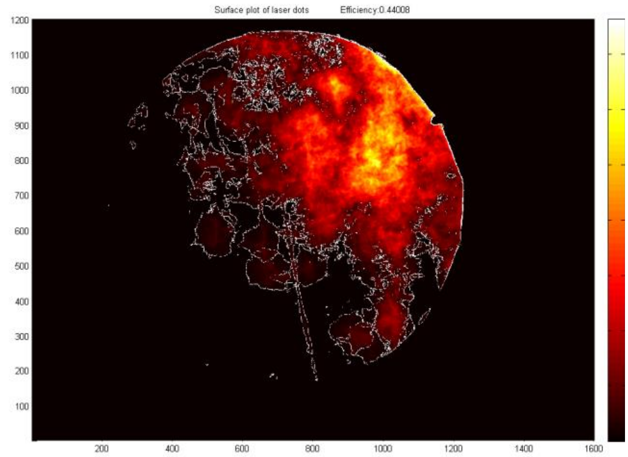

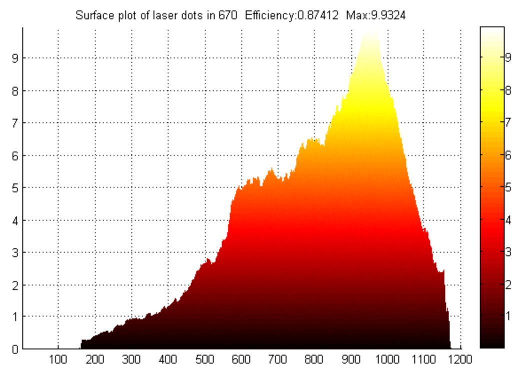

b Dist: 708 mm, Eff. 0.553, Intensity 9.1, Angle 1,7

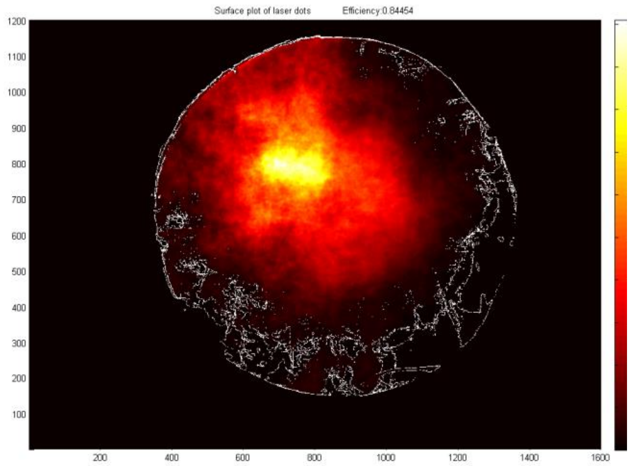

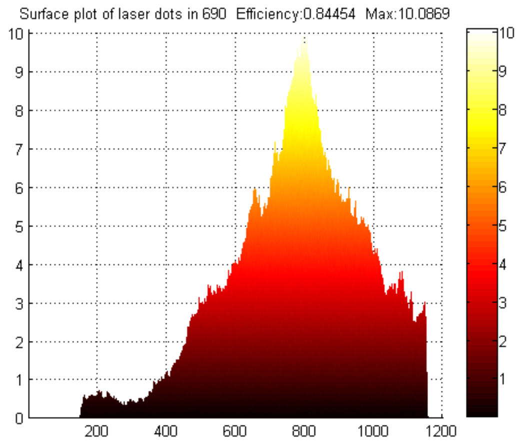

c Dist: 703 mm, Eff. 0.845, Intensity 10.1, Angle 1,3

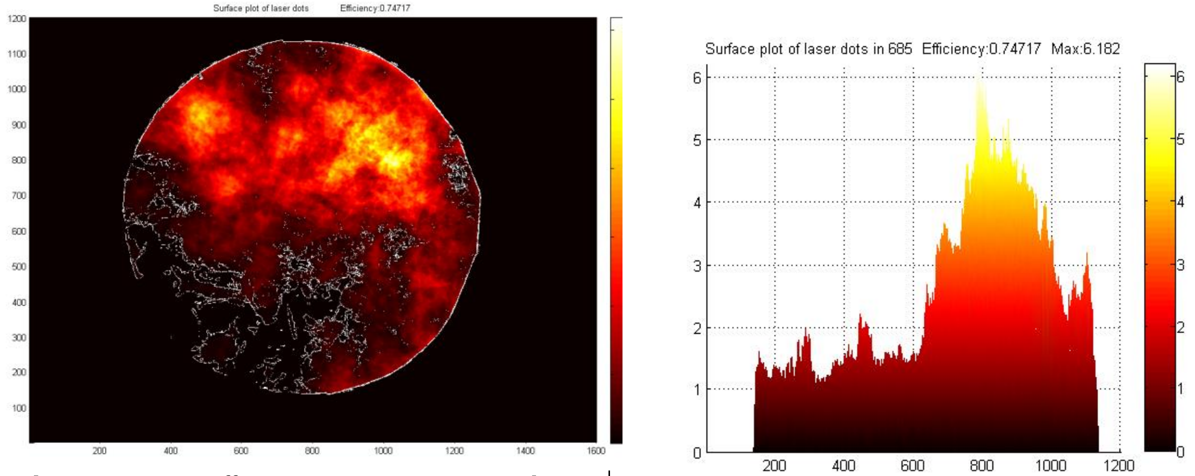

d Dist: 698 mm, Eff. 0.747, Intensity 6.15 , Angle 0

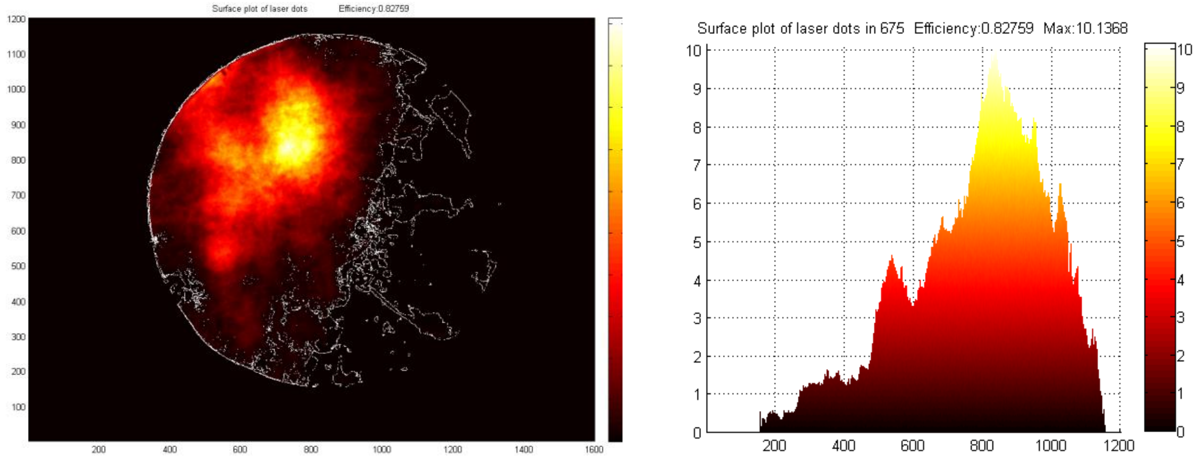

e Dist: 688 mm, Eff. 0.828, Intensity 610.2, Angle 1,4

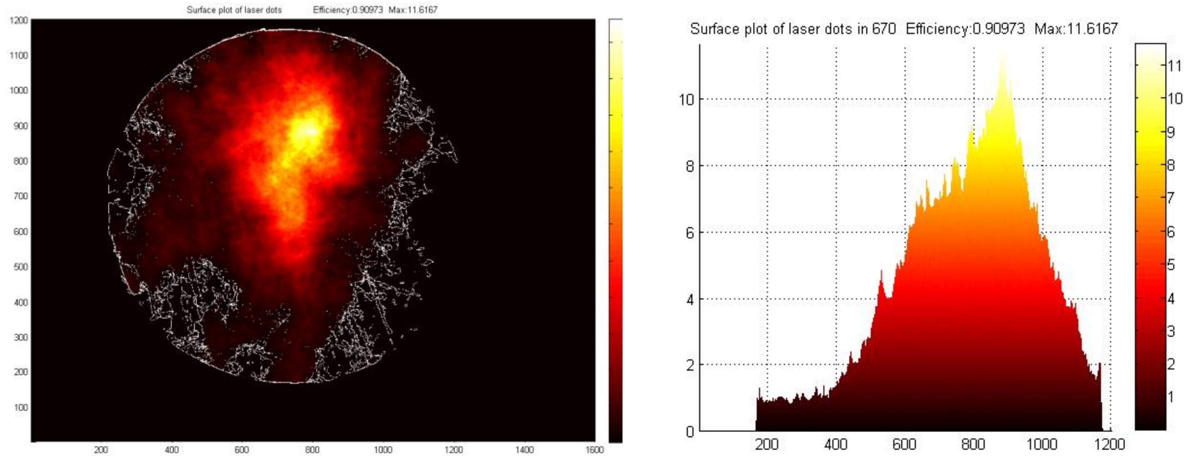

f Dist: 683 mm, Eff. 0.910, Intensity 911.61, Angle 0.9

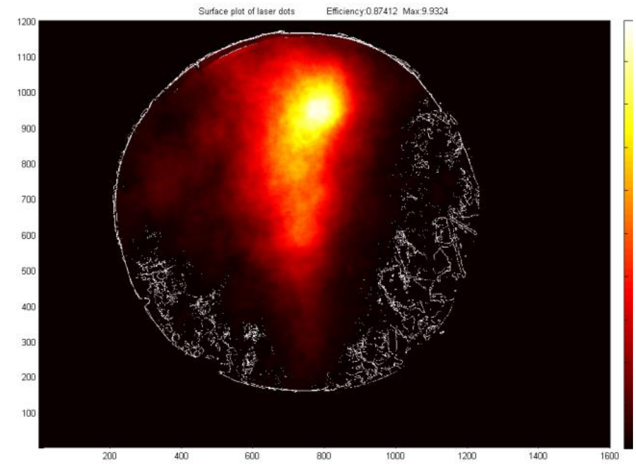

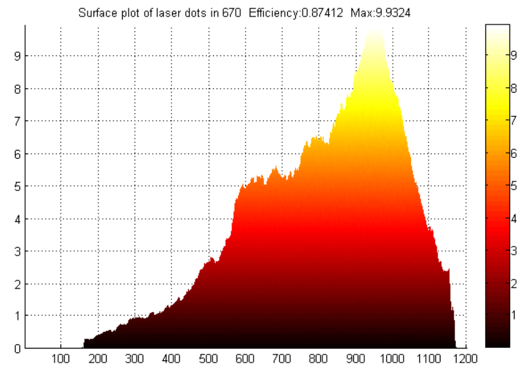

g Dist: 683 mm, Eff. 0.874, Intensity 9.93, Angle 0,9

References

Blackwell, J. and S. Thornton Mastering Optics: An Applications Guide to Optical Engineering, McGraw-Hill.

Incopera, D., Bergmann, Lavine (2007). Fundamentals of Heat and Mass transfer. United States of America, John Wiley and Sons.

John A. Duffie, W. A. B. (2006). Solar engineering of thermal processes, Hoboken, N.J. : Wiley.

Kalogirou, S. A. (2004). "Solar thermal collectors and applications." Progress in Energy and Combustion Science **30**(3): 231-295.

Kaykaty, G. (1966). Analysis of Performance of Double-Reflector System for Collecting Solar Energy, DTIC Document.

Mlatho, J. S. P., M. McPherson, et al. (2010). "Determination of the spatial extent of the focal point of a parabolic dish reflector using a red laser diode." Renewable Energy **35**(9): 1982-1990.

Oberg, E., F. D. Jones, et al. Machinery's Handbook (29th Edition) & Guide to Machinery's Handbook, Industrial Press**:** 480.

OMEGA_Engineering. "Introduction to thermocouples." 2013, from http://www.omega.com/prodinfo/thermocouples.html.

Sharma, A. "Review on thermal energy storage with phase change materials and applications." Renewable ans Sustainable Energy Reviews (13): 318-345.

Sharma, G. and A. Thé. "Automating Image Registration with MATLAB." 2013, from www.mathworks.se.

SIU. "The Norwegian Programme for Development, Research and Education (NUFU)

" Retrieved 28.11, 2013, from http://www.siu.no/eng/Front-Page/Programme-information/Development-cooperation/NUFU.

UCSB. "Innovative Datasets for Environmental Analysis by Students." Retrieved 05.11., 2013, from http://www.geog.ucsb.edu/ideas/Insolation.html.

UO-SRML. "Sun path chart program." from http://solardat.uoregon.edu/SunChartProgram.html.

Woh, F. C. (2011). Experimental and numerical investigations of a small scale double-reflector concentrating solar system with latent heat storage. Trondheim : Norwegian University of Science and Technology, Faculty of Engineering Science and Technology, Department of Energy and Process Engineering.